UNIVERSITÀ
DEGLI STUDI
DI PALERMO

Università degli Studi di Palermo

DOTTORATO DI RICERCA IN SCIENZE CHIMICHE
SSD CHIM/12 Chimica dell'Ambiente e Beni Culturali

Caratterizzazione delle vernici da antichi strumenti musicali

—

Characterization of the varnishes from historical musical instruments

Candidato:
Francesco Caruso

Tutor e Cotutor:
Prof. Eugenio Caponetti e
Prof.ssa Delia Francesca Chillura Martino

Coordinatore:
Prof. Michelangelo Gruttadauria

XXII ciclo – A.A. 2008–2010

Abstract

The characterization of materials such as glues, paints, pigments, binders and varnishes used to create artworks, continues to provide art historians and conservators with precious information. Such a knowledge enables restoration and conservation processes to be carried out properly without causing any damage to the original artefacts and also helps to understand the techniques used by the artists.

The varnishing of musical instruments has been an interesting debating point since the end of the 19^{th} century for lute-makers and industries focused onto the (re)production of high quality instruments.

To date, there is considerable scientific interest in recovering the original formulations (the *secrets* of the old masters) and transferring such knowledge to restorers, conservators, lute-makers and musicologists.

Ample scientific efforts have been made to identify the organic and the inorganic portions of the surface layers of several historical stringed instruments, although the interest has mainly been focused on North-Italian ones.

This doctoral dissertation is devoted to the use of a non standard multi-analytical method for the characterization of the varnish of a selection of historical stringed musical instruments from the "Musical Instruments Museum" in Brussels and the "Vincenzo Bellini" Conservatory in Palermo. A series of non-destructive and micro-destructive instrumental techniques was applied for obtaining information about the composition of the varnishes of the instruments.

Particular attention was given to the implementation of a Curie Point Pyrolysis Gas Chromatography coupled with Mass Spectrometry methodology for the study of the organic portions of the micro-samples without any special pre-treatment.

This is the first systematic scientific work on the art works of such collections and one of the few in the field of chemical sciences applied to the conservation of historical musical instruments.

Acknowledgements

CONSERVATORIO DI MUSICA
VINCENZO BELLINI
PALERMO

I would like to thank the director and the vice-director of the "Vincenzo Bellini" Conservatory in Palermo, Maestro Carmelo Caruso and Maestro Luigi Rocca, and the conservators of the "Musical Instruments Museum" in Brussels, Dr Anne-Emmanuelle Ceulemans and Dr Jorge De Valck, for providing the historical musical instruments and their precious collaboration.

I would like to thank Dr Cosimo Di Stefano from the Centro Regionale per la Progettazione ed il Restauro – Regione Siciliana in Palermo for his precious support and the assistance with the analysis by m-XRF.

I would like to thank Dr Steven Saverwyns and Dr Marina Van Bos from the Koninklijkinstituut voor het Kunstpatrimonium – Institut Royal du Patrimoine Artistique in Brussels for their precious support during my internship in Brussels and the assistance with the analysis by GC-MS, Cp-Py-GC-MS, μ-FTIR, μ-XRF.

I would like to thank Dr Lucia Burgio from the Victoria and Albert Museum in London for her precious support during my internship in London and the assistance with the preparation and the analysis of cross sections by polarized light microscopy.

I acknowledge an Erasmus LLP Placement scholarship for my internship at the Koninklijkinstituut voor het Kunstpatrimonium – Institut Royal du Patrimoine Artistique in Brussels.

I would like to thank Dr Giovanni Paolo Di Stefano from the Università degli Studi di Palermo for his precious support in the organological information about the instruments from the the "Vincenzo Bellini" Conservatory in Palermo.

Finally, I would like to thank all the colleagues of Prof Caponetti's research group, Dr Maria Luisa Saladino, Dr Antonio Zanotto, Alberto Spinella, Giorgio Nasillo, for their support during the last three years.

Dedication

I would like to dedicate this doctoral dissertation to my beloved family (my mum Angela, my father Antonino, my brother Fulvio, and my girlfriend, Alessandra). Thank you very much for everything.

Contents

List of Tables

List of Figures

Chapter 1

Introduction

This introductory chapter presents a brief history of the collections of the studied stringed musical instruments. The chapter also reviews the existing relevant scientific literature about the studies on the varnishes from historical musical instruments.

1.1 History of the collection of the "Vincenzo Bellini" Conservatory in Palermo

The "Vincenzo Bellini" Conservatory was born in 1618 under the name of "Conservatorio del Buon Pastore" or "Casa degli Spersi". Like other important Italian conservatories, the Conservatory of Palermo owns an important collection of historical stringed musical instruments. The origin of the collection is uncertain because of the massive bombings of the archive of the Conservatory during the Second World War and a few pieces of information are available [1].

The most important surviving instrument of the collection is probably the 18^{th} century double bass by Vincenzo Trusiano (also known as Panormus). The instrument, probably given to the Conservatory at the beginning of the 18^{th} century, has been the object of an extensive conservation project [2, 3, 4].

The Sicilian minister Gaetano Daita reports about the presence of two violas by Antonio Stradivari and Nicolò Amati (both lost or stolen), a violin by Jacobus Steiner, a cello by unknown (probably, the one attributed to Carlo D'Avenia) and a double bass by D'Avena[1] [1, 5].

At the beginning of the 20^{th} century, the maintenance of the instruments was given to the well-known luthier Antonio Sgarbi who kept a laboratory

[1]The author was not precise in his booklet because the instrument is probably the above mentioned double bass by Trusiano and he mistook the cello with the double bass [1]

inside the Conservatory. Subsequently, Alfredo Averna, active until the end of 1970s, was appointed as luthier of the Conservatory [1].

1.2 History of the "Musical Instruments Museum" in Brussels

[2]

Since January 1992 the "Musical Instruments Museum" (now known as the "mim") has been part of the Royal Museums of Art and History as Department IV. By royal decree, the State has recognised the scientific character of its activities and provided it with two sections: the early music section and the section of modern (19^{th} and 20^{th} centuries), popular and traditional music.

Figure 1.1: The entrance of the "Vincenzo Bellini" Conservatory in Palermo. Photograph by A. Cataldo.

The original creation of the Brussels "Musical Instruments Museum" dates back to February 1877, when it was attached to the Brussels Royal Music Conservatory with the educational purpose of showing early instruments to the students.

When the Brussels Musical Instruments Museum was created, two collections of instruments were joined together.

One belonged to the celebrated Belgian musicologist François-Joseph Fétis (1784-1871). In 1872, it was bought by the Belgian government and stored on deposit in the Conservatory where Fétis was the first director. The other was offered to King Leopold II in 1876 by the Rajah Sourindro Mohun Tagore (1840–1914) and comprises about a hundred Indian instruments.

With these two original collections, the "Musical Instruments Museum" was already remarkably rich for its time. But its first *conservateur*, Victor-Charles Mahillon (1841–1924), was considerably to increase the collections, thus placing it among the finest in the world.

[2] Adapted from [6]

Figure 1.2: Since 2000, the Art Nouveau "Old England" building has been hosting the "Musical Instruments Museum" at Mont des Arts, in Brussels. Photograph by the author.

At his death in 1924, the "Musical Instruments Museum" counted some 3666 articles, among which 3177 were original musical instruments. As a collector and maker of wind instruments and a noted acoustics expert, Mahillon performed his job with an enthusiasm, competence and dynamism that exceeded any of the expectations that his purely honorary title might have aroused.

Thanks to his activity and connections, the museum rapidly gained international fame, not only for the quantitative importance of its collections but also for their diversity, and for the quality and rarity of the items brought together.

Furthermore, between 1880 and 1922 Mahillon described the collections of the museum in a monumental five-volume catalogue. The catalogue also includes the four versions of his "Essay on the methodical classification of all instruments, ancient and modern" that was to serve as the basis for the classifications of E.M. von Hornbostel and C. Sachs which are still used today. This classification of musical instruments entitled him to be considered as one of the pioneers of organology, the science of musical instruments.

Beginning in 1877, Mahillon created a restoration workshop inside the museum where he employed and trained a worker, Franz de Vestibule, to restore damaged articles, and also to make copies of historical instruments from collections from other countries (England, France, Italy, Hungary, Germany and other) [7].

In the 1880s, historical concerts on early instruments or copies were organised by François-Auguste Gevaert, who succeeded Fétis at the head of the Brussels Royal Music Conservatory. Performed by Conservatory professors and students, these concerts were a great success in Brussels and London at the end of the 19^{th} century.

Under the direction of Gevaert, Mahillon adopted a modern four-classes division for the instruments [8]:

1. *autophones*, or self-vibrators;
2. *membranophones*, or skin-vibrators;
3. *aerophones*, or wind-vibrators;
4. *chordophones*, or string-vibrators.

Through clever judgement, Mahillon obtained large augmentations of the collections by calling on philanthropists, mixing with erudite amateurs who sometimes became generous donors (eg César Snoeck), and through friendly relations with Belgian diplomats in foreign posts such as Jules Van Aalst at Canton (China) and Dorenberg at Puebla (Mexico), who brought back several instruments from beyond Europe.

Figure 1.3: Victor-Charles Mahillon. Retrieved October 31, 2010, from `http://www.rjmartz.com/horns/Mahillon_055/`

It was thus that Mahillon received or purchased isolated pieces of great historical and organological value, but also homogeneous ensembles whose interest today is considerable. Mahillon followed all the large public sales of musical instruments and bought the pieces he needed to complete the ideal collection that he was determined to build at the "Musical Instruments Museum".

The growth of the collection slowed sharply after Mahillon's death in 1924. His successor, Ernest Closson (1870–1950) was nonetheless motivated by the same scientific curiosity regarding musical instruments. He wrote several articles on Belgian luthiers for the National Biography and devoted a long monograph to "La facture des instruments de musique en Belgique" which appeared in 1935, during the Universal Exhibition held in Brussels. Besides organological information, statistics show the volume of Belgian instrument exports in the mid-19$^{\text{th}}$ century and highlight the reversal of trends in the 1920s and 1930s, namely the disappearance of most of the instrument builders in Low Countries.

With the arrival of Roger Bragard (1903–1985), curator from 1957 to 1968, the situation improved considerably. This eminent Latinist, drawn to musicology by his persistent interest for ancient treatises relating to music, was able to attract the attention of the Minister of Culture at the time and particularly of Miss Sara Huysmans: budgets were substantially augmented, the exhibition rooms were renovated, guides and scientific personnel were hired, and concerts of early music on original instruments or copies were organised. Once again, rare pieces could be acquired for the collections. Bragard's efforts were continued by René de Maeyer (from 1968 to 1989), who hired about ten scientific collaborators, each specialised in a different

field of organology. Nicolas Meeùs assumed the interim from 1989 to 1994: he launched the project for moving to the Art Nouveau "Old England" building designed by the Belgian architect Paul Saintenoy in 1899. Under Malou Haine, such a project has been realised.

The collection of western string instruments of the "Musical Instruments Museum" comprises all instruments used in western classical and art music [9]. In numbers, there are:

- 421 bowed string instruments;
- 243 plucked string instruments;
- 12 struck string instruments;
- More than 200 among bows, incomplete and experimental instruments, spare parts, etc.

1.3 Scientific studies on the varnish of historical musical instruments

The conservation and restoration of complex and delicate artefacts, such as historical musical instruments, require a multidisciplinary approach. The role of the scientific investigation is to characterize the artefact, assess its state of preservation and the reliability of possible conservation/restoration methods.

Wood restoration techniques vary from case to case and particular attention should be given for painted or varnished material.

After the prior eventual disinfestation from insects or parasites — in an inert gas chamber, if possible [10] — and the cleaning of the surface, the restoration process consists of the substitution of damaged parts of the artwork, using the same kinds of wood (ancient or artificially aged, when possible) and varnish [11]. In fact, the restorer has to deal with two aspects related with the problem of the varnish [12]: what kind was originally used and which ones among the established products are suited for the restoration.

The varnishing and finishing of musical instruments has been an interesting debating point since the end of the 19^{th} century for modern lute-makers and industries focused onto the (re)production of high quality instruments [13, 14].

A good varnish on a musical instrument should, in fact, meet the following requirements [15]:

- protective action on wood;
- enhancement of the aesthetical properties;

- good grip and chemical compatibility with the underlying layer;
- lack of formation of dangerous (for the wood) ageing products;
- compatibility with dyes and lacquers;
- permeability to steam;
- plasticity;
- good transparency;
- avoiding cracking

Apart from the above cited roles of the varnish, its influence on the quality of the emitted sound is not yet demonstrated even if some authors claim the importance of such a contribution (eg [14]) to compensate for possible structural defects of the wood substrate.

Therefore there is nowadays considerable scientific interest in recovering the original formulations (the *secrets* of the Old Masters) and transferring such knowledge to restorers, conservators, lute-makers and musicologists. Actually, the skills and the experience in the finishing of such Old Masters were outstanding and comparable to their building technique [16].

Varnishes for musical instruments are complex mixtures of both organic and inorganic compounds and are usually distinguished on the basis of their *solvents*:

1. spirit- or alcohol-based;
2. siccative oil-based (linseed oil, walnut oil, poppy-seed oil, etc);
3. essential oil-based (turpentine, lavender oil, etc).

Considerable scientific efforts have been made to identify the organic and the inorganic portions of the surface layers of several historical stringed instruments, although the interest has mainly been focused on North-Italian ones [17].

In some of the papers by Nagyvary *et al.*, the authors found mineral preparatory layers and/or chemical treatments in the wood of some Guarneri, Del Gesù and Stradivari's instruments [18, 19, 20, 21]. Their investigations were carried out by several micro- and non destructive (ND) analytical techniques such as wavelength and energy dispersive X-ray spectrometry (WDS and EDS), solid state ^{13}C cross polarization magic angle spinning nuclear magnetic resonance, Fourier transform infrared spectroscopy (FTIR). The authors claim that these preparatory layers and/or chemical treatments are relevant aspects of the finishing and partly responsible for the high quality of sound of such instruments.

The inorganic portion has been studied by destructive, micro-destructive and ND techniques [17].

A ND energy dispersive X-Ray Fluorescence (EDXRF) study was conducted on 15 North-Italian instruments dated from the 16^{th} to the 18^{th} century from the collection of the "Musée de la Musique" in Paris [22]. The author found the presence of lead, arsenic and mercury. Lead-based compounds were likely referable to the use of an oil-based varnish whereas arsenic- and mercury-based compounds were used as pigments.

Von Bohlen and Meyer carried out the total-reflection XRF characterization of micro-samples from North-Italian, Austrian, English and French instruments dated from the 16^{th} to the 20^{th} century [23, 24]. They found that iron, arsenic and lead are in a higher relative quantity in the samples from historical instruments (16^{th}-18^{th} century ones), whereas manganese, copper, cobalt, zinc and lead are more present in the varnishes of recent instruments (20^{th} century ones).

Von Bohlen and co-workers characterized small samples and varnished wood pieces from Guarneri, Grancino, Ceruti and Widhalm's stringed instruments by external micro-particle induced X-ray emission spectrometry [25]. No mineral-based intermediate layer was found. In fact, the weak response collected was probably attributed by the authors to the presence of mineral components, residues and contaminating traces associated to the usual processing of the wood.

A partial characterization of the varnish and the glue of an important 18^{th} century double bass, made by the Sicilian luthier Vincenzo Trusiano, was carried out by gas chromatography coupled with mass spectrometry (GC-MS) [3, 4]. It was found that one of the components of the varnish was walnut oil and the glue was of animal origin. Another GC-MS study by Echard *et al.* was conducted on the varnish of three 16^{th}-18^{th} centuries' stringed instruments from la Cité de la Musique, in Paris [26]. Echard and coworkers identified siccative oils, resinous materials, inorganic pigments, fillers and siccatives present in the samples. Chiavari *et al.* carried out a pyrolysis-GC-MS study on some materials used in the varnishes by luthiers (colophony, Manila copal, sandarac, elemi, benzoin and amber) and compared the obtained results with the pyrograms from an 18^{th} century violin by Marchi and a 20^{th} century violin by Bignami [27]. Apart from finding Py-GC-MS a feasible technique for this kind of investigation, they found that the formulation of the varnish on the violin by Marchi included a siccative oil and colophony whereas the varnish on the modern violin by Bignami included benzoin and colophony.

A review on the characterization of the varnishes from historical stringed musical instruments was published by Echard and Lavédrine [17]. The authors proposed a sequential approach consisting of both in situ non-destructive analyses (UV photography, polarized light microscopy of the surface, EDXRF) and micro-invasive and micro-destructive analyses (mi-

croscopy of cross-sections, micro-FTIR, SEM-EDX, Py-GC-MS and synchrotron-based XRD and FTIR). Following the proposed protocol, Echard *et al.* studied four Stradivari's stringed instruments. They found that the famous luthier from Cremona employed commonly available materials (siccative oils, *Pinaceae* resins, cochineal dye and iron oxides pigments) concluding that he might not have a secret recipe, but outstanding skills in manufacturing [28].

1.4 The analysed instruments and their labels

1.4.1 The instruments from the "Vincenzo Bellini" Conservatory in Palermo

The instrument, the number of inventory and the transcription of the inner label of the analysed instruments from the "Vincenzo Bellini" Conservatory in Palermo are reported in table 1.1.

Table 1.1: Instruments, number of inventory and transcription of the label of the studied stringed musical instruments from the "Vincenzo Bellini" Conservatory in Palermo.

Instrument and no. of inventory	Transcription of the inner label
Viola d'amore 1993	Printed: "Cav. Antonio Sgarbi Palermo 1914". The date is handwritten
Viola 1996	Handwritten: "Viola Tedesca riparata in Palermo l'anno 1896 da ASgarbi". The parts "Viol" and "riparat in Palermo l'anno 1896 da" are printed
Violin 1999	Printed: "Jacobus Stainer in Absam prope Oenipontum 1767"
Violin 2002	No visible label
Violin 2021	Printed: "Nicolaus Gagliano Filius Alexandri fecit Neap. 1781"
Cello 2173	Printed: "Carlo d'Avenia in Napoli 1716". Another more recent label is handwritten: "Violoncello Napoletano riparato in Palermo l'anno 1896 da ASgarbi". The parts "Viol" and "riparat in Palermo l'anno 1896 da" are printed

The six analysed instruments — among the most important ones, excluding Trusiano's double bass — were chosen with the help of the vice-director

and the responsible of the collection of the "Vincenzo Bellini" Conservatory, Maestro Luigi Rocca, with the main aim of obtaining new scientific information on the varnish of early South-Italian instruments. Such knowledge will support the conservators in the project of creating a museum out of this collection.

An historical picture of the ensemble of the collection is shown in figure 1.4.

1.4.2 The instruments from the "Musical Instruments Museum" in Brussels

The instrument, the number of inventory and the transcription of the inner labels of the analysed instruments from the "Musical Instruments Museum" in Brussels are reported in table 1.2.

Table 1.2: Instruments, number of inventory and transcription of the label of the studied stringed musical instruments from the "Musical Instruments Museum" in Brussels.

Instrument and no. of inventory	Transcription of the inner label
Violin 1338	Printed: "Benoit-Joseph Boussu, me / Luthier à Bruxelles 1750"
Cello 1372	Handwritten: "Benoit Joseph Boussu ME / luthier A Bruxelles 1757"
Cello 1374	Printed: "Gaspar Borbon / tot Brussel 1688". The last two digits of the label are handwritten
Pochette 2764	Handwritten: "Gaspar Borbon tot Brussel 1686"
Violin 2774	Printed: "GASPAR BORBON / tot Brussel 16.."
Violin 2781	Handwritten: "Boussu, a / ....1750"
Violin 2782	Handwritten: "B. I. Boussu, a Etterbeecke / près de Bruxelles, Le / 20 8bre 1752 n° 36"
Violin 2784	Printed: "Benoit Joseph BOUSSU, / Maître Luthier à Bruxel- / les 1753". The last digit of the label is handwritten
Violin 2836	Printed: "Gaspar Borbon tot Brusselles 1692"

Figure 1.4: An early 20^{th} century picture of the collection of "Vincenzo Bellini" Conservatory in Palermo (from reference [1]).

The nine analysed instruments were chosen by the conservators of the "Musical Instruments Museum" because they presented issues in the authentication, the state of preservation, peculiarity of their manufacture, and others.

All the instruments are among the finest of the "Musical Instruments Museum": four by Benoit-Joseph Boussu and five by Gaspar Borbon. Benoit-Joseph Boussu was a luthier active from 1747 to 1760 in Brussels. His instruments, on the model by Nicolò Amati, are qualitatively comparable to the finest North-Italian ones. Gaspar (or Jaspar) Borbon was a member of the renowned family of Belgian musicians and luthiers. He was born in 1632 or 1635, was active from 1664 to 1702 and died in 1710 [29, 30].

Cello 1374 is of particular interest because of the manufacturing technique. The latter is a special one, typical of the Low Countries, called *archaicé*. The luthiers employing it did not use a mould for making the instruments [31].

Violin 2836 is exceptional because it is almost entirely kept in its original state. It is very fragile because of several ancient wormholes, which made its use impossible from early on.

Chapter 2

Experimental

This chapter describes the sampling operations and the experimental conditions during *in situ* and the laboratory parts of this research work.

It is furtherly divided into two sections: non destructive and micro-destructive techniques.

2.1 Non destructive techniques

2.1.1 Photography in visible and UV light

To answer questions concerning the various aspects of interest in an artefact, two types of methods are generally applied: area and point examinations.

Area examinations examine the states of the total or greater parts of surface of an object (including macro- and microscopic investigations). This meets the holistic approach of art historians. Aims of these methods are to make invisible or imperceptible surface states or the inner structure of opaque objects visible to the naked eye. Visible and UV illumination and their digital photographic documentation may serve for this purpose [32].

The musical instruments of the "Vincenzo Bellini" conservatory were photographed in visible light with an Olympus SP-500UZ 6 MP digital camera, with manual white balance and automatic parameters for exposure time, F-number, and ISO speed.

The musical instruments of the "Musical Instruments Museum" were photographed in both visible and UV light with a Nikon D40x 10 MP digital camera, mounting a Nikkor VR 18-105 mm lens, with manual white balance and automatic parameters for exposure time, F-number, and ISO speed.

2.1.2 m- and μ-X-ray Fluorescence

X-ray Fluorescence spectroscopy (XRF) is the technique that relies on the emission of X-rays from a sample, after the photo-electric absorption of higher energy incoming photons from an X-ray tube, a radioisotope or a

synchrotron source. It can be schematically described as a two step process involving: i) the creation of inner electronic vacancies (ionization of atoms of the sample); and ii) photo emission due to the electronic transition inside the inner orbitals of the atoms. As a function of the type of transition, this yields the so-called K, L and M lines on the spectra. This phenomenon is exploited by XRF spectrometers to analyse the elemental composition of an object. Thus, the information that can be drawn from such a technique regards qualitative and semi-quantitative elemental (from Be, $Z = 4$, to U, $Z = 92$) composition. The energy and the intensity of the emitted photons are related to specific elements present and their concentration, respectively.

A typical XRF equipment includes an X-ray source, a target, a detector and an analysing system (electronics). Remarkable studies about XRF technique and instrumentation can be found throughout the physico-chemical literature (eg [33, 34, 35, 36]).

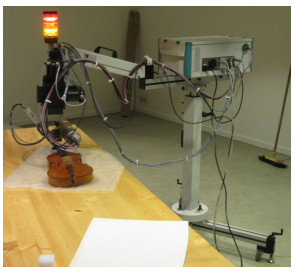

Figure 2.1: The ARTAX μ-XRF portable instrument by Bruker during the measurements at the "Musical Instruments Museum" in Brussels. Photograph by the author.

XRF spectroscopy is an exploratory technique which is well-suited to cultural heritage analyses because of its being portable, non-destructivity, non-invasiveness and rapidity. It allows researchers to establish what kind of further diagnostic investigations should be carried out. It can also be used to obtain information on an entire painted surface (preparation layers, artificial and natural inorganic pigments, degradation products) exploiting its state of conservation. It has also been applied to many different types of materials in the field of cultural heritage including stony artefacts, organic materials, metallic ones, paintings, and so on [37, 38, 39].

On the other hand, XRF analyses often need to be integrated with results from other techniques (eg Fourier Transform Infrared Spectroscopy, Raman Spectroscopy, X-ray Diffraction).

Two were the instruments used for the elemental characterisation of the inorganic additives of the varnishes of the musical instruments.

The first instrument was used for the characterisation of the varnish of some instruments from the "Vincenzo Bellini" Conservatory in Palermo whereas the second one was used for characterising the varnish of selected instruments from the "Musical Instruments Museum" in Brussels.

The first instrument used was a Lithos 3000 by Assing (Assing S.p.A., Monterotondo, Italy). It is composed of an air-cooled conventional source, with a Mo target and a W filament, developing a maximum power of 15 W under a 30 kV and 500 μA, maximum acceleration potential and current, respectively. The used acceleration potential and current were 24 kV and 200 μA, respectively. The radiation was Zr-filtered. The EDS detector,

Peltier effect cooled, guarantees a resolution of 158 eV on the iron line. It has an area of 7 mm^2. The head of the instrument features: a red laser interferometer with a resolution of 60 mm to correctly establish the focal distance (10 mm) and a mini CCD b/w camera that enables to point to the analysed area. The analysed area ranges from 2.9 mm^2 to 105.0 mm^2. The instrument is mounted on a suitably modified professional photographic Manfrotto tripod and it is connected to a Windows XP laptop through a DAQCard – 6024E by National Instruments (National Instruments Corporation, Austin, TX, USA). The data collecting and analysing software is the XQ Assing bundle. Measurements were done in air. The collection times varied from 100 s to 300 s.

The second instrument used was the ARTAX μ-XRF portable instrument by Bruker (Bruker Belgium S.A./N.V., Brussels, Belgium). It includes an air-cooled metal ceramic X-ray tube with a W target. The applied acceleration potential and current were 50 kV and 600 μA, respectively. The radiation was not filtered and collimated to 200 μm. The Si drift detector (SDD) was cooled at a temperature of -15 °C by a Peltier element. The SDD allows a resolution of less than 155 eV at 10 kcps and has an area of 10 mm^2. The head of the instrument is mounted on a tripod and connected to a Windows PC through an interface. The data collecting and analysing software was the ARTAX package by Bruker. Measurements were carried out in air and the collection time was 200 s.

The analysed areas were selected to provide good statistical information and on the basis of the presence of interesting points (evidenced during the prior observation under visible and UV light).

2.2 Micro-destructive techniques

2.2.1 Sampling

Six instruments from the "Vincenzo Bellini" Conservatory in Palermo were sampled from different areas, close to scratched and damaged regions (see figure 2.2).

μg-samples (well below the 0.1 mg recommended by Stuart in her recent book [40]) from the from historical musical instruments were taken by gently scraping the surface of the instrument with a scalpel with a rounded head sterile mini blade.

The sampling maps are shown in figures 2.3, 2.4, 2.5, 2.6, 2.7, 2.8 and a summary of the number of the taken sample is shown in table 2.1.

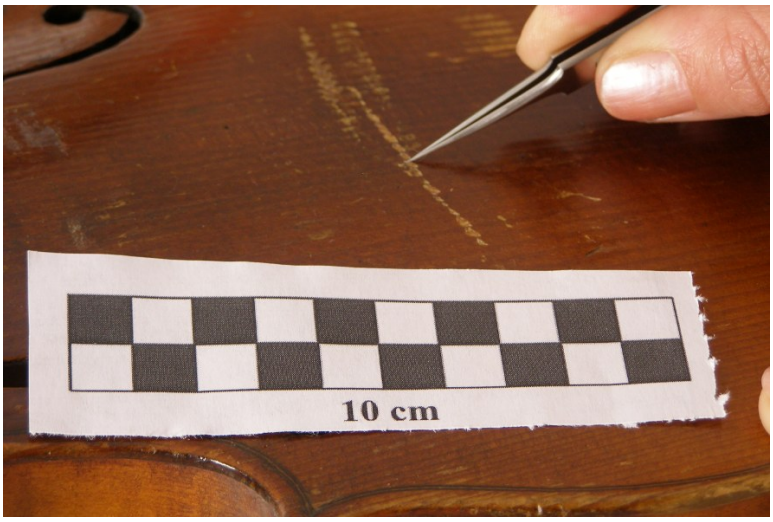

Figure 2.2: Micro-destructive sampling on one of the instruments of the "Vincenzo Bellini" Conservatory.

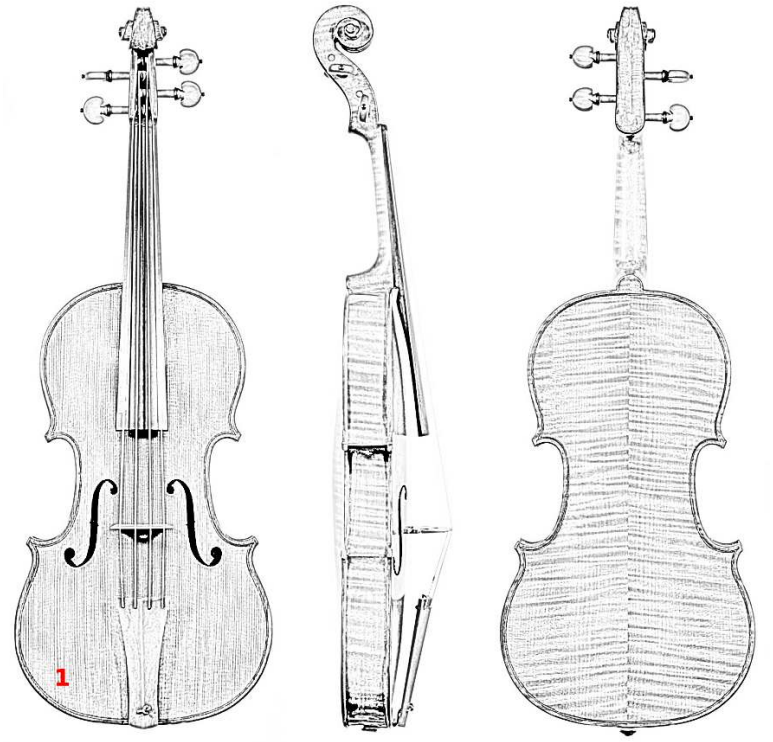

Figure 2.3: The map of the sampled spots of the *viola d'amore* 1993 by A. Sgarbi.

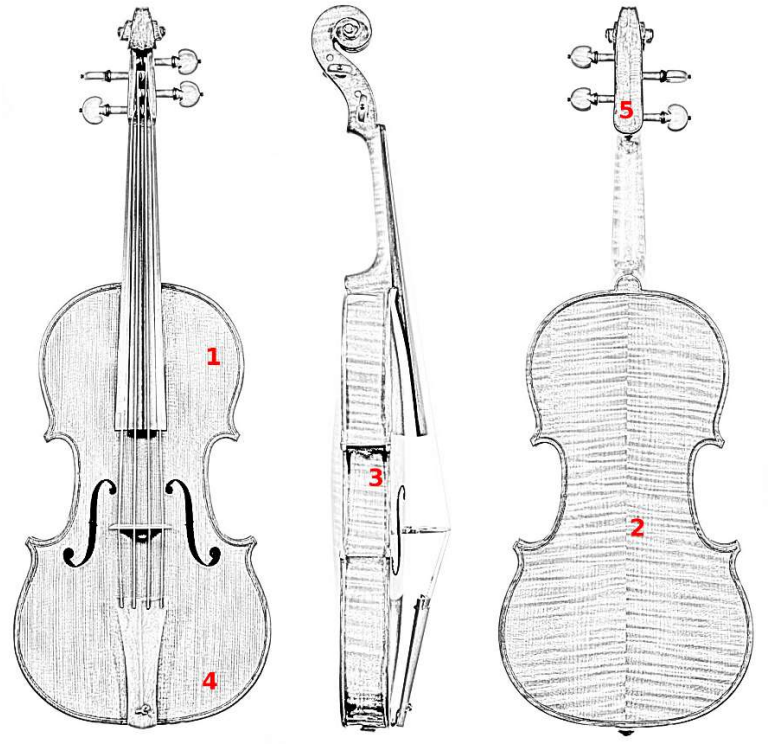

Figure 2.4: The map of the sampled spots of the German viola 1996 by unknown.

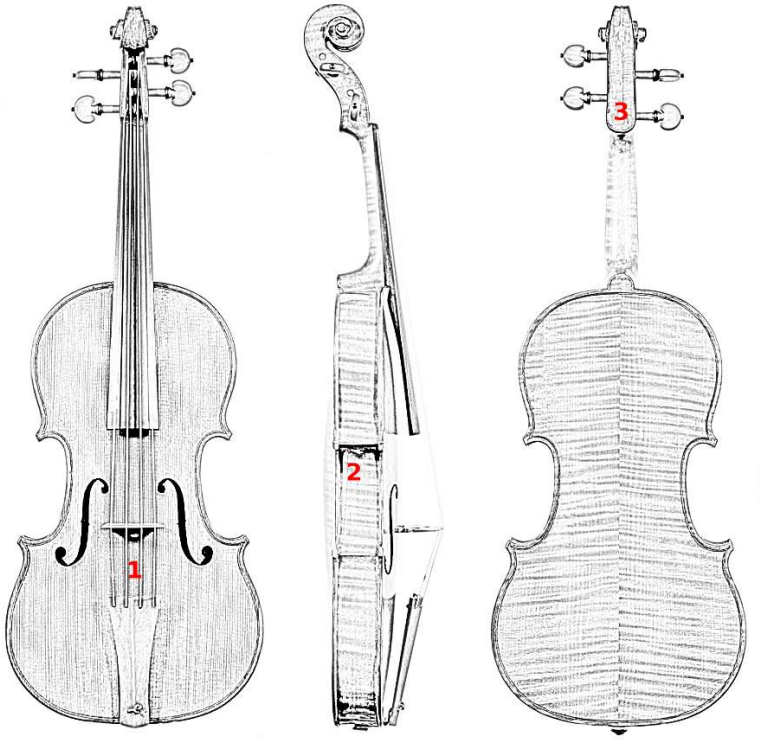

Figure 2.5: The map of the sampled spots of the violin 1999 by J. Stainer.

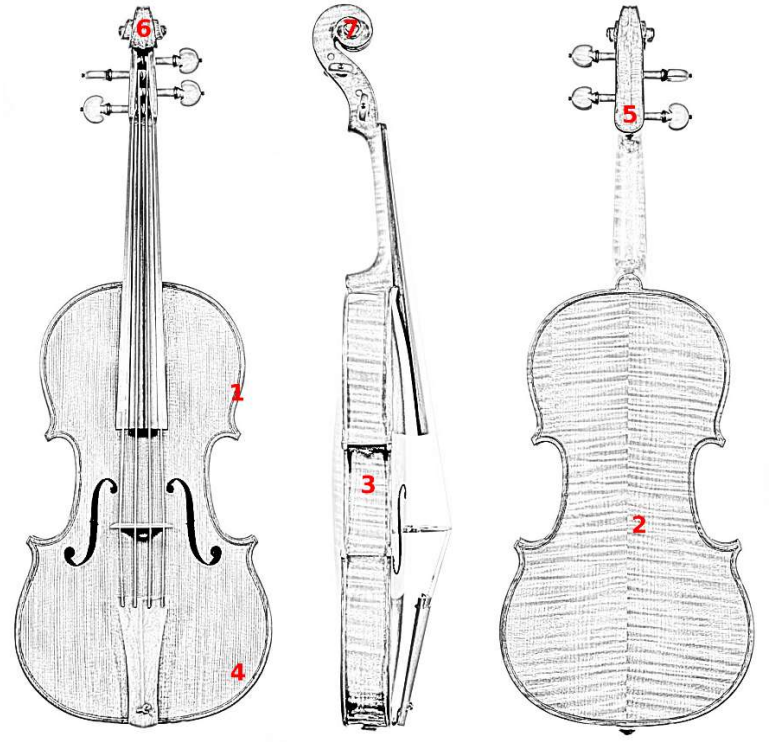

Figure 2.6: The map of the sampled spots of the violin 2002 by unknown.

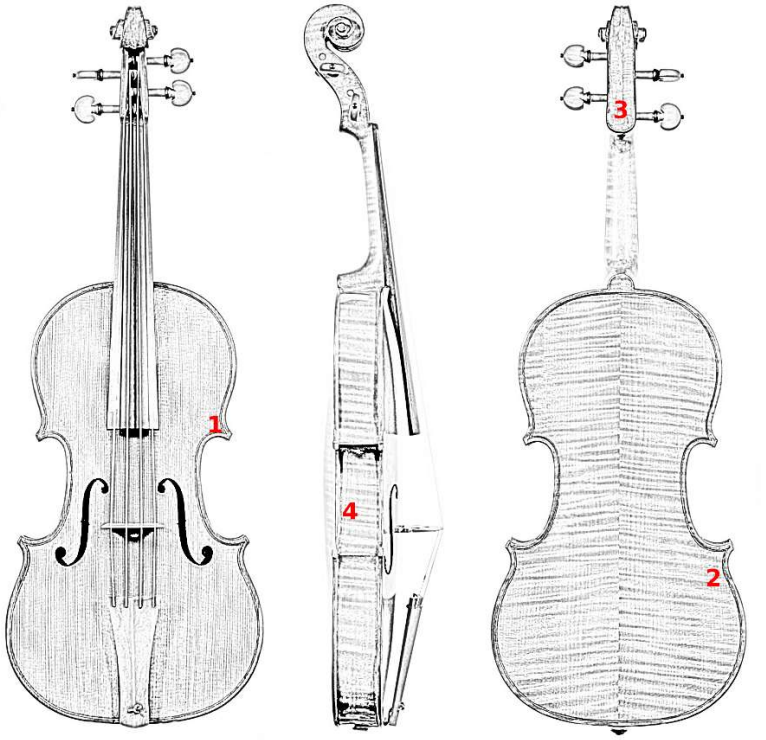

Figure 2.7: The map of the sampled spots of the violin 2021 by N. Gagliano.

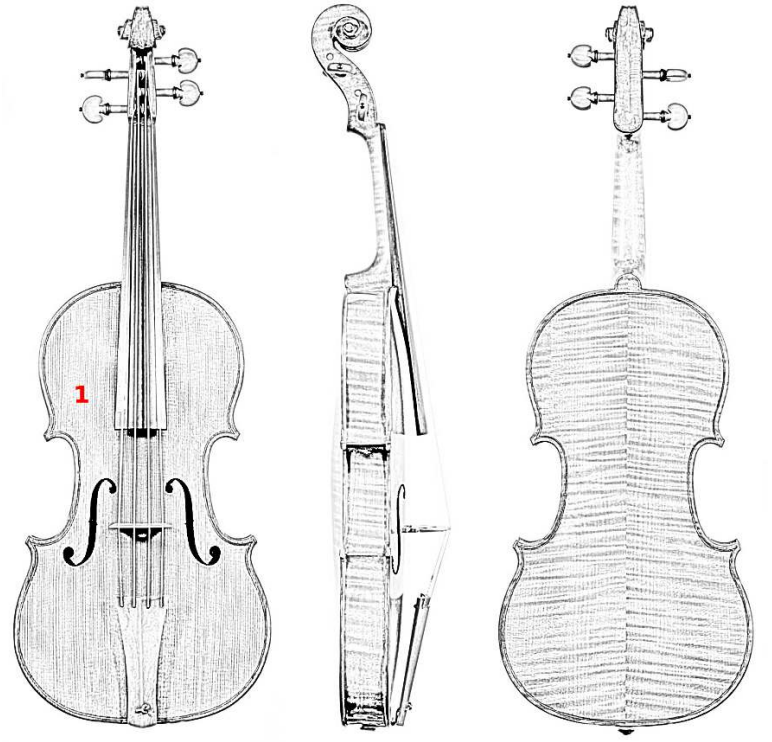

Figure 2.8: The map of the sampled spots of the cello 2173 by C. d'Avenia.

Table 2.1: Number of inventory and number of samples of the studied musical instruments of the "Vincenzo Bellini" Conservatory in Palermo (Italy)

No. of inventory	No. of samples
1993	1 sample
1996	5 samples
1999	3 samples
2002	6 samples
2021	6 samples
2173	1 sample

2.2.2 Polarized Light Microscopy

Polarized light microscopy (PLM) analysis is used to gather information about the structure and characteristics of a sample, not appreciable by naked eye inspection [40]. In the case of varnished wooden artefacts, PLM can be used for obtaining information on the chemical nature of the varnish, its thickness, the number of layers applied, the possible presence of pigments, and so on.

Portions of the samples were embedded in polyester resin (Tiranti clear casting resin. Alec Tiranti Ltd. Thatcham, UK) and wet polished with SiC papers up to 4000 mesh/in and, subsequently, with a water suspension of micrometer sized Al_2O_3.

The cross-sections were analysed under a Leica Laborlux M12 microscope equipped with a mercury burner and a filter for selecting far blue (435 nm) and near UV (365 nm) radiation (Leica Microsystems GmbH, Wetzlar, Germany). Analyses were carried out in reflection. The equipment is shown in figure 2.9.

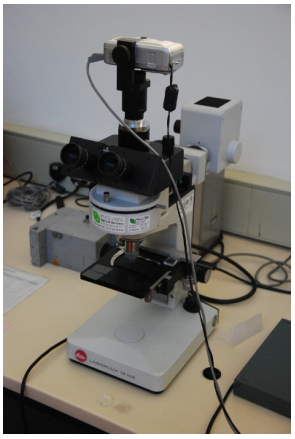

Figure 2.9: The Leica Laborlux M12 microscope employed for the analysis of the cross-sections. Photograph by the author.

2.2.3 μ-Fourier Transform Infrared spectroscopy

Infrared radiation comprises the radiation that can be detected from heat sources. In this spectral region, a vibrorotational energy is at stake and a molecule is able to absorb an infrared photon only when its vibration can vary the dipolar electric moment [41].

The great value of infrared spectra is to give

information on functional grous present when determining the structure of a new or unidentified compound. The absorption band of particular groups are well established and tables of these are to be found in the specialized literature of the subject [42]. The attribution of every band of a spectrum to a functional group cannot always be carried out because of the spreading and overlapping of bands.

The wavelength range is between 2.5 and 50 μm (in wavenumbers, between 4000 and 200 cm^{-1}).

A typical Fourier Transform equipment for infrared spectroscopy (FTIR, non-dispersive instrument) is set up as follows: a source, a collimator, a beam splitter, a moving mirror, a fixed mirror, a sample holder, a detector and an analysing system (electronics). More information about the technique can be found elsewhere [42, 43].

μ-FTIR is an established method for rapidly characterizing and differentiating reference materials and objects of interest in the field of cultural heritage. Furthermore, the coupling of the spectrometer with a microscope makes FTIR a unique tool allowing the analysis, mapping and imaging of tiny samples from works of art [40, 44, 45, 46].

A set of organic reference materials — selected among the ones listed in the review by Echard and Lavédrine [17] — was analysed by FTIR, GC-MS and Py-GC-MS.

They were:

- five diterpenic resins: Venice turpentine, colophony, Strasbourg turpentine, sandarac, copal;
- three triterpenic resins: mastic, elemi, dammar;
- two insect and fossil resins: shellac and Baltic amber;
- Dragon's Blood and beeswax.

The recorded spectra of these materials are reported in appendix B.

Micro-samples were compressed in a diamond cell and analysed in transmission mode using a Bruker Vertex 70 Fourier transform infrared spectrometer coupled with a Bruker Hyperion 3000 microscope (Bruker Optik GmbH, Ettlingen, Germany) equipped with a dedicated liquid nitrogen cooled narrow-band mercury cadmium telluride detector. Spectra were acquired within the range 4000 – 600 cm^{-1} by accumulating 64 scans at a spectral resolution of 4 cm^{-1}.

When analysing micro-samples with remaining wood, only regions with varnish were chosen for the analysis.

Every spectrum was subtracted of the background and corrected for the baseline.

2.2.4 Gas Chromatography coupled with Mass Spectrometry

Gas chromatography (GC) is a technique described, for the first time, by Martin and James in 1952 [47]. It is based upon the partition of the analytes between two phases: an inert, not very viscous, highly pure carrier gas as mobile phase and a liquid or solid stationary phase. Since the 1980s and with the introduction of fused silica capillary columns (which guarantee higher resolution than the packed ones [48]), the interest conveyed on GC has considerably grown [49].

The introduction of low cost and little cumbersome mass spectrometers (MS) justifies its use as universal and non specific detectors for GC. In a MS, the identification of an analyte is achieved by the ionization of a molecule, its fragmentation into smaller ions and their separation on the basis of the mass/charge ratio by an analyser. This may be a quadrupole, an ion trap or a magnetic sector.

By the coupling of the mentioned techniques, it is possible to draw qualitative and quantitative information about the composition of micro quantities of complex organic solutions.

A typical equipment for modern GC-MS roughly consists of a cylinder containing the carrier gas, an injector, a capillary column in a furnace, a flowmeter, an interface (by which most of the carrier gas is depleted), a mass spectrometer and the electronics. More detailed information about the technique and its theory can be found elsewhere [50, 51].

Although requiring the destruction of micro-samples and, sometimes, a rather long analytical procedure in some cases, GC-MS is considered as the main and the best tool for the analysis of varnishes (eg the works by Colombini *et al.* [52, 53] or [54]) because it allows the separation and identification of analytes in complex organic matrices with a high degree of sensitivity and specificity.

Derivatization (a preliminary chemical treatment) make compounds more volatile or less polar and consequently suitable for GC analysis [50]. The used derivatizion process is here reported.

Solid samples were put into plastic vials with glass insert and treated with 40 μL (30 μL for the samples from musical instruments) of a 33% (v/v) Meth-Prep II solution (Grace, Deerfield, IL, USA) in NORMAPUR grade toluene (VWR International, Fontenay sous Bois, France). Meth-Prep II is a 0.2 N methanolic solution of (*m*-trifluomethylphenyl) trimethylammonium hydroxide. This reagent allows the low temperature (220-300 °C) online derivatization (methylation) of fatty acids and resin compounds avoiding the extraction step [55]. The vial was shaken with a vortex mixer, put into the oven at 65 °C for one hour and shaken again with a vortex mixer. The sample was then centrifuged with a Sorvall Super T21 super speed refrigerated centrifuge by DuPont (Mechelen, Belgium) at 3000 rpm at 21

°C for 3 min and the supernatant was taken for the GC-MS analysis.

Analyses were carried out with a Thermo Finnigan GC Trace coupled with a Thermo Finnigan Polaris Q ion trap mass spectrometer (Thermo Fisher Scientific Inc., Waltham, MA, USA).

The temperatures of the injector and of the interface were 230 and 290 °C, respectively. GC separation was achieved on a Restek Rtx-5MS fused silica capillary column with integrated guard column (30 + 5 m × 0.25 mm id, 0.25 μm film thickness, Restek Corporation, Bellefonte, PA, USA). The following temperature program was set up: isothermal conditions at 65 °C for 1 min, up to the temperature of 100 °C with a rate increase of 30.0 °C/min, up to the final temperature of 290 °C with a rate increase of 4.0 °C/min and isothermal conditions at 290 °C for 32 min. Ultrapure grade helium (purchased from Praxair, Inc., Danbury, CT, USA) was the carrier gas and its flow rate was 1.3 mL/min. The injection volume was 1.0 μL and the injection mode was splitless (splitless time = 0.70 min).

Mass spectrometer conditions were as follows: 50–600, m/z range of analysis; 0.55 s, scan event time; 7.00 min, solvent cut; 3, number of microscans; 25 ms, max ion time. The ion source was at 220 °C and positive ions were analysed. Analysis was conducted in full scan mode.

The same set of reference materials studied by FTIR was analysed by GC-MS.

2.2.5 Pyrolysis Gas Chromatography coupled with Mass Spectrometry

Pyrolysis is the technique that exploits thermal energy to decompose large molecules into smaller volatile products. Much of the degradation is caused by free radical reactions initiated by bond breaking. The way a molecule decomposes (in a characteristic way) is reproducible, thus making pyrolysis an analytical instrument.

When coupled to a GC-MS, the pyrolyzer decomposes — in micro scale, in the gas stream at the start of the column — a material yielding characteristic low molecular weight products. The resulting volatile products are separated in the usual way. Thus, Py-GC-MS allows the sensitive determination of the components of complex materials for which simple derivatization is not effective such as tire rubber [56], dried paint [57], glue [58], paper additives [59], petrochemical sources [60, 61], plant materials [62], bacteria [63, 64], and the whole range of synthetic polymers [65, 66].

The most commonly used devices for pyrolysis are the microfurnace, the resistively heated filament and the Curie point pyrolyzer [48, 67]:

1. *Microfurnaces* are devices that ensure a constantly heated, isothermal pyrolytic environment to the liquid or solid sample;

2. in the *resistively heated filament*, the sample is attached to a metal (often platinum) circuit that is heated to a programmed temperature with a controllable rate by a flowing current;

3. the *Curie point pyrolyzer* is a ferromagnetic alloy that is rapidly heated by induction of a high frequency coil until its Curie temperature[1]. The cross-section diagram of a Curie point pyrolyzer is shown in figure 2.11. On the basis of the composition of the alloy, the Curie temperature changes.

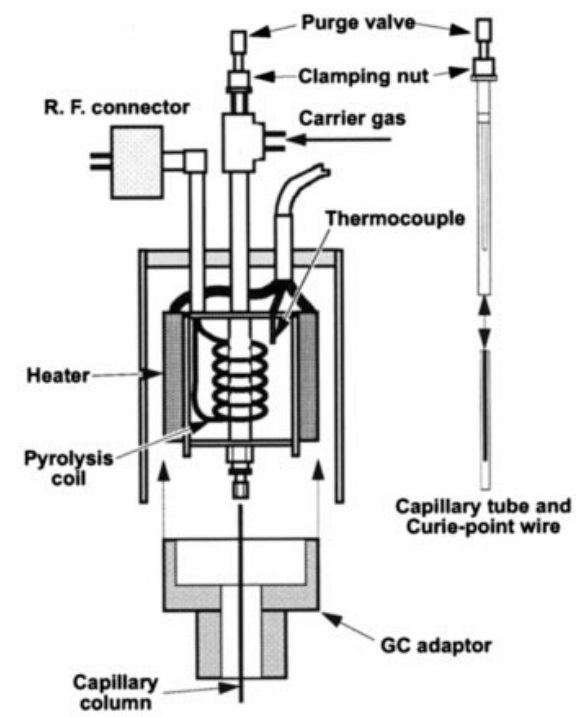

Figure 2.11: Diagram of a cross-section of a Curie point device for pyrolysis and its interface to a GC capillary system (adapted from reference [68]).

The last two devices are nowadays the most used and it has been demonstrated that the results derived from their use are comparable [68].

With the aim of having greater structural information, increased sensitivity and better chromatographic behavior of polymeric or complex structures, thermochemolysis (aka thermally assisted hydrolysis and methylation) can be used. First introduced by Challinor in 1989 with the name of pyrolysis-derivatisation-gas chromatography [69], thermochemolysis is a form of analytical pyrolysis in which the heat of the pyrolyser is used to drive a reaction between the acidic groups of the analyte and an alkylating agent producing

[1]The temperature at which the ferromagnetic material loses its magnetism.

alkyl esters and ethers [69, 70, 71]. One of the most widely used alkylating agent is tetramethylammonium hydroxide (TMAH) [72]. The reaction that produces with carboxylic acids is the following:

$$RCOOH + (CH_3)_4^+NOH^- \xrightarrow{\Delta} RCOOCH_3 + (CH_3)_3N + H_2O$$

Figure 2.10: The Thermo Finnigan GC Trace coupled with the Polaris Q ion trap mass spectrometer in pyrolysis configuration employed for the analysis. The red high frequency coil is well visible. Photograph by the author.

Py-GC-MS (with and without thermochemolysis) has successfully been applied to the characterization of natural complex materials such as paint binding media and varnishes [44, 73, 74]. A Round Robin sample comprising of several materials (dried linseed oil, Paraloid B82 resin, sandarac, succinic acid, mastic, gum arabic, egg white) present in works of art has recently been studied by van Keulen [75].

One of the main issue of Py-GC is the handling of micro-samples. The following proposed solution can ease the manipulation.

The samples, managed under a stereomicroscope with a microscalpel (to possibly remove excess of sample) and a metallic micro-tip, were placed onto a microscopy slide. The samples should be placed in the *eye* of the Ni-Fe wire (Curie point temperature = 625 °C), purchased from GSG Mess- und Analysigeräte, Bruchsal, Germany.

They were treated with about 1.0 μL of a 25% (w/w) TMAH (purchased from Sigma-Aldrich Corporation, St. Louis, MO, USA) aqueous solution and put into the oven at 65 °C for one hour for evaporating the solvent and sticking the samples to the wire as can be seen in figure 2.12. The wire was then inserted in the glass tube and ready for the Cp-Py-GC-MS injection.

Pyrograms were obtained by interfacing the pyrolyser (a Pyromat unit by GSG) to the instrument used for GC-MS analysis. The temperature of the pyrolyser interface was 250 °C and the pyrolysis was carried out for 10 s.

The temperatures of the injector and of the GC-MS interface were 250 and 290 °C, respectively. GC separation was achieved on a Restek Rtx-5MS fused silica capillary column with integrated guard column. The following temperature program was set up: isothermal conditions at 50 °C for 5 min, up to the temperature of 175 °C with a rate increase of 8.0 °C/min, up

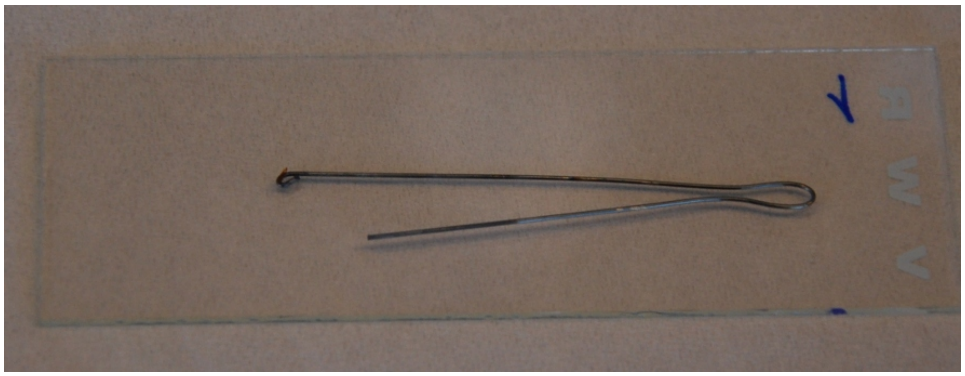

Figure 2.12: A micro-sample of varnish stuck on a Ni-Fe wire for pyrolysis after the experimental treatment and ready for the injection. Photograph by the author.

to the final temperature of 290 °C with a rate increase of 2.0 °C/min and isothermal conditions at 290 °C for 15 min. Ultrapure grade helium was the carrier gas and its flow rate was 1.3 mL/min. The injection mode was split (split ratio = 8; split flow = 10 mL/min).

Mass spectrometer conditions were as follows: 50–500, m/z range of analysis; 0.49 s, scan event time; 3, number of microscans; 25 ms, max ion time. The ion source was at 220 °C and positive ions were analysed. Analysis was conducted in full scan mode.

The same set of reference materials studied by FTIR and GC-MS was analysed by Py-GC-MS.

Chapter 3

Results and discussion

This chapter presents the results of the *in situ* and laboratory experiments carried out on the instruments from the "Musical Instruments Museum" in Brussels and the "Vincenzo Bellini" Conservatory in Palermo. A comparison with existing literature about previously analysed instruments is also presented.

3.1 Non destructive techniques

Bringing technical equipments from the laboratory to the artwork has particular advantages. Any risk (and costs, if insurances are considered) related to the transportation of precious and fragile objects into a laboratory is avoided. Furthermore, results are obtained practically in real time, thus creating higher interaction between scientists and conservators [76].

3.1.1 m-X-Ray Fluorescence

This part of the research was carried out at the "Vincenzo Bellini" Conservatory in Palermo to obtain preliminary information about the inorganic additives present in the varnish of historical musical instruments. Measurements were carried out onto two instruments: the *viola d'amore* 1993 and the cello 2173.

Viola d'amore 1993

This is a 20^{th} century Sicilian violin by Antonio Sgarbi. The printed label inside reports: "Cav. Antonio Sgarbi Palermo 1914". The date is handwritten. A picture under white light is shown in figure 3.1.

Measures were carried out onto five spots. A typical spectrum recorded on the surface of the top of the *viola d'amore* 1993 is reported in figure 3.2.

XRF spectra reflect the use of a poorly pigmented and naturally golden coloured varnish. Iron peaks caused by the probable presence of red-brown

Figure 3.1: The *viola d'amore* 1993 by A. Sgarbi photographed under white light. Picture used by permission of the "Vincenzo Bellini" Conservatory, Palermo.

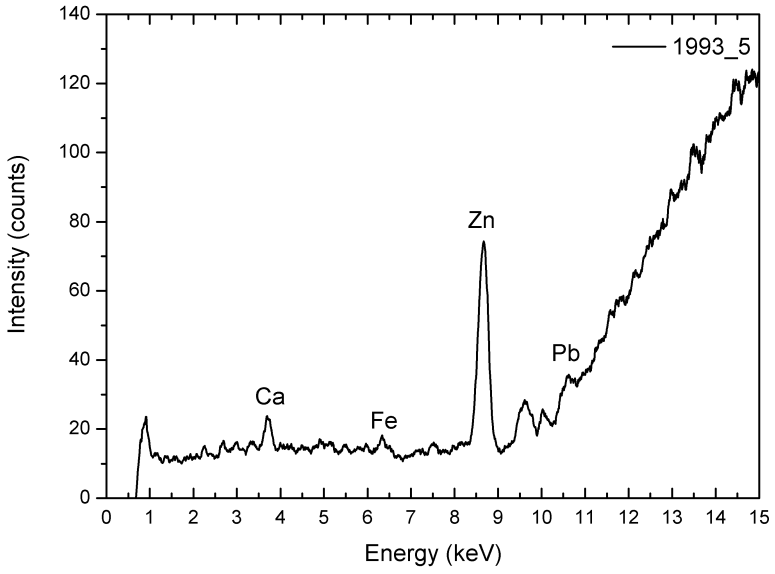

Figure 3.2: Smoothed XRF spectrum of the fifth sampled spot on the surface of the *viola d'amore* 1993. The drift is attributable to the target of the instrument. An average on 15 points was run to smooth the original spectrum for graphical reasons.

earth, such as Fe_2O_3 are faint but visible. Peaks centred at 10.55 keV can be attributed to the presence of lead. Lead-based compound (such as massicot or litharge, PbO, lead white, $2PbCO_3 \cdot Pb(OH)_2$, and red lead, $2PbO \cdot PbO_2$) were often added as pigments to accelerate and uniform the desiccation of an oil-based varnish [22, 23, 24, 77, 78]. The presence of lead can be, thus, regarded as an indicator (though not the only one [17]) for the use of an oil-based varnish [23, 77].

The presence of zinc is attributed to either the secretion of human sweat [22, 79] or some residual polish impurities [25].

Cello 2173

This is a 17^{th} century Neapolitan cello by Carlo D'Avenia. The printed label inside reports: "Carlo d'Avenia in Napoli 1716". The instrument was refurbished by Antonio Sgarbi in 1896. A picture under white light is shown in figure 3.3.

Figure 3.3: The cello 2173 by C. D'Avenia photographed under white light. Picture used by permission of the "Vincenzo Bellini" Conservatory, Palermo.

Measures were carried out onto six spots. A typical spectrum recorded on the surface of the top of the cello 2173 is reported in figure 3.4.

The signals in the XRF spectra recorded on the cello 2173 are significantly more intense than the ones recorded on the *viola d'amore* 1993. The darker colour of the surface of the cello also reflects the higher presence of inorganic elements.

The floral decoration present on the surface of the back of the cello was also analysed. It is shown in figure 3.5.

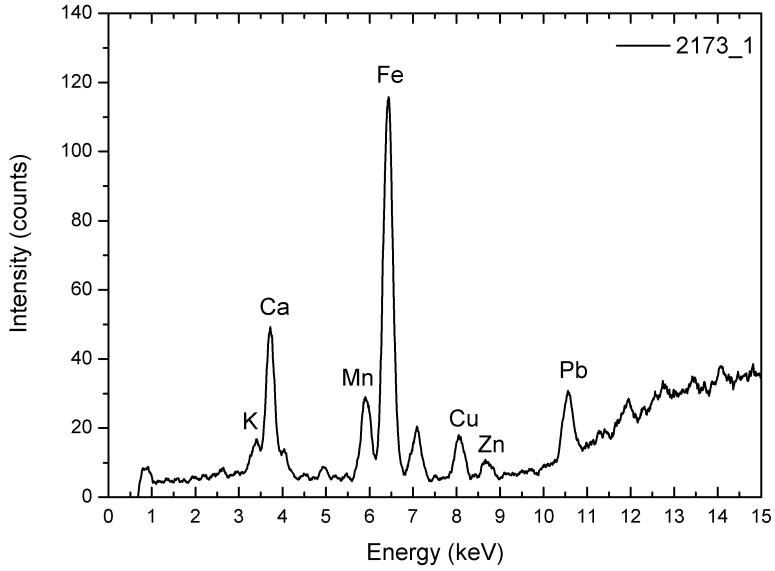

Figure 3.4: Smoothed XRF spectrum of the fifth sampled spot on the surface of the cello 2173. The drift is attributable to the target of the instrument. An average on 15 points was run to smooth the original spectrum for graphical reasons.

Figure 3.5: The floral decoration present on the back of the cello 2173 by C. D'Avenia photographed under white light. Picture used by permission of the "Vincenzo Bellini" Conservatory, Palermo.

The spectra relative to the different colours of the decoration are shown in figure 3.6.

All the spectra show the extensive presence of lead. This element, as lead white, has been extensively used since the antiquity as a cosmetic and white paint because of its excellent light fastness and rapid drying capabilities when used in combination with a siccative oil. For toxicity reasons, it was partly replaced by zinc and, subsequently, titanium white by the 19^{th} century [80, 81].

The red pigment is mainly constituted by mercury (probably as vermilion from cinnabar, HgS). Known since the antiquity[1], vermilion has excellent body and hiding power. It is quite stable although darkens when exposed to direct sunlight, especially in wet environment [83]. The preparation of the synthetic one has been known since the 12^{th} century. Cennino Cennini also described its preparation in his famous "Il Libro dell'Arte" [84].

The black one is mainly constituted by lead. It is possible that the used pigment was carbon black (carbon, not detectable) which can be used in a mixture with lead white (eg [85]). Furthermore, lead pigments may turn to black because of the reaction with the atmospheric hydrogen sulphide giving the black lead sulphide, PbS [77, 86].

[1] In 315 BC, Theophrastus reports the vicinity of Ephesus, Turkey, as one of the extraction centres of the time [82].

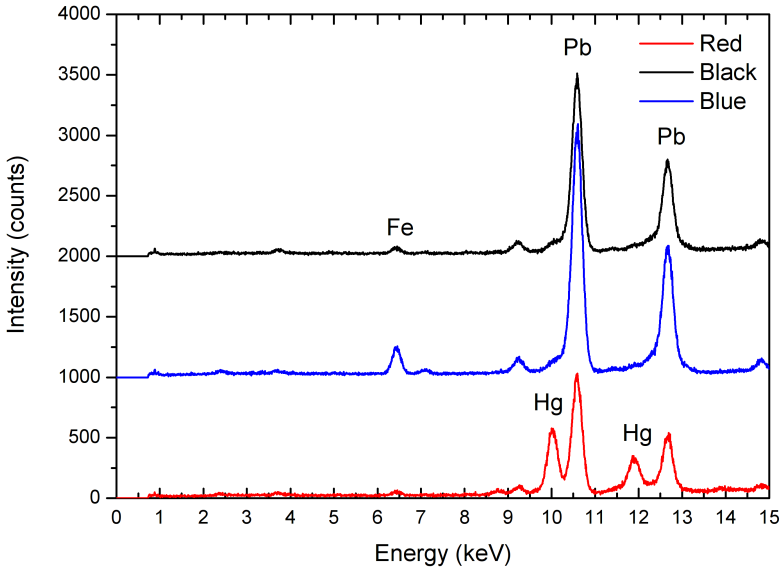

Figure 3.6: XRF spectra of the different colours of the floral decoration present on the back of the cello 2173 by C. D'Avenia. The spectra of the blue and black colours are shifted by 1000 and 2000 counts, respectively, for clarity.

The most known blue pigment in literature containing iron is Prussian Blue, $Fe_4[Fe(CN)_6]_3$. Prussian blue is an artificial pigment, known since the beginning of the 18^{th} century, it is very finely divided and with low hiding power. It is resistant to dilute acids but attacked by bases [77, 83]. For such a reason, it is not suitable for use on frescoes.

3.1.2 μ-X-Ray Fluorescence and photography in visible and UV light

Once the feasibility of the technique was established and preliminary information obtained about the instruments of the "Vincenzo Bellini" Conservatory in Palermo, a much more systematic study was carried out with a higher performance instrument at the "Musical Instruments Museum" in Brussels.

In this section, the main results on these instruments are presented and discussed. Extended results (including the maps of the sampled areas, pictures in visible and UV light) are reported in appendix A.

The analysed areas were selected to have good statistical information and on the basis of the presence of interesting points (evidenced during the prior observation under visible and UV light).

Potassium and calcium were detected in every analysed area of every instruments. These elements, along with sulphur and chlorine (also often found), can be attributed to the secretion of human sweat [22] or to the inorganic portion of the wood below the varnish. In fact, potassium and calcium are the most abundant inorganic elements for spruce, beech and bark [87, 88].

The occurrence of the other detected elements on the surface of the analysed musical instruments is shown in table 3.1.

Table 3.1: Occurrence of the detected elements on the surface of the analysed musical instruments of the "Musical Instruments Museum" in Brussels (Belgium). The number indicates the percentage of the sampled spots in which an element was found.

Element	1338	1372	1374	2764	2774	2781	2782	2784	2836
Fe	100	100	100	100	100	100	100	100	100
Mn	87	91	33	100	94	94	100	84	71
Ti	3	9	57	14	24	22	32	24	48
Pb	9	9	82	29	41	17	36	32	38
Zn	19	9	49	86	35	39	68	20	57
Cu	0	0	4	0	12	0	9	8	19
Sr	0	0	2	0	0	11	5	0	5

Iron, manganese, titanium, lead and zinc were found on the surface of every musical instrument. Copper and strontium were found on the surface of five and four instruments, respectively.

Iron combined with manganese is an indication for earth pigments like siennas and umbers giving a range of yellow-red-brown tints [77, 38, 89].

The presence of titanium can be attributed to impurities of the iron-based pigments [38].

Lead was found in three spots of the surface of the instrument. As above mentioned, such an element, coming from siccatives, may be regarded as an indicator for the use of an oil-based varnish. Furthermore, the values of the areas of the lead peaks are correlated with the areas of iron ones (ρ_{FePb}, the Pearson index of correlation[2], is more than 0.5 for every instrument and up to 0.95 in the case of instrument 2781) meaning that lead was likely added to the original recipe.

Zinc — again attributable to the secretion of human sweat [22] or to some residual polish impurities — was found in six spots. The L lines of the tungsten target partly superimpose to the zinc signals [38].

Chromium was found in the 98% of the analysed spots on the varnish of the cello 1374. To the best of our knowledge, this is the first time that a chromium pigment is found in the varnish of an historical musical instrument.

A typical spectrum recorded on the surface of the cello 1374 is reported in figure 3.7.

The occurrence of chromium on the whole surface of the instrument, its relative high content (mean value of the chromium peak area = 1317 keV $\cdot$ counts) and a very low correlation ($\mathrm{R}^2 = 0.06$, $\rho_{\mathrm{FeCr}} = 0.25$) between the values of the areas of the chromium peaks and the iron ones exclude the possibility that such an element is an impurity of iron-based pigments [38]. Analogue considerations can be drawn out about the low correlation between the values of the areas of the chromium peaks and the lead ones ($\mathrm{R}^2 = 0.17$, $\rho_{\mathrm{PbCr}} = 0.42$), thus excluding the possibility of the use of Chrome red (basic lead chromate).

Two reasonable hypotheses would explain the presence of a chromium-based pigment in cello 1374:

1. G. Borbon used an uncommon pigment for colouring the varnish;

2. the instrument was re-varnished, at the earliest in the beginning of the 19^{th} century.

[2]Pearson correlation coefficient is a rescaled covariance:

$$r_{XY} = \frac{s_{XY}}{s_X s_Y}$$

where s_{XY} is the sample covariance and s_X and s_Y are sample standard deviations[90]

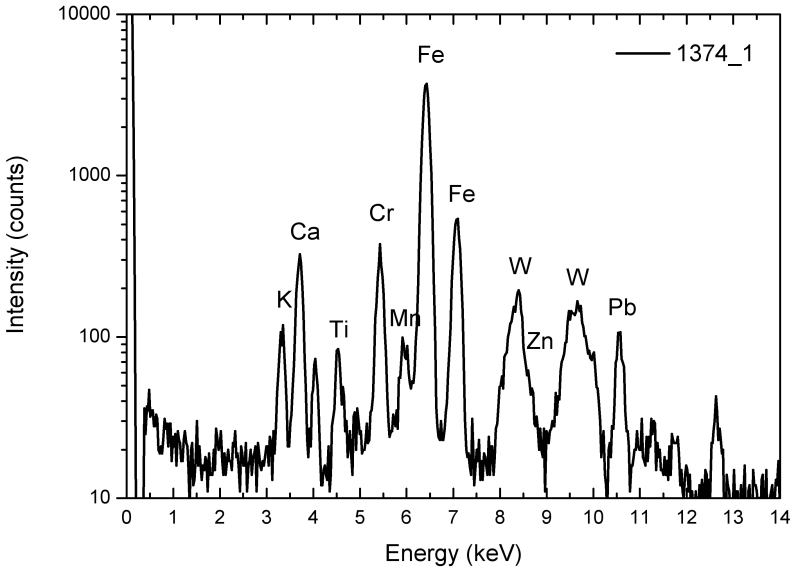

Figure 3.7: XRF spectrum of the first sampled spot on the surface of the cello 1374 attributed to G. Borbon. Tungsten peaks are attributable to the target of the instrument. A logarithmic scale is used on the axis of intensity for clarity.

To further support the above-mentioned hypotheses and to explore pattern recognition, principal component analysis (PCA) was carried out on XRF data.

PCA is a mathematical procedure that transforms the possibly correlated variables of a set of multivariate data into uncorrelated variables (the so-called principal components) by applying a geometrical transformation.

Such multivariate technique allows the exploration of possible patterns in the data, discriminating the useful information from noise or meaningless variations herein contained [91].

PCA was carried out using a specifically designed R [92] program. The source code with every line commented is here reported[3].

```
x=as.matrix(read.table("datafile.txt",header=TRUE)) #the
#program reads the data in the file. The option
#header=TRUE makes the program reads the first row of
#every column as row. The command as.matrix transforms
#a data frame into a numerical matrix
y=t(x) #the x matrix is transposed
z=cov(y,y) #the z covariance matrix is calculated
a=eigen(z) #the a matrix of the eigenvalues of the
#covariance matrix is calculated
b=cbind(a$vectors[,1:2]) #the b matrix of the first
#two principal components is created
d=t(b) #the b matrix is transposed
e=d%*%x #the d matrix is multiplied by the x matrix
plot(e[1,],e[2,],xlab="PC1",ylab="PC2") #the two
#principal components are plotted in a x,y graph
f=read.table("labels.txt") #the file of the labels is
#uploaded
text(e[1,],e[2,],labels=f[,1],cex=.5,pos=1,offset=.5)
#the labels are added to the data points in the plot
```

The matrix dataset is composed of the average areas (factors) of the peaks of six elements (iron, manganese, titanium, lead, zinc, chromium) found in every instrument. The data relative to spots in which the varnish is particularly thick were excluded (eg figure 3.8) in the matrix dataset because statistically meaningless. The plot of scores of the first two components is reported in figure 3.9.

The first component (PC1) mainly contains the variance of the iron signal whereas lead and chromium accounts for less weight. The second component (PC2) mainly contains the variance due to the lead signal.

[3]The statistical treatment should be carried out after the normalization of the data and the subtraction of the mean from every single observation.

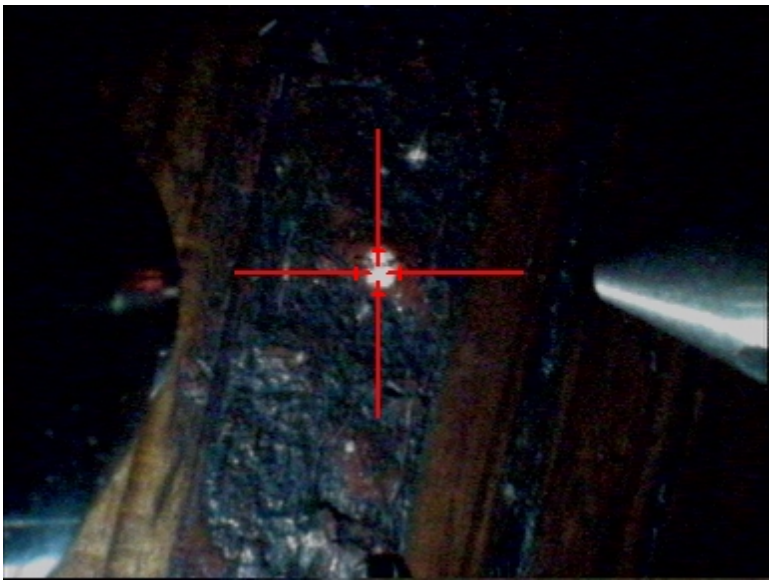

Figure 3.8: One of the sampled spots on the surface of the violin 2836 in which the varnish is particularly thick.

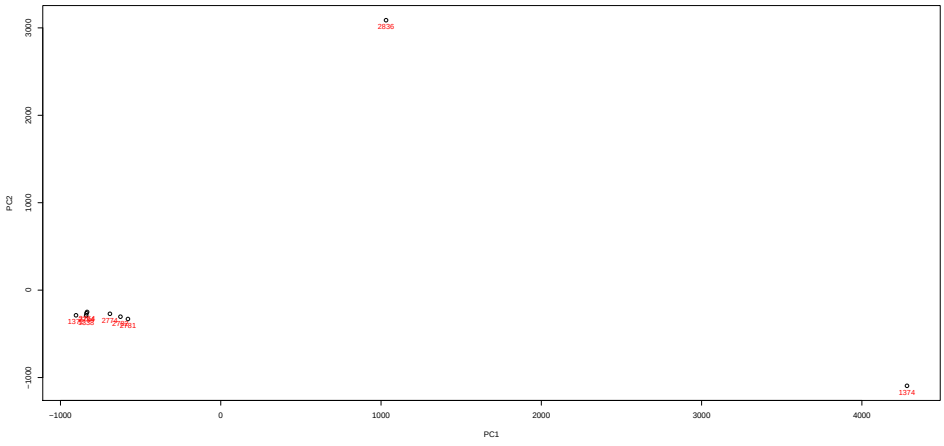

Figure 3.9: Plot of scores of the first two principal components of the XRF data recorded on the surface of the nine instruments from the "Musical Instruments Museum", Brussels.

In the plot, a main cluster is visible and two outliers. Instruments 1338, 1372, 2764, 2774, 2781, 2782, 2784 are included in the main cluster. Cello 1374 is out of the main cluster because of the above-mentioned presence of chromium, absent in the other instruments, and the high counts for iron whereas violin 2836 shows high mean peaks area values for lead and iron. This manipulation of the data confirms the above mentioned peculiarity of such musical instruments.

A particularly interesting spot on the surface of the violin 2781 by B.-J. Boussu is on the bottom right part of the top. The surface of the instrument is slightly carved in such a region. This is well-evidenced when illuminated under UV light in 3.10.

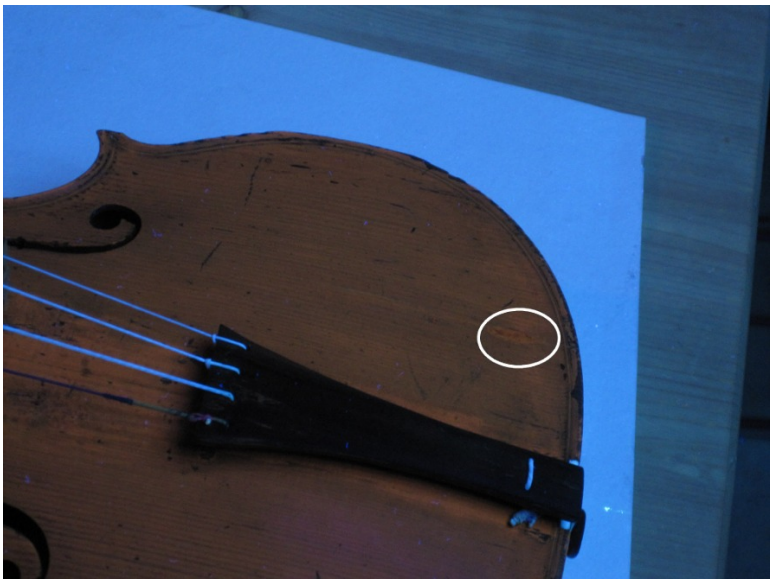

Figure 3.10: Bottom right part of the top of the violin 2781 by B.-J. Boussu illuminated by UV light. The white circle indicates a region with a probable retouch of the varnish. Picture used by permission of the "Musical Instruments Museum", Brussels.

The spectrum of such a region is reported in figure 3.11.

The simultaneous presence of barium and cadmium is likely referable to the use of a cadmium yellow lithopone. It is an artificial mixture of cadmium sulphide (CdS) and barium sulphate ($BaSO_4$) (from cadmium sulphate, $CdSO_4$, and barium sulphide, BaS) with heat and light resistance properties [83]. It was introduced in 1927 [77, 89]. As a consequence, this region could have been retouched with such a pigment after its acquisition by the "Musical Instruments Museum".

Mercury-based (such as mercury sulphide, ie cinnabar or vermilion [22]) and tin-based pigments (such as lead-tin yellow) were not found. A weak

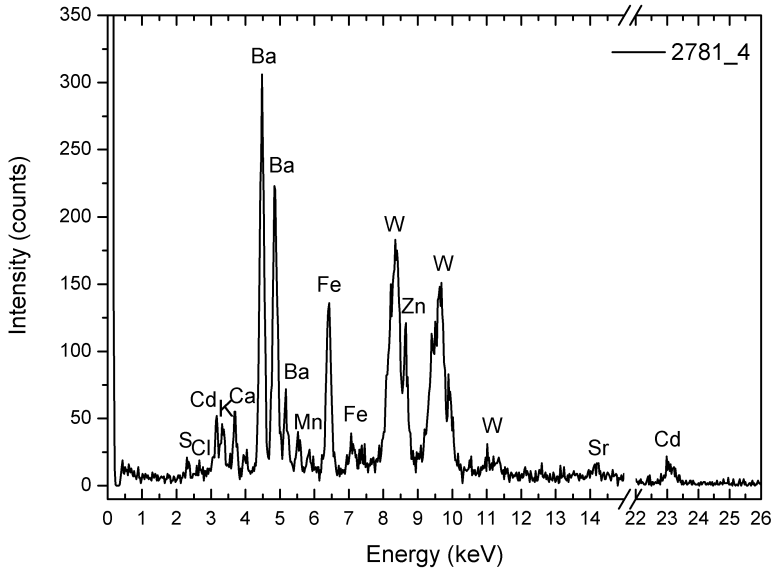

Figure 3.11: XRF spectrum of the fourth sampled spot on the surface of the violin 2781. Tungsten peaks are attributable to the target of the instrument.

signal attributable to arsenic was detected only in one spot of the cello 1374.

The results here shown differ somewhat from the ones reported in other publications (mainly on North-Italian instruments) because of the absence of arsenic- and mercury-based pigments [17, 22, 28]. Conversely, a study on five Stradivari's instruments reports the presence of a pure ochre (in place of an earth) pigment in three of them [28], resembling the results here reported. The possibility of micro-sampling such instruments and carrying out an elemental analysis could be very useful to assess the presence of other light element-based material (such as potash alum [28] or borate [21]).

3.2 Micro-destructive techniques

Among the variety of modern instrumental techniques of analysis that are currently available, non destructive ones are preferred. But to answer questions about the structure of complex paint layers or the chemical nature of binding media in paints, sampling is unavoidable, a procedure that is always destructive.

3.2.1 Polarised Light Microscopy

***Viola d'amore* 1993**

Two micrographs at two different magnifications (100× and 250×) were taken on the cross section of the sample 1993_1. They are shown in figure 3.12.

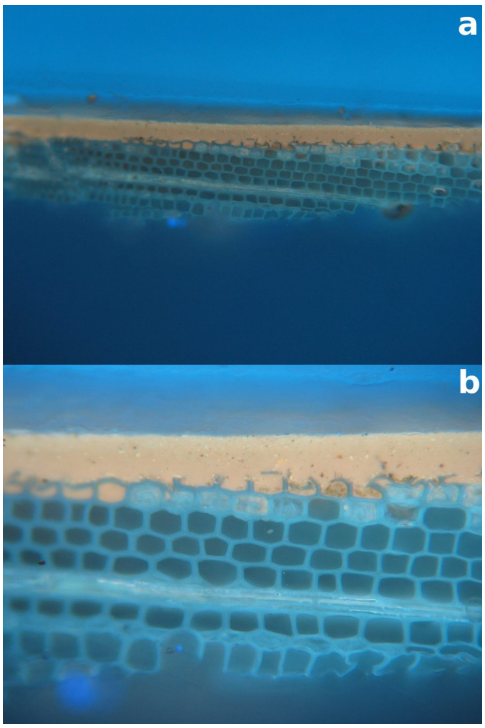

Figure 3.12: Cross section of a portion of the first sample from the *Viola d'amore* 1993 taken at two different magnifications under far blue light: 100× (a) and 250× (b).

It is noticeable the presence of a single layer of pigmented varnish that penetrates the first two layers of cells in the wood. An orange fluorescence is observed. This is usually referable to shellac resin [93].

Shellac is the only animal resin that has been used for painting purposes.

Despite being known since ancient times in the Far East (India, China and Japan), it became popular in Europe only in 17^{th} century. It is excreted by some female insects from the superfamily *Coccoidea*. The drops of shellac are scratched from the trees, thoroughly washed and purified by sieving the melt. The shellac is bleached with hypochlorite and the shellac wax is separated by saponification. The dried shellac sheets are dissolved in alcohol, thereby generating a spirit varnish. Sometimes it is mixed with other components of varnishes, such as copal or mastic [77, 94].

A few very small particles in the layer appear to be red and are likely to be made of organic dyes, possibly anthraquinone-based [28]. Anthraquinoid dyes provide the most important red dyes and lakes used in artistic paintings. Although their organic nature, they are quite resistant to chemical and physical (but not to direct light!) agents [77, 95].

Other particles exhibit the yellow-green fluorescence typical of zinc white [40]. Zinc oxide (ZnO), occurs naturally as the mineral zincite and was introduced as a white pigment (zinc or Chinese white) at the end of the 18^{th} century. Finely divided and giving a pure cold white, zinc white is a non-poisonous pigment but has poor drying qualities in linseed oil [83, 96].

Viola 1996

A picture under white light of the viola 1996 is shown in figure 3.13.

Figure 3.13: The German viola 1996 photographed under white light. Picture used by permission of the "Vincenzo Bellini" Conservatory, Palermo.

Two micrographs at two different magnifications (100× and 250×) were taken on the cross section of the sample 1996_3. They are shown in figure 3.14.

In the cross section of sample 1996_3, two superimposed thin layers of pigmented varnishes are observed, the upper one being faintly pink. The first three-four layers of wood cells are highly degraded. Such damage was possibly caused by a mechanical, chemical or thermal treatment carried out during either the original finishing or a subsequent application of varnish.

Two micrographs at two different magnifications (100× and 250×) were

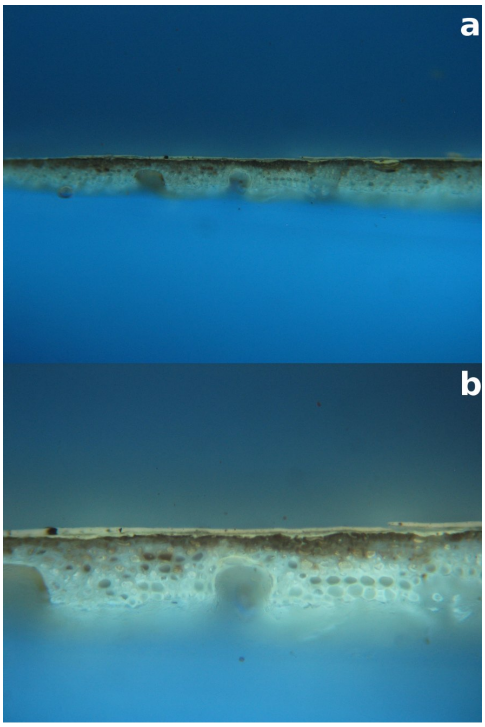

Figure 3.14: Cross section of a portion of the third sample from the viola 1996 taken at two different magnifications under far blue light: 100× (a) and 250× (b).

taken on the cross section of the sample 1996_4. They are shown in figure 3.15.

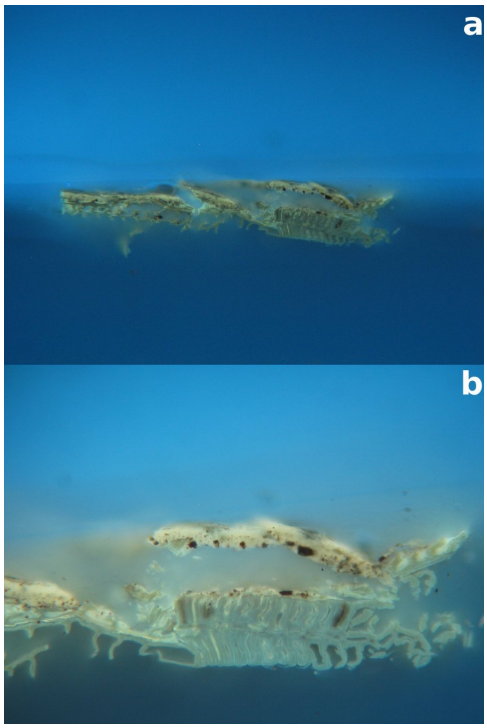

Figure 3.15: Cross section of a portion of the fourth sample from the viola 1996 taken at two different magnifications under far blue light: 100× (a) and 250× (b).

In this case, the pigmented varnish is detached and no clear information about the number of layers is inferable.

Violin 2002

A picture under white light of the violin 2002 is shown in figure 3.16.

Figure 3.16: The violin 2002 by unknown photographed under white light. Picture used by permission of the "Vincenzo Bellini" Conservatory, Palermo.

One micrograph of the cross section of the sample 2002_3 was taken at 250×. It is shown in figure 3.17.

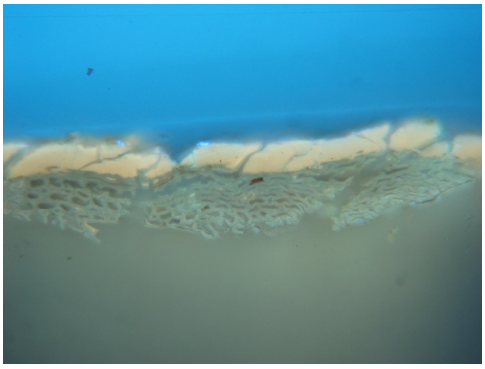

Figure 3.17: Cross section of a portion of the third sample from violin 2002 taken at 250× under far blue light.

One micrograph of a portion of the fourth sample from the violin 2002 was taken at 250×. It is shown in figure 3.18.

One micrograph of the cross section of a portion of the fifth sample from the violin 2002 was taken at 100×. It is shown in figure 3.19.

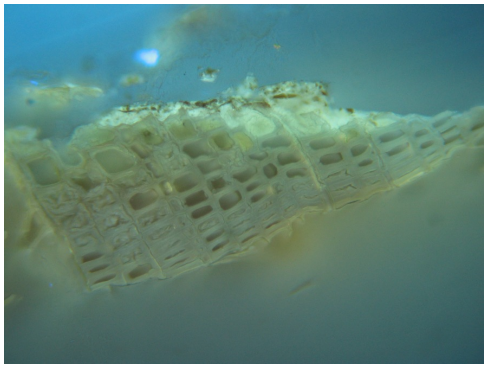

Figure 3.18: Cross section of a portion of the fourth sample from the violin 2002 taken at 250× under far blue light.

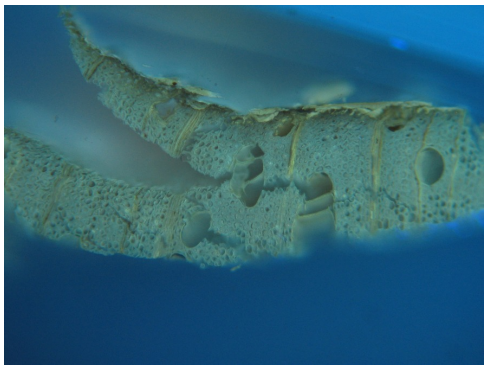

Figure 3.19: Cross section of a portion of the fifth sample from the violin 2002 taken at 100× under far blue light.

Violin 2021

A picture under white light of the violin 2021 is shown in figure 3.20.

Figure 3.20: The violin 2021 by N. Gagliano photographed under white light. Picture used by permission of the "Vincenzo Bellini" Conservatory, Palermo.

Four micrographs at two different magnifications (100× and 250×) and at two different wavelength (far blue and near UV) were taken on the cross section of a portion of the first sample from violin 2021. They are shown in figure 3.21.

The cross section of sample 2021_1 shows the presence of at least three layers, the first two ones being likely wax and dirt. The bottom one is a deep orange and penetrates the first two layers of cells in the wood.

Four micrographs at two different magnifications (100× and 250×) and at two different wavelength (far blue and near UV) were taken on the cross section of the sample 2021_4. They are shown in figure 3.22.

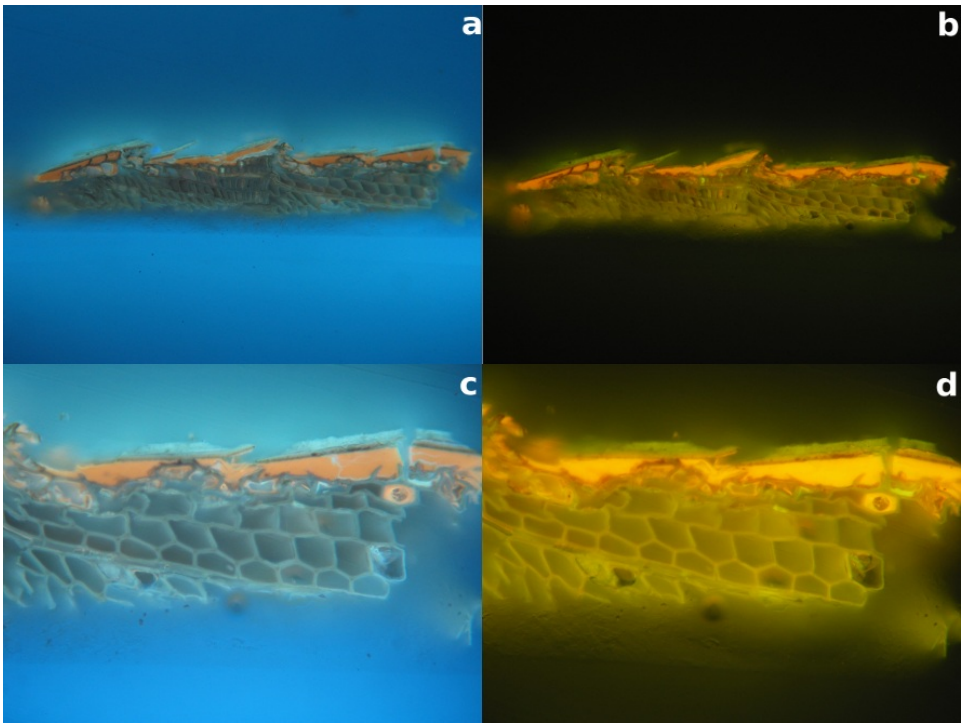

Figure 3.21: Cross section of a portion of the first sample from violin 2021 taken at 100× under far blue (a) and near UV (b) light and at 250× under far blue (c) and near UV (d) light.

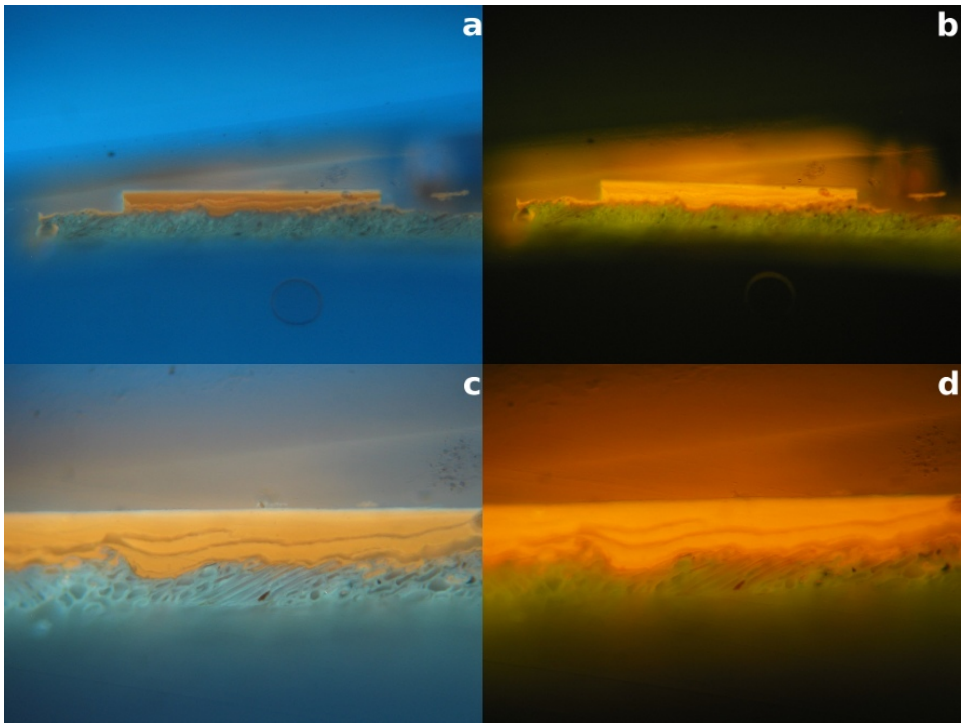

Figure 3.22: Cross section of a portion of the fourth sample from violin 2021 taken at 100× under far blue (a) and near UV (b) light and at 250× under far blue (c) and near UV (d) light.

Cello 2173

Two micrographs at two different magnifications (100× and 250×) and were taken on the cross section of a portion of the only sample from cello 2173. They are shown in figure 3.23.

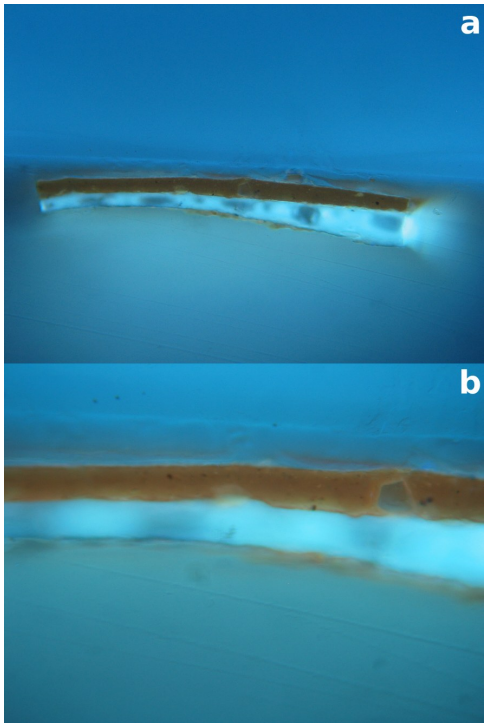

Figure 3.23: Cross section of a portion of the only sample from cello 2173 taken at two different magnifications under far blue light: 100× (a) and 250× (b).

The cross-section of sample 2173_1 did not show any wood substrate and the colour of the varnish is brown with black particles under far blue illumination, thus indicating the possible use of a siccative oil and carbon black and the absence of shellac (or its use to a minor extent).

3.2.2 μ-Fourier Transform Infrared spectroscopy

The FTIR spectra of the materials used as references are reported in appendix B.

μ-FTIR analysis was conducted on samples from all the considered musical instruments from the "Vincenzo Bellini" Conservatory. As an example of typical recorded spectra, figure 3.24 shows the μ-FTIR spectrum of a portion of the only sample from cello 2173:

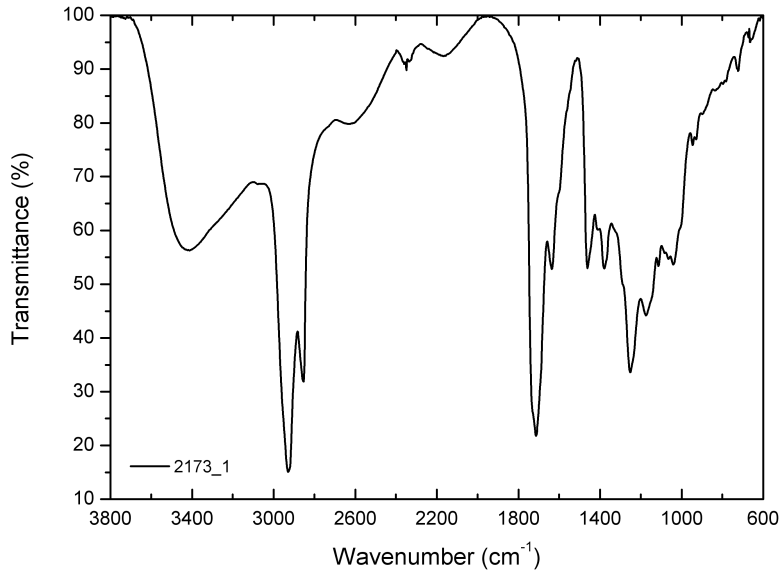

Figure 3.24: Normalized FTIR spectrum of a portion of the only sample from cello 2173.

Spectra of both reference and musical instrument samples can be roughly divided into four regions:

1. Broad bands due to OH stretches are around 3400 cm^{-1}. Such a contribution is enhanced for the samples from the musical instruments because of the presence of traces of wood;

2. bands from 2800 to 3200 cm^{-1} due to carbon aliphatic stretches;

3. peaks from 1500 to 1750 cm^{-1} due to the carbonyl group;

4. below 1500 cm^{-1} bands are referred to as fingerprints (C-H, C-O; C-C wagging and bending vibrations).

As a result, it is possible to distinguish different resins on the basis of the position of characteristic absorption bands [97]. The analysed reference materials and real samples were distinguished on the basis of two frequency ranges: 1690–1755 cm^{-1} (carbonyl bands) and 2915–2955 cm^{-1} (C-H aliphatic stretches). The histograms reported in figure 3.25 show the wavenumbers of maximum absorption in the selected regions for the different materials taken into account.

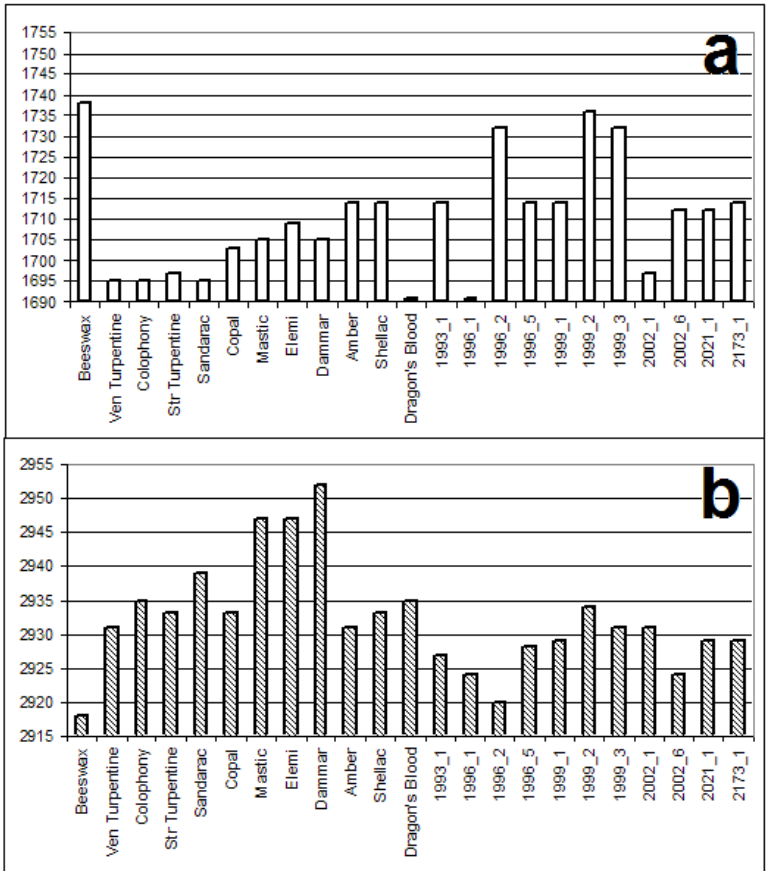

Figure 3.25: Histograms of the maximum absorption of the reference and analysed samples in two selected regions: 1690–1755 cm^{-1} (C=O) (a) and 2915–2960 cm^{-1} (C-H stretches) (b).

It is noticeable that diterpenic and triterpenic resins are easily distinguishable and that only shellac and amber frequencies are partially superimposed. The following evidence may be derived from the analysis of the samples from the musical instruments examined in this study:

1. The possible use of shellac — and/or Baltic amber, to a less likely extent — in the samples from instruments 1993, 1999, 2021 and 2173. To confirm further this assumption, it was found that many of the spectra

examined show patterns similar (not shown) to shellac in other two distinctive frequency ranges: 1730–1738 cm^{-1} and 1635–1645 cm^{-1};

2. the absence of use of triterpenic resins;

3. no sample seems to have been treated with beeswax. A further element supporting the absence of waxes is the absence of the doublet in the 1450–1480 cm^{-1} range (CH_2/CH_3 bending modes) [28], see figure 3.26 as an example;

4. there are large variations in the position of the peaks in the spectra of samples 1996 and 2002. Therefore, it is not possible to give precise indications about the presence of manufacturing materials.

The absence of bands around 1035–1055 cm^{-1} (ν(C-O-C)) and 1530–1570 cm^{-1} (amide II) in all the spectra refers to the absence of gums and proteinaceous materials, respectively.

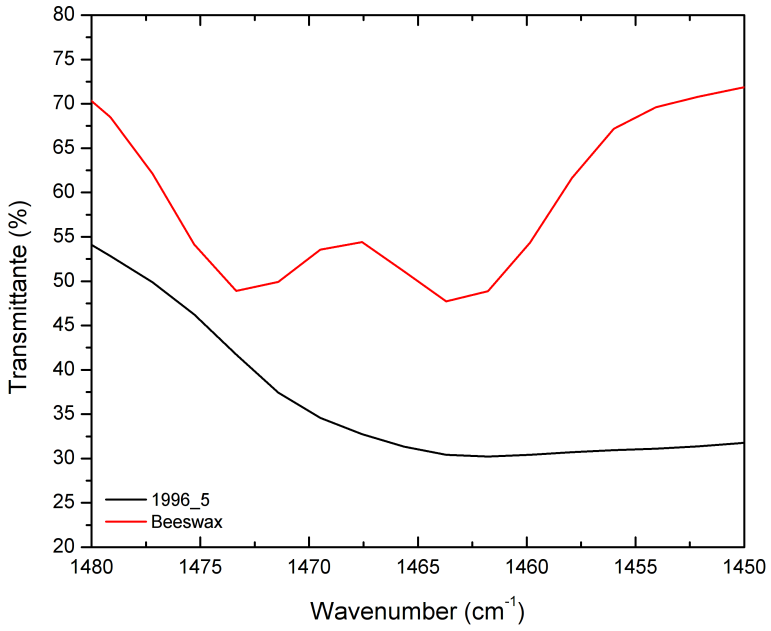

Figure 3.26: Comparison of the FTIR spectra of beeswax and a portion of the fifth sample from viola 1996 in the range 1450–1480 $^{-1}$.

3.2.3 Gas Chromatography coupled with Mass Spectrometry

The results hence obtained by FTIR and PLM are indicative but give rise to interpretation problems because of the limitations of the techniques. To identify the composition of the organic portion of the varnish, separative techniques, such as GC-MS and Py-GC-MS, are needed.

As observed by PLM, the varnishes of the musical instruments from the "Vincenzo Bellini" Conservatory are, in some cases, made by more than one layer. The sampling technique employed here results in the analysis of the entire stratigraphy making it impossible to differentiate between the different layers.

Analytes were identified as their methyl esters by direct comparison with reference materials, by use of a customized digital library (mainly based on the NIST one) and by interpreting the corresponding mass spectra. GC-MS analysis was performed on samples from all the musical instruments investigated and all the reference materials. A typical recorded total ion chromatogram (TIC) is shown in figure 3.27:

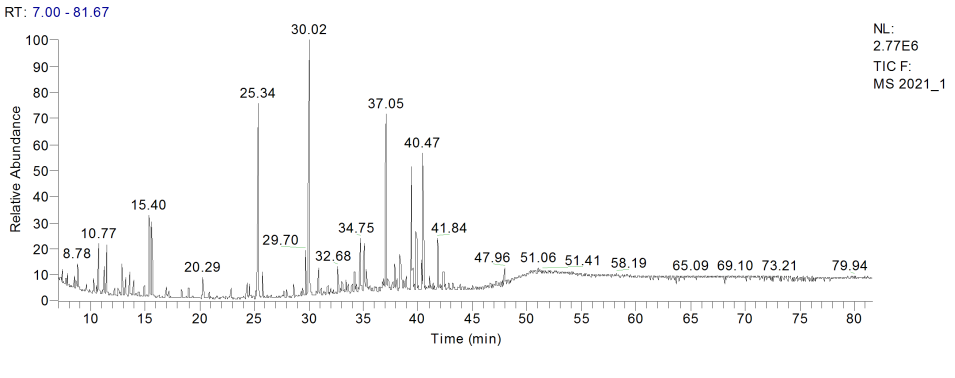

Figure 3.27: TIC of the first sample from violin 2021.

The proposed compound identification and the mean retention time of the detected substances are reported in 3.2.

Table 3.2: Proposed compound identification and mean retention time of the detected substances in the analysed samples from the "Vincenzo Bellini" Conservatory. Where possible, the common name of the corresponding fatty acid was used along with the symbology Cx:y. x and y indicate the number of carbon atoms and of unsaturations, respectively.

Identified analyte and mean retention time (min)	1993_1	1996_3	1999_1	1999_2	2002_1	2002_2	2002_3	2002_4	2002_5	2002_6	2021_1	2021_2	2173_1
Pelargonic acid (C9:0) (7.44)					X			X	X	X	X	X	X
Adipic acid (7.87)	X	X			X			X	X	X	X	X	X
Cinnamic acid (?) (9.41)													X
Capric acid (C10:0) (9.69)													X
Pimelic acid (10.25)	X		X	X	X			X	X	X	X	X	X
Suberic acid (12.89)	X	X	X	X	X	X	X	X	X	X	X	X	X
Lauric acid (C12:0) (14.91)	X	X	X	X	X	X	X	X	X	X	X	X	X
Azelaic acid (15.61)	X	X	X	X	X	X	X	X	X	X	X	X	X
Veratric acid (16.92)	X	X	X	X	X	X	X	X	X	X	X	X	X
3,4,5-trimethoxybenzaldehyde (17.24)		X		X						X		X	
Sebacic acid (18.34)	X							X	X				X
Myristic acid (C14:0) (20.28)	X	X	X	X	X	X	X	X	X	X	X	X	X
Trimethylgallic acid (20.38)		X		X		X	X			X	X	X	X
Undecanoic acid (C11:0) (20.99)				X						X	X		X
Unidentified fatty acid (21.91)					X			X		X			X
Unidentified (22.42)	X		?					X	X		X	X	X
Pentadecanoic acid (C15:0) (22.85)	?	X			X	?	?	X	X	X	X	X	X
Butolic acid (23.78)	X		X		X				X			?	X
6-oxomyristic acid (?) (24.58)	X				X		?	?	X	?			X
Palmitoleic acid (C16:1) (24.73)	X	X			X	X	?	X	?	X	?	?	
Typical peak of shellac (25.14)	X		X	X	X		X	X	X	?	X	X	X
Palmitic acid (C16:0) (25.33)	X	X	X	X	X	X	X	X	X	X	X	X	X
Brassylic acid (26.02)			X	X									
Unidentified (26.83)										X			

Unidentified (27.04)								?		X			X
Heptadecanoic acid (C17:0) (27.71)		X			X	X		X		X	X	X	X
Unidentified fatty acid (28.94)	X		X	X					X			X	
Unidentified (29.09)	X								X				X
Linoleic acid (C18:2) (29.28)		X	X	X			X	?		X	X	X	
Oleic acid (C18:1) (29.41)	X	X	X	X	X	X	X	X	X	X	X	X	X
Shellolic acid (29.68)	X	X	X	X	X	X	X	X	X	?	X	X	X
Unidentified fatty acid (29.94)												X	X
Stearic acid (C18:0) (30.01)	X	X	X	X	X	X	X	X	X	X	X	X	X
Typical peak of shellac (30.89)	X		X	X	X		X	X	X	X	X	X	X
Methylsecodehydroabietic acid (31.03)	X		X	X	X			X	X	X	X		X
Methylsecodehydroabietic acid (31.50)	X		X	X									X
Unidentified fatty acid (32.18)										X			
Sandaracopimaric acid isomer (32.53)	X			X	X		X	?	X	X			X
Typical peak of shellac (32.67)	X	X	X	X	X	X	X	X	X	?	X	X	X
Sandaracopimaric acid isomer (32.91	X	X	X	X	X	X	X	X	X		X		X
Larixol (33.08)					X			X					X
Long chain hydrocarbon (33.43)										X			
Retinoic acid (33.58)	X		X	X	X			X	X		X		
Isopimaric acid (33.80)	X	X	X	X	X		X	X	X				X
Isopimaric acid (33.89)	X		X	X	X			X					
Arachidic acid (C20:0) (34.33)		X	X	X	X	X	X	X		X	X		X
Dehydroabietic acid (34.73)	X	X	X	X	X	X	X	X	X	X	X	X	X
Larixyl acetate (35.26)			X		X		X	X	X				X
Abietic acid (35.63)	X		X	X									X
Henicosanoic acid (C21:0) (26.30)										X			
Typical peak of pine resins (36.92)	X		X	X	X			X	X	X	X	X	X
7-methoxytetradehydroabietic acid (37.04)	X	X	X	X	X		X	X	X	X	X	X	X

Peak of pine resins (?) (37.97)													X
15-methoxydehydroabietic acid (38.04)	X		X	X	X			X	X	?	X		X
Behenic acid (C22:0) (38.27)										X			
Peak of pine resins (38.49)	X		X	X	X			X	X	X	X		X
7-oxodehydroabietic acid (39.42)	X	X	X	X	X		X	X	X	X	X	X	X
7,15-dimethoxytetradehydroabietic acid (39.86)			X	X	X			X	X	X	X		X
Tricosanoic acid (C23:0) (40.14)										X			
Typical peak of shellac (41.84)	X	X	X	X	X	?	X	X	X	?	X	X	?
Lignoceric acid (C24:0) (41.97)										X			
Agathic acid (?) (42.90)												X	
Unidentified long chain fatty acid (43.27)										X			
Unidentified long chain fatty acid (43.74)										X			
Unidentified long chain fatty acid (45.42)										X			
Typical peak of shellac (47.97)	?										X	X	

Samples show very similar composition indicating that a re-varnishing could have occurred for most of them. This evidence is consistent with the PLM analysis.

The TIC of sample 2002_2 shows fewer components than the others because of the resulting high dilution of the analysed solution (figure 3.28).

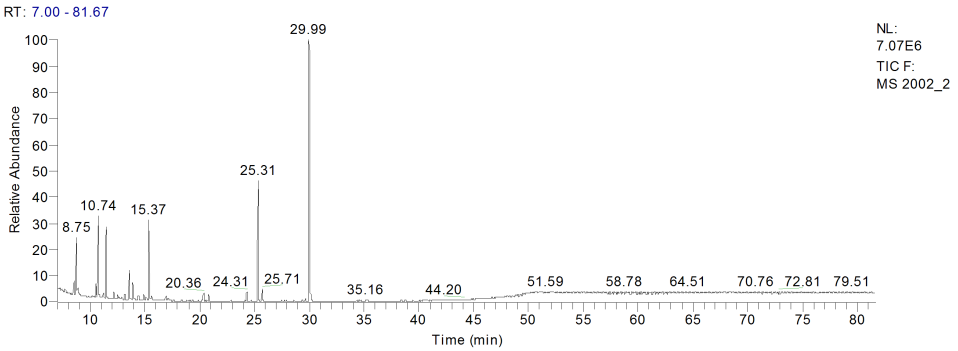

Figure 3.28: TIC of the second sample from violin 2002.

A number of mono- and dicarboxylic fatty acids were detected. The latter are due to the oxidation of the unsaturated fatty acids present in siccative oils [3, 98, 44].

The power of a siccative oil is, in fact, strictly connected to the presence of unsaturated fatty acids. In a good siccative oil, their concentration should be at least the 65% (w/w). The presence of linolenic acid (C18:3) is particularly important for a fast drying process. The rate of drying for the member of the C18 fatty acids series is: C18:3 > C18:2 > C18:1 >> C18:0. The oxidative degradation products[4] of long chain fatty acids are dicarboxylic acids [99].

Chromatograms reported in figures 3.29 and 3.30 are representative for the absence of triterpenic substances in every analysed sample, confirming the results obtained by μ-FTIR.

The ions selected in the SIM chromatograms in figure 3.30 are 410, 218 and 385 m/z because they are markers for 28-norolean-17-en-3-one, amyrins and the methyl ester of dammarenolic acid, respectively. In fact, the latter compounds are abundant in aged mastic, elemi and dammar resins, respectively [100, 101].

The presence of shellac is also confirmed in every sample analysed (except sample 2002_6) because of the detection of peaks at 25.14, 29.68 (shellolic acid), 32.67, 41.84, 47.97 min (see figure 3.31).

The presence of dehydroabietic, sandaracopimaric, isopimaric acids and their derivate products is an indicator for the use of a diterpenic *Pinaceae*

[4]The reaction mechanism probably involves the formation of peroxide intermediates [44].

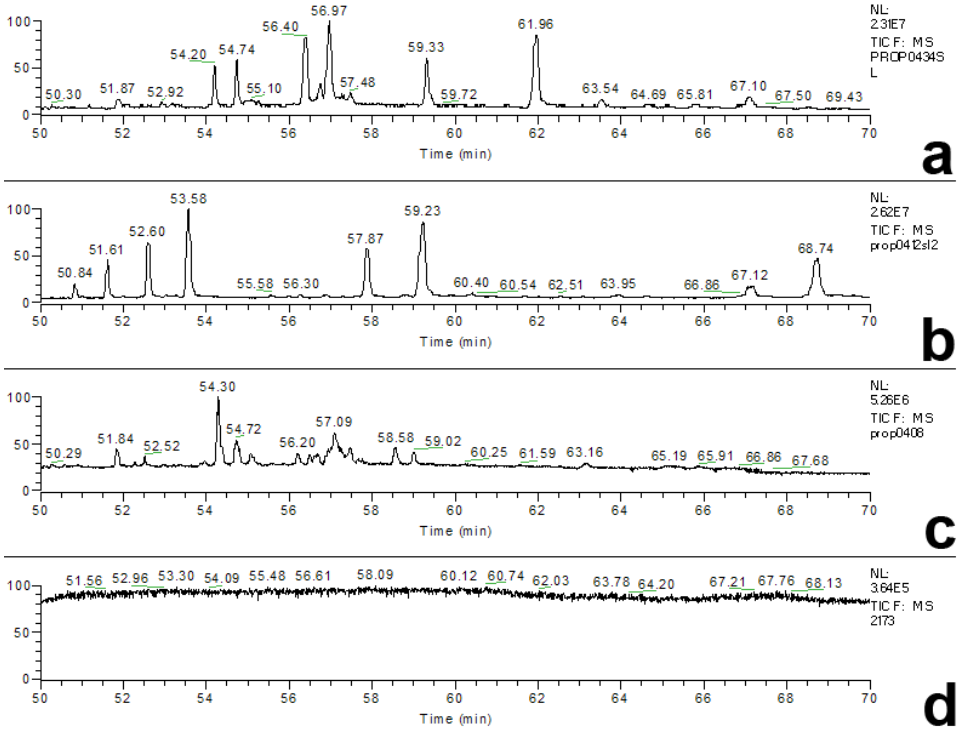

Figure 3.29: Details of the TICs of mastic (a), elemi (b), dammar (c) and the only sample from cello 2173 (d) in the range from 50 to 70 min.

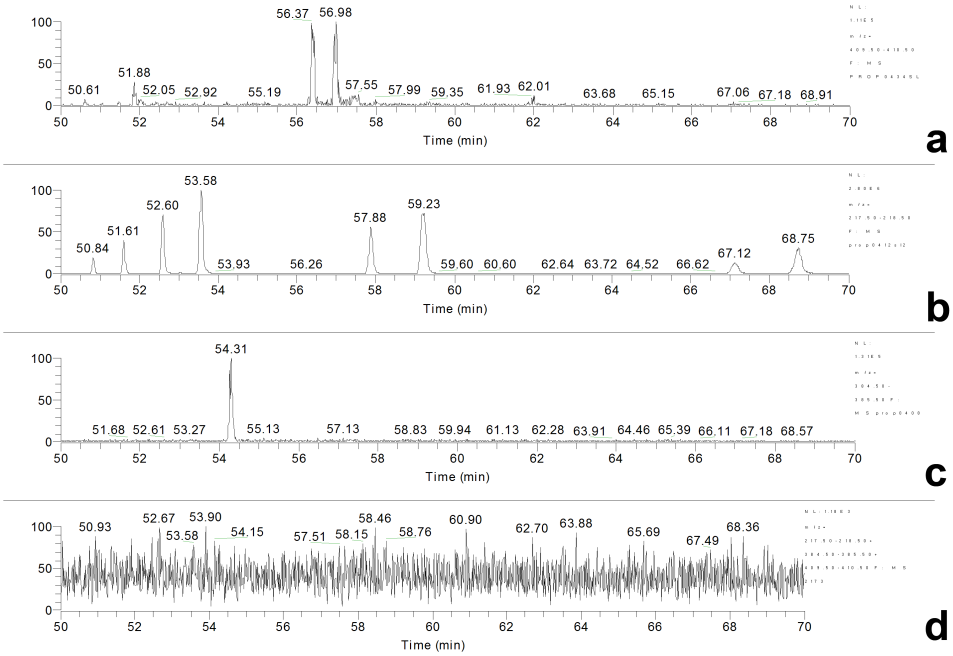

Figure 3.30: Details of the SIM chromatograms of mastic (a), elemi (b), dammar (c) and the only sample from cello 2173 (d) in the range from 50 to 70 min. The selected fragments were 410 (a,d), 218 (b,d) and 385 (c,d) m/z.

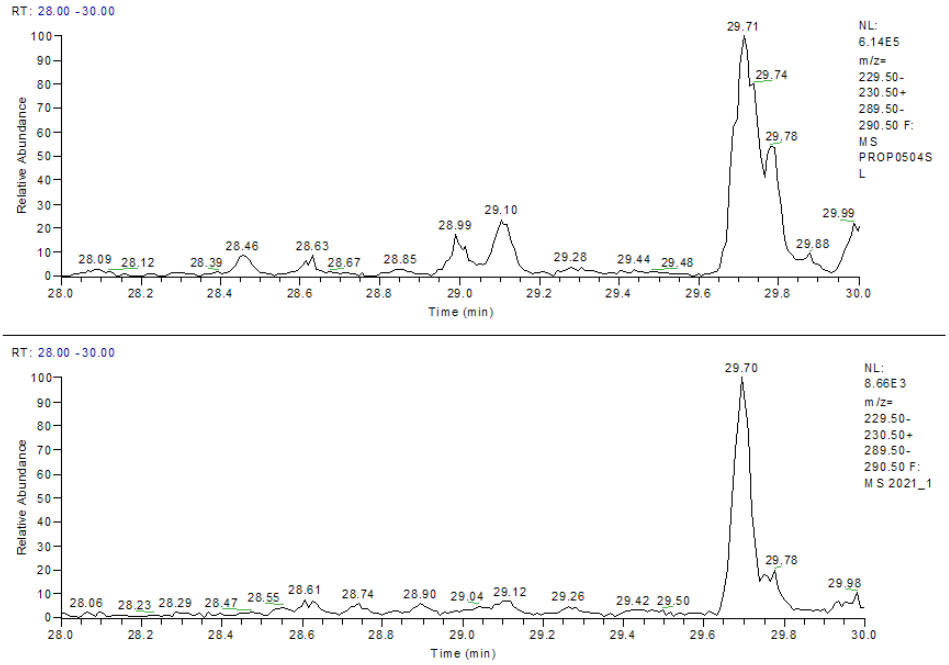

Figure 3.31: Details of the SIM chromatograms of the samples 2021_1 (bottom) and shellac (top) from 28 to 30 min. The selected fragments were 230 and 290 m/z.

resin [26, 27].

Larixol and larixyl acetate are characteristic of the presence of Venice turpentine and make it distinguishable among the other diterpenic resins [44, 100]. Tiny peaks of such compounds were found in samples from instruments 1999, 2002 and 2173 meaning that Venice turpentine was probably used in their varnish. This is in agreement with sources about the finishing of 18$^{\text{th}}$ century stringed musical instruments from Italy [13].

Venice turpentine (and its variety, Strasbourg turpentine) is the exudate of the *Larix decidua*. Known since the antiquity, it was often used with sandarac in varnishes and for veiling technique, although it is not recommended as a finishing varnish. Venice turpentine has got a yellowish and sticky aspect. Venice turpentine was used to produce a transparent green, when mixed with verdigris copper pigment. It does not cause further yellowing when aged [77, 102].

The TIC of the sixth sample from violin 2002 is the only one showing peaks corresponding to long chain fatty acids and hydrocarbons. It is known that these substances reveal the probable use of beeswax [44]. Figure 3.32 reports the selected ion monitoring (SIM) chromatograms for fragments 352 and 384 m/z for samples 2002_6 and fresh beeswax.

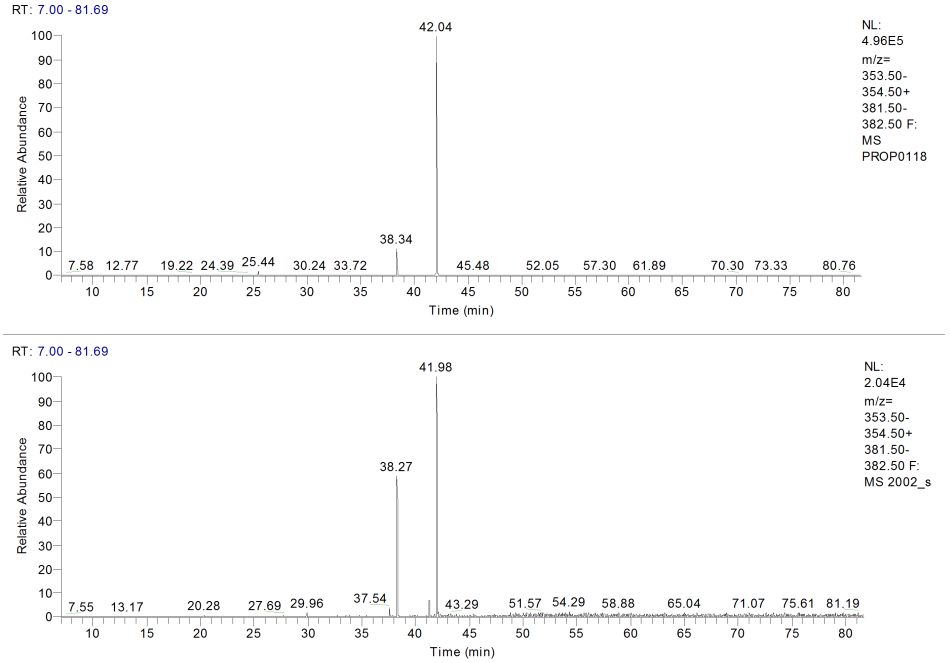

Figure 3.32: SIM chromatograms of the samples 2002_6 (bottom) and fresh beeswax (top). The selected fragments were 354 and 382 m/z.

The ions selected in the SIM chromatograms in figure 3.32 are 354 and 382 m/z because they are markers for the methyl esters of docosanoic and

tetradecanoic acids, respectively. In fact, the latter compounds — and, especially, tetradecanoic acid — are abundant in beeswax [103].

Beeswax is a natural animal product with various origin, that is from *Apis dorsata*, *Apis florea*, *Apis indica*, *Apis mellifera adansonii*, *Apis mellifera*. Since the prehistory, it has been used as a lighting and sealing agent. It was used as a varnish and, until Middle Ages, as a binder for encaustic painting technique [74].

The presence of beeswax apparent contrast with the results from μ-FTIR analysis but is explained by the much higher sensitivity of GC-MS.

Finally, 3,4,5-trimethoxybenzaldehyde and cinnamic, veratric and trimethylgallic acids are hydrolysis products of the lignin moiety [104] because of some traces of wood present in the samples.

3.2.4 Pyrolysis Gas Chromatography coupled with Mass Spectrometry

Measurements were carried out only on samples from instruments 1993, 2021 and 2173. Some total ion pyrograms are shown in figure 3.33.

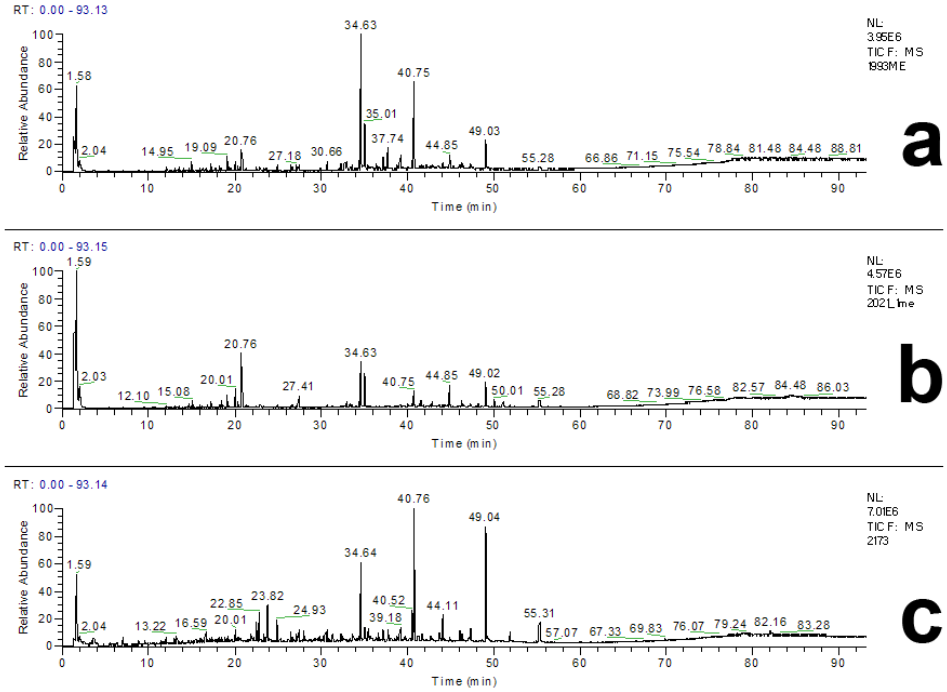

Figure 3.33: Total ion pyrograms of the only sample from *viola d'amore* 1993 (a), the first sample from violin 2021 (b) and the only sample from cello 2173 (c).

Peaks at 20.01–20.02 (attributable to azelaic acid), 34.63–34.64 (attributable to a compound of shellac), 40.75–40.76 (attributable to dehydroabietic acid), 49.02–49.04 min (attributable to 7-oxodehydroabietic acid) are well-visible.

Unlike GC-MS, by Cp-Py-GC-MS, it was possible to carry out analyses on Baltic amber.

Its pyrogram was compared to the ones of the samples from musical instruments (see figure 3.34).

The ion selected in the SIM pyrogram in figure 3.34 is 115 m/z because it is a marker for the dimethyl esters of succinic acid. In fact, the latter compound is abundant in Baltic amber [27, 105, 106] and it was found that the analysed samples show the corresponding peak at 10.73 min.

In the overall, the obtained data further corroborate the *picture* drawn from GC-MS analyses (ie presence of shellac, a siccative oil, a *Pinaceae*

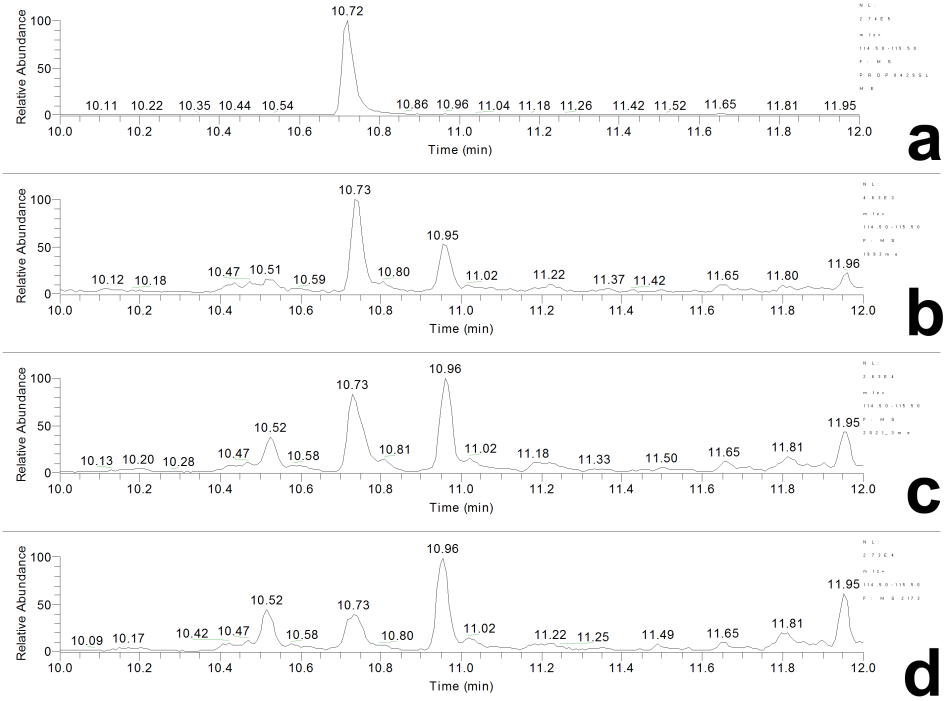

Figure 3.34: Details of the SIM chromatograms of Baltic amber (a), the only sample from *viola d'amore* 1993 (b), the third sample from violin 2021 (c) and the only sample from cello 2173 (d) in the range from 10 to 12 min. The selected fragment was 115 m/z

resin and Venice turpentine). Apart from the presence of Baltic amber, the results are consistent with studies carried out on the varnishes of musical instruments using the same technique [28, 27].

Finally, combining the data arising from both chromatographic techniques, it was possible to build a table (3.3) for marker fragments correlated to compounds likely present in aged and fresh varnishes for their rapid identification[5].

Table 3.3: Marker fragments, compounds and attributable substances in aged and fresh varnishes.

Fragment (m/z)	Compound	Substance
75	Typical peak of shellac	Shellac
113	Typical peak of shellac	Shellac
115	Succinic acid, methyl ester	Baltic amber
152	Azelaic acid, dimethylester	Siccative oil
216	Typical peak of shellac	Shellac
218	Amyrins	Elemi
229 and 187	Typical peak of shellac	Shellac
230 and 290	Shellolic acid	Shellac
232	Oleanonic aldehyde	Mastic
244	Typical peak of (degraded?) shellac	Shellac
248	Moronic acid, methyl ester	Mastic
255	Larixol and larixol acetate (?)	Venice turpentine
262	Ursonic acid, methyl ester	Dammar
277	Typical peak of copal	Copal
284	Typical peak of dragon's blood	Dragon's blood
300	Typical peak of dragon's blood	Dragon's blood
303	Methyl copalate	Copal
354	Docosanoic acid, methyl ester	Beeswax
355	Hydroxydammarenone (I or II)	Dammar
358	Typical peak of dammar	Dammar
382	Tetracosanoic acid, methyl ester	Beeswax
385	Dammarenolic acid, methyl ester	Dammar
410	28-norolean-17-en-3-one and hexacosanoic acid, methyl ester	Mastic and beeswax
424	Dammaradienone (?)	Dammar
438	Octacosanoic acid, methyl ester	Beeswax
453	(Iso)masticadienoic acid, methyl ester	Mastic
466	Tricontanoic acid, methyl ester	Beeswax
468 and 262	Oleanonic acid, methyl ester	Mastic and dammar

[5]The presence of a compound should also be assessed by comparison with the corresponding retention times.

Chapter 4

Conclusions

A multi-analytical approach — comprising of both non destructive and micro-destructive techniques — was used for the first time for the study of the varnishes of a selection of historical stringed musical instruments from the collection of the "Vincenzo Bellini" Conservatory in Palermo and the collection of the "Musical Instruments Museum" in Brussels.

The results here presented are relevant for chemistry and conservation fields.

On a conservation point of view, for the instruments of "Vincenzo Bellini" Conservatory, it was consistently found that on instruments 1996, 1999, 2002, 2021 and 2173 a varnish with similar formulation — based on a *Pinaceae* diterpenic resin, shellac and a siccative oil — was used. Markers for Venice Turpentine were found in three instruments (1999, 2002 and 2173), two of which date back to the 18^{th} century. Markers for Baltic amber were found in the three instruments analysed by Cp-Py-GC-MS (1993, 2021, 2173). Iron- and lead-based compounds were found in the varnishes of the viola d'amore 1993 and the cello 2173. The inorganic elements present in the pigments of a decoration of the cello 2173 were also detected.

For the instruments of the "Musical Instruments Museum", it was found that all the instruments considered were treated with a varnish with earth pigments (iron-based with different amounts of manganese and titanium). In the case of instruments 1374, 2774, 2782, 2784, 2836, lead-based compounds were found. In the case of instrument 1374 (dated back to the 17^{th} century), the presence of a chromium pigment was detected, meaning that the instrument was either re-varnished or built in a peculiar way. A modern retouch was also found on the surface of the instrument 2781.

This thesis contributes to the existing literature about scientific examination of historical musical instruments by expanding the knowledge of the varnish employed and bringing to light some conservation issues on the studied instruments.

On a chemical science point of view, this work dealt with the imple-

mentation of a non-standard approach to the study of micro-samples from complex organic (and inorganic traces) matrices. The analysis of such samples by Cp-Py-GC-MS was also carried out, easing the problem of managing a solid micro-sample and building a list of molecular markers for the identification of specific compounds in substances occurring in varnishes.

Furthermore, the results of this thesis could translate into a know-how for conservators, restorers and lute-makers interested in the use of compatible and historically consistent materials for early stringed musical instruments.

References

[1] G.P. Di Stefano. Vincenzo Trusiano Panormo and the Double Bass of the Conservatory of Music in Palermo. In Regione Siciliana. Assessorato dei Beni Culturali, Ambientali e della Pubblica Istruzione. Dipartimento dei Beni Culturali, Ambientali e dell'Educazione Permanente. Centro Regionale per la Progettazione e il Restauro, editor, *Il Restauro Conservativo del Contrabbasso Panormo*, pages 137–144. Regione Siciliana. Assessorato dei Beni Culturali, Ambientali e della Pubblica Istruzione. Dipartimento dei Beni Culturali, Ambientali e dell'Educazione Permanente, Palermo, 2008.

[2] Regione Siciliana. Assessorato dei Beni Culturali, Ambientali e della Pubblica Istruzione. Dipartimento dei Beni Culturali, Ambientali e dell'Educazione Permanente. Centro Regionale per la Progettazione e il Restauro, editor. *Il Restauro Conservativo del Contrabbasso Panormo*. Regione Siciliana. Assessorato dei Beni Culturali, Ambientali e della Pubblica Istruzione. Dipartimento dei Beni Culturali, Ambientali e dell'Educazione Permanente, Palermo, 2008.

[3] F. Caruso, S. Orecchio, M.G. Cicero, and C. Di Stefano. Gas chromatography-mass spectrometry characterization of the varnish and glue of an ancient 18th century double bass. *Journal of Chromatography A*, 1147:206–212, 2007.

[4] F. Caruso, S. Orecchio, M.G. Cicero, and C. Di Stefano. Determinazione di componenti della vernice e della colla del contrabbasso "Panormo" di Vincenzo Trusiano. In Regione Siciliana. Assessorato dei Beni Culturali, Ambientali e della Pubblica Istruzione. Dipartimento dei Beni Culturali, Ambientali e dell'Educazione Permanente. Centro Regionale per la Progettazione e il Restauro, editor, *Science and Cultural Heritage in the Mediterranean Area. Proceedings of the 3rd international congress "La materia e i segni della storia"*, pages 614–620, 2009.

[5] G. Daita. *Sul Collegio di Musica in Palermo. Appendice al cenno storico artistico ed organico.* Tipografia Corselli, Palermo, 1875.

[6] The Musical Instruments Museum. History, 2010. `http://www.mim.be/history`.

[7] E. Fontana. Copies of historic musical instruments in the collection of the University of Leipzig. In G.R. Rognoni, editor, *Restoration and Conservation of Early Musical Instruments – The spinetta ovale by Bartolomeo Cristofori*. Nardini, Firenze, 2008.

[8] F. Galpin. *A textbook of European musical instruments – Their origin, history and character*. Williams & Norgate, London, 1937.

[9] A.-E. Ceulemans. Western string instruments, 2010. `http://www.mim.be/western-string-instruments`.

[10] A. Gambetta, E.L. De Capua, M. Mercadini, and P. Cicolani. Studio sull'impiego di gas non tossici nella disinfestazione di manufatti lignei e di materiale cartaceo. *Bollettino ICR - Nuova Serie*, 2, 2001.

[11] C. Quaglierini and L. Amorosi. *Chimica e Tecnologia dei Materiali per l'Arte*. Zanichelli, Bologna, 1991.

[12] V. Massa and G. Scicolone. *Le Vernici per il Restauro – I Leganti*. Nardini, Firenze, third edition, 1998.

[13] J. Michelman. *Violin Varnish – A Plausible Re-creation of the Varnish Used by the Italian Violin Makers Between the Years 1550 and 1750, A.D.* W.B. Conkey Company, Cincinnati, 1946.

[14] S.F. Sacconi. *I Segreti di Stradivari*. Libreria del Convegno, Cremona, 1979.

[15] G. Tavlaridis. Technology of Materials Employed for the Construction of Bowed Musical Instruments. In Regione Siciliana. Assessorato dei Beni Culturali, Ambientali e della Pubblica Istruzione. Dipartimento dei Beni Culturali, Ambientali e dell'Educazione Permanente. Centro Regionale per la Progettazione e il Restauro, editor, *Il Restauro Conservativo del Contrabbasso Panormo*, pages 170–173. Regione Siciliana. Assessorato dei Beni Culturali, Ambientali e della Pubblica Istruzione. Dipartimento dei Beni Culturali, Ambientali e dell'Educazione Permanente, Palermo, 2008.

[16] L. Colombo. Il secolo XVIII e le vernici per liuteria. In V. Gheroldi, editor, *Vernici e segreti curiosissimi – Cremona 1747*, pages 169–199. Cremonabooks Srl, Cremona, 1999.

[17] J.-P. Echard and B. Lavédrine. Review on the characterization of ancient stringed musical instrument varnishes and implementation of an analytical strategy. *Journal of Cultural Heritage*, 9:420–429, 2008.

[18] J. Nagyvary. The chemistry of a Stradivarius. *Chemical & Engineering News*, 66:24–31, 1988.

[19] J. Nagyvary. Investigating the secrets of the Stradivarius. *Education in Chemistry*, 42:96–98, 2005.

[20] J. Nagyvary, J.A. DiVerdi, N.L. Owen, and H.D. Tolley. Wood used by Stradivari and Guarneri. *Nature*, 444:565, 2006.

[21] J. Nagyvary, R.N. Guillemette, and C.H. Spiegelman. Mineral Preservatives in the Wood of Stradivari and Guarneri. *PLoS ONE*, 4:e4245, 2009.

[22] J.-P. Echard. In situ multi-element analyses by energy-dispersive X-ray fluorescence on varnishes of historical violins. *Spectrochimica Acta B*, 59:1663–1667, 2004.

[23] A. Von Bohlen and F. Meyer. Microanalysis of old violin varnishes by total-reflection X-ray fluorescence. *Spectrochimica Acta B*, 52:1053–1056, 1997.

[24] A. Von Bohlen. Total reflection X-ray fluorescence spectrometry – A versatile tool for ultra-micro analysis of objects of cultural heritage. *e-PS*, 1:23–34, 2004.

[25] A. von Bohlen, S. Röhrs, and J. Salomon. Spatially resolved element analysis of historical violin varnishes by use of μPIXE. *Analytical and Bioanalytical Chemistry*, 387:781–790, 2007.

[26] J.-P. Echard, C. Benoit, J. Peris-Vicente, V. Malecki, J.V. Gimeno-Adelantado, and S. Vaiedelich. Gas chromatography/mass spectrometry characterization of historical varnishes of ancient italian lutes and violin. *Analytica Chimica Acta*, 584:172–180, 2007.

[27] G. Chiavari, S. Montalbani, and V. Otero. Characterisation of varnishes used in violins by pyrolysis-gas chromatography/mass spectrometry. *Rapid Communications in Mass Spectrometry*, 22:3711–3718, 2008.

[28] J.-P. Echard, L. Bertrand, A. von Bohlen, A.-S. Le Hô, C. Paris, L. Bellot-Gurlet, B. Soulier, A. Lattuati-Derieux, S. Thao, L. Robinet, B. Lavédrine, and S. Vaiedelich. The nature of the extraordinary finish of Stradivari's instruments. *Angewandte Chemie International Edition*, 49:197–201, 2010.

[29] M. Haine and N. Meeùs. *Dictionnaire des facteurs d'instruments de musique en Wallonie et à Bruxelles du 9e siècle à nos jours.* P. Mardaga, Bruxelles, 1986.

[30] M. Haine and N. Meeùs. *Instruments de Musique anciens à Bruxelles et en Wallonie – 17e-20e siècles.* P. Mardaga, Bruxelles, 1986.

[31] K. Moens. La "nascita" del violino nei Paesi Bassi del sud: alla ricerca di un luogo dove collocare l'inizio della storia del violino. In M. Tiella, editor, *Monteverdi, imperatore della musica (1567-1643)*, pages 84–131. Accademia roveretana di musica antica – Istituto per la ricerca organologica ed il restauro, Rovereto, 1993.

[32] F. Mairinger. UV-, IR- and X-ray imaging. In K. Janssens and R. Van Grieken, editors, *Non-destructive Micro Analysis of Cultural Heritage Materials*, Comprehensive Analytical Chemistry. Elsevier, Amsterdam, 2004.

[33] M.N. Filippov, T.A. Kupriyanova, and O.I. Lyamina. Simultaneous Determination of the Concentration of Elements and Their Speciation in Solid Samples Using X-ray Fluorescence Spectrometry. *Journal of Analytical Chemistry*, 56:729–735, 2001.

[34] N.M. Mukhamedshina and A.A. Mirsagotova. Application of X-ray fluorescence for the analysis of some technological materials. *Applied Radiation and Isotopes*, 63:715–722, 2005.

[35] G.V. Pavlinsky, A.Yu. Dukhanin, E.O. Baranov, and A.Yu. Portnoy. Theory of the Implementation of the Fundamental Parameter Method for the X-ray Fluorescence Determination of Low-Atomic-Number Elements. *Journal of Analytical Chemistry*, 61:654–661, 2006.

[36] P.J. Potts. Introduction, Analytical Instrumentation and Application Overview. In P.J. Potts and M. West, editor, *Portable X-ray Fluorescence Spectrometry – Capabilities for In Situ Analysis*, pages 1–12. The Royal Society of Chemistry, Cambridge, 2008.

[37] R. Cesareo, S. Ridolfi, M. Marabelli, A. Castellano, G. Buccolieri, M. Donativi, G.E. Gigante, A. Brunetti, and M.A. Rosales Medina. Portable Systems for Energy-Dispersive X-Ray Fluorescence Analysis of Works of Art. In P.J. Potts and M. West, editor, *Portable X-ray Fluorescence Spectrometry – Capabilities for In Situ Analysis*, pages 206–246. The Royal Society of Chemistry, Cambridge, 2008.

[38] C. Seccaroni and P. Moioli. *Fluorescenza X – Prontuario per l'Analisi XRF Portatile Applicata a Superfici Policrome.* Nardini, Firenze, 2004.

[39] F. Caruso, C. Di Stefano, M.L. Saladino, and E. Caponetti. X-Ray Fluorescence spectroscopy applied to the study of three Sicilian works of art. In E.A. Varella and E. Caponetti, editors, *Proceedings of the*

2nd Residential Summer School – Chemistry and Conservation Science 2008, pages 77–85, 2009.

[40] B.H. Stuart. *Analytical Techniques in Materials Conservation*. John Wiley & Sons, Ltd, Chichester, 2007.

[41] P. Mazzeo. *Spettroscopia analitica chimica – L'analisi chimica quantitativa con metodi spettrofotometrici*. La Nuova Italia Scientifica, Roma, 1996.

[42] J. Chalmers and P. Griffiths, editors. *Handbook of Vibrational Spectroscopy*. John Wiley & Sons, Ltd, Chichester, 2001.

[43] B.H. Stuart. *Infrared Spectroscopy: Fundamentals and Applications*. Analytical Techniques in the Sciences. John Wiley & Sons, Ltd, Chichester, 2004.

[44] J.S. Mills and R. White. *The Organic Chemistry of Museum Objects*. Butterworth-Heinemann, Oxford, second edition, 1994.

[45] M.R. Derrick, D. Stulik, and J.M. Landry. *Infrared Spectroscopy in Conservation Science*. Scientific tools for conservation. The Getty Conservation Institute, Los Angeles, 1999.

[46] S. Prati, E. Joseph, G. Sciutto, and R. Mazzeo. New Advances in the Application of FTIR Microscopy and Spectroscopy for the Characterization of Artistic Materials. *Accounts of Chemical Research*, 43:792–801, 2010.

[47] A.T. James and A.J.P. Martin. Gas-liquid partition chromatography: the separation and micro-estimation of volatile fatty acids from formic acid to dodecanoic acid. *Biochemistry Journal*, 50:679–690, 1952.

[48] T.P. Wampler. Introduction to pyrloysis-capillary gas chromatography. *Journal of Chromatography A*, 842:207–220, 1999.

[49] I.A. Fowlis. *Gas Chromatography*. Analytical Chemistry by Open Learning. John Wiley & Sons, Ltd, Chichester, second edition, 1995.

[50] R.L. Grob and E.F. Barry, editors. *Modern Practice of Gas Chromatography*. John Wiley & Sons, Inc, Hoboken, fourth edition, 2004.

[51] H.M. McNair and J.M. Miller. *Basic Gas Chromatography*. John Wiley & Sons, Inc, Hoboken, second edition, 2009.

[52] M.P. Colombini, F. Modugno, S. Giannarelli, R. Fuoco, and M. Matteini. GC-MS characterization of paint varnishes. *Microchemical Journal*, 67:385–396, 2000.

[53] M.P. Colombini, A. Andreotti, I. Bonaduce, F. Modugno, and E. Ribechini. Analytical Strategies for Characterizing Organic Paint Media Using Gas Chromatography/Mass Spectrometry. *Accounts of Chemical Research*, 43:715–727, 2010.

[54] M.R. Schilling. Paint Media Analysis. In National Academy of Sciences, editor, *Scientific Examination of Art: Modern Techniques in Conservation and Analysis*. The National Academies Press, Washington, 2003.

[55] K. Sutherland. Derivatisation using m-(trifluoreomethyl)phenyltrimethylammonium hydroxide of organic materials in artworks for analysis by gas chromatography – mass spectrometry: Unusual reaction products with alcohols. *Journal of Chromatography A*, 1149:30–37, 2007.

[56] G. Sarkissian. The Analysis of Tire Rubber Traces Collected After Braking Incidents Using Pyrolysis-Gas Chromatography/Mass Spectrometry. *Journal of Forensic Sciences*, 52:1050–1056, 2007.

[57] M.F. Silva, M.T. Doménech-Carbó, L. Fuster-López, M.F. Mecklenburg, and S. Martin-Rey. Identification of additives in poly(vinylacetate) artist's paints using PY-GC-MS. *Analytical and Bioanalytical Chemistry*, 397:357–367, 2010.

[58] H. Ling, N. Maiqian, G. Chiavari, and R.Mazzeo. Analytical characterization of binding medium used in ancient Chinese artworks by pyrolysis-gas chromatography/mass spectrometry. *Microchemical Journal*, 85:347–353, 2007.

[59] B. Sitholé, B. Ambayec, and R. Beaudoin. Py-GC/MS analysis of fluorochemical sizing agents in paper. *Canadian Journal of Analytical Sciences and Spectroscopy*, 49:148–155, 2004.

[60] R.P. Philp. Application of pyrolysis - GC and pyrolysis - GC-MS to fossil fuel research. *Trends in Analytical Chemistry*, 1:237–241, 1982.

[61] Y. Sun, Z. Yang, L. Xie, Y. Zhang, and P. Chai. Pyrolysis-gas chromatography-mass spectrography as a method to evaluate hydrocarbon generation potential of Oligocene source rocks from Qiongdongnan Basin, offshore South China Sea. *Shiyou Xuebao/Acta Petrolei Sinica*, 31:579–585, 2010.

[62] S. Takeno, T. Bamba, Y. Nakazawa, E. Fukusaki, A. Okazawa, and A. Kobayashi. High-Throughput and Highly Sensitive Analysis Method for Polyisoprene in Plants by Pyrolysis-Gas Chromatography/Mass Spectrometry. *Bioscience, Biotechnology, and Biochemistry*, 74:13–17, 2010.

[63] P.B. Smith and A.P. Snyder. Chracterization of bacteria by quartz tube pyrolysis-gas chromatography/ion trap mass spectrometry. *Journal of Analytical and Applied Pyrolysis*, 24:23–38, 1992.

[64] P.B. Smith and A.P. Snyder. Characterization of bacteria by oxidative and non-oxidative pyrolysis-gas chromatography/ion trap mass spectrometry. *Journal of Analytical and Applied Pyrolysis*, 24:199–210, 1993.

[65] S. Tsuge and H. Ohtani. Structural characterization of polymeric materials by Pyrolysis-GC/MS. *Polymer Degradation and Stability*, 58:109–130, 1997.

[66] C. Watanabe, S. Tsuge, and H. Ohtani. Development of new pyrolysis-GC/MS system incorporated with on-line micro-ultraviolet irradiation for rapid evaluation of photo, thermal, and oxidative degradation of polymers. *Polymer Degradation and Stability*, 94:1467–1472, 2009.

[67] K.L. Sobeih, M. Baron, and J. Gonzalez-Rodriguez. Recent trends and developments in pyrolysis-gas chromatography. *Journal of Chromatography A*, 1186:51–66, 2008.

[68] B.A. Stankiewicz, P.F. van Bergen, M.B. Smith, J.F. Carter, D.E.G. Briggs, and R.P. Evershed. Comparison of the analytical performance of filament and Curie-point pyrolysis devices. *Journal of Analytical and Applied Pyrolysis*, 45:133–151, 1998.

[69] J.M. Challinor. A pyrolysis-derivatisation-gas chromatography technique for the structural elucidation of some synthetic polymers. *Journal of Analytical and Applied Pyrolysis*, 16:323–333, 1989.

[70] J.M. Challinor. Review: the development and applications of thermally assisted hydrolysis and methylation reactions. *Journal of Analytical and Applied Pyrolysis*, 61:3–34, 2001.

[71] F. Shadkami and R. Helleur. Recent applications in analytical thermochemolysis. *Journal of Analytical and Applied Pyrolysis*, 89:2–16, 2010.

[72] I. Bonaduce and A. Andreotti. Py-GC/MS of Organic Paint Binders. In M.P. Colombini and F. Modugno, editors, *Organic Mass Spectrometry in Art and Archaeology*. John Wiley & Sons, Ltd, Chichester, 2009.

[73] D. Scalarone and O. Chiantore. Py-GC/MS of Natural and Synthetic Resins. In M.P. Colombini and F. Modugno, editors, *Organic Mass Spectrometry in Art and Archaeology*. John Wiley & Sons, Ltd, Chichester, 2009.

[74] I. Bonaduce and M.P. Colombini. Characterisation of beeswax in works of art by gas chromatography-mass spectrometry and pyrolysis-gas chromatography-mass spectrometry procedures. *Journal of Chromatography A*, 1028:297–306, 2004.

[75] H. van Keulen. Gas chromatography/mass spectrometry methods applied for the analysis of a Round Robin sample containing materials present in samples of works of art. *International Journal of Mass Spectrometry*, 284:162–169, 2009.

[76] C. Miliani, F. Rosi, B.G. Brunetti, and A. Sgamellotti. In Situ Non-invasive Study of Artworks: The MOLAB Multitechnique Approach. *Accounts of Chemical Research*, 43:728–738, 2010.

[77] M. Matteini and A. Moles. *La Chimica nel Restauro – I Materiali dell'Arte Pittorica*. Nardini, Firenze, 2004.

[78] M. Cotte, E. Checroun, J. Susini, and P. Walter. Micro-analytical study of interactions between oil and lead compounds in paintings. *Applied Physics A: Materials Science & Processing*, 89:841–848, 2007.

[79] J.R. Cohn and E. A. Emmett. The excretion of trace metals in human sweat. *Annals of Clinical and Laboratory Science*, 8:270–275, 1978.

[80] G. Fortunato, A. Ritter, and D. Fabian. Old Masters' lead white pigments: investigations of paintings from the 16th to the 17th century using high precision lead isotope abundance ratios. *The Analyst*, 130:898–906, 2005.

[81] E. Welcomme, P. Walter, P. Bleuet, J.-L. Hodeau, E. Dooryhee, P. Martinetto, and M. Menu. Classification of lead white pigments using synchrotron radiation micro X-ray diffraction. *Applied Physics A: Materials Science & Processing*, 89:825–832, 2007.

[82] N. Eastaugh, V. Walsh, T. Chaplin, and R. Siddall. *Pigment Compendium – A Dictionary and Optical Microscopy of Historical Pigments*. Butterworth-Heinemann, Oxford, 2008.

[83] R.J. Gettens and G.L. Stout. *Painting Materials – A short encyclopaedia*. Dover Publications, Inc., New York, 1966.

[84] C. D'Andrea Cennini. *The Craftsman's Handbook. The Italian "Il Libro dell'Arte"*. Dover Publications, Inc, New York, 1933.

[85] P. Vandenabeele, F. Verpoort, and L. Moens. Non-destructive analysis of paintings using Fourier transform Raman spectroscopy with fibre optics. *Journal of Raman Spectroscopy*, 32:263–269, 2001.

[86] D. Goltz, J. McClelland, A. Schellenberg, M. Attas, E. Cloutis, and C. Collins. Spectroscopic Studies on the Darkening of Lead White. *Applied Spectroscopy*, 57:1393–1398, 2003.

[87] S.C. van Lith, V. Alonso-Ramirez, P.A. Jensen, F.J. Frandsen, and P. Glarborg. Release to the Gas Phase of Inorganic Elements during Wood Combustion. Part 1: Development and Evaluation of Quantification Methods. *Energy & Fuels*, 20:964–978, 2006.

[88] S.C. van Lith, P.A. Jensen, F.J. Frandsen, and P. Glarborg. Release to the Gas Phase of Inorganic Elements during Wood Combustion. Part 2: Influence of Fuel Composition. *Energy & Fuels*, 22:1598–1609, 2008.

[89] A. Casoli, M.P. Colombini, and M. Matteini. La chimica dei materiali pittorici. In L. Campanella, editor, *Chimica per l'Arte*. Zanichelli, Bologna, 2007.

[90] J.L. Rodgers and W.A. Nicewander. Thirteen Ways to Look at the Correlation Coefficient. *The American Statistician*, 42:59–66, 1988.

[91] R. Brereton. *Chemometrics – Data Analysis for the Laboratory and Chemical Plant*. John Wiley & Sons, Ltd, Chichester, 2003.

[92] R Development Core Team. R: A Language and Environment for Statistical Computing, 2010. `http://www.R-project.org`.

[93] N. Umney and S. Rivers. *Conservation of Furniture*. Butterworth-Heinemann, Oxford, 2003.

[94] P. Vandenabeele, B. Wehling, L. Moens, H. Edwards, M. De Reu, and G. Van Hooydonk. Analysis with micro-Raman spectroscopy of natural organic binding media and varnishes used in art. *Analytica Chimica Acta*, 407:261–274, 2000.

[95] L. Rafaëlly, S. Héron, W. Nowik, and A. Tchapla. Optimisation of ESI-MS detection for the HPLC of anthraquinone dyes. *Dyes and Pigments*, 77:191–203, 2008.

[96] A.M. Correia, R.J.H. Clark, M.I.M. Ribeiro, and M.L.T.S. Duarte. Pigment study by Raman microscopy of 23 paintings by the Portuguese artist Henrique Pousão (1859–1884). *Journal of Raman Spectroscopy*, 38:1390–1405, 2007.

[97] M. Derrick. Fourier Transform Infrared Spectral Analysis of Natural Resins Used in Furniture Finishes. *Journal of the American Institute for Conservation*, 28:43–56, 1989.

[98] M.P. Colombini, I. Bonaduce, and G. Gautier. Molecular Pattern Recognition of Fresh and Aged Shellac. *Chromatographia*, 58:357–364, 2003.

[99] A. Casoli, P.C. Musini, and G. Palla. Gas chromatographic-mass spectrometric approach to the problem of characterizing binding media in paintings. *Journal of Chromatography A*, 731:237–246, 1996.

[100] U. Baumer, P. Dietemann, and J. Koller. Identification of resinous materials on 16th and 17th century reverse-glass objects by gas chromatography/mass spectrometry. *International Journal of Mass Spectrometry*, 284:131–141, 2009.

[101] G. Cartoni, M.V. Russo, F. Spinelli, and F. Talarico. GC-MS Characterisation and Identification of Natural Terpenic Resins Employed in Works of Art. *Annali di Chimica*, 94:767–782, 2004.

[102] G. Chiavari, D. Fabbri, R. Mazzeo, P. Bocchini, and G.C. Galletti. Pyrolysis Gas Chromatography-Mass Spectrometry of Natural Resins Used for Artistic Objects. *Chromatographia*, 41:273–281, 1995.

[103] J.J. Jiménez, J.L. Bernal, S. Aumente, L. Toribio, and J. Bernal Jr. Quality assurance of commercial beeswax II. Gas chromatography-electron impact ionization mass spectrometry of alcohols and acids. *Journal of Chromatography A*, 1007:101–116, 2003.

[104] D.W. Ribbons. Chemicals from lignin. *Philosophical transactions of the Royal Society of London*, 321:485–494, 1987.

[105] L. Carlsen, A. Feldthus, T. Klarskov, and A. Shedrinsky. Geographical classification of amber based on pyrolysis- and infra-red spectroscopy data . *Journal of Analytical and Applied Pyrolysis*, 43:71–81, 1997.

[106] E.C. Stout, C.W. Beck, and K.B. Anderson. Identification of rumanite (Romanian amber) as thermally altered succinite (Baltic amber). *Physics and Chemistry of Minerals*, 27:665–678, 2000.

Appendix A

XRF results on the instruments from the "Musical Instruments Museum" in Brussels

The extended XRF results on the instruments from the "Musical Instruments Museum" in Brussels are reported in this appendix.

Violin 1338

A picture under white and UV light of the instrument is shown in figure A.1.

Figure A.1: The violin 1338 by B.-J. Boussu photographed under white (a) and UV (b) light. Picture used by permission of the "Musical Instruments Museum", Brussels.

Measures were carried out onto 32 spots. The sampling map is shown in figure A.2.

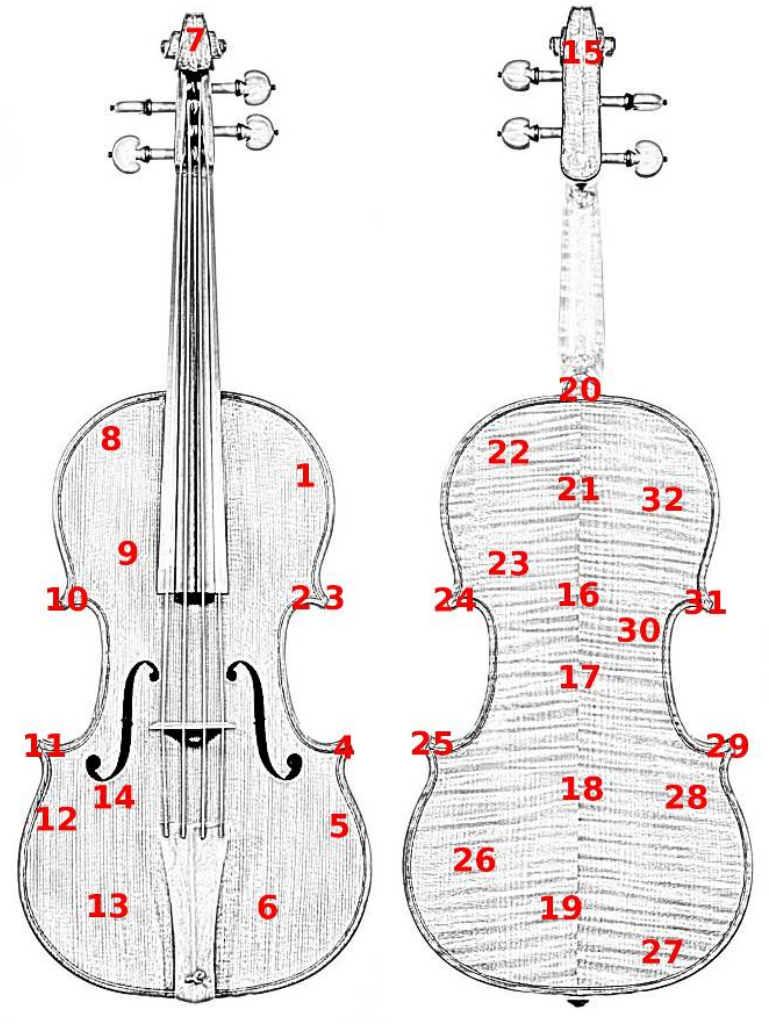

Figure A.2: The map of the spots of the violin 1338 by B.-J. Boussu analysed by μ-XRF.

Among the others, three *special* spots were also analysed:

1. The third sampled spot, a black-coloured region;
2. The fifth sampled spot, a carved part of the top;
3. The twelfth sampled spot, an area in which some *droplets* of varnish are visible.

A typical spectrum recorded on the surface of the top of the violin 1338 is reported in figure A.3.

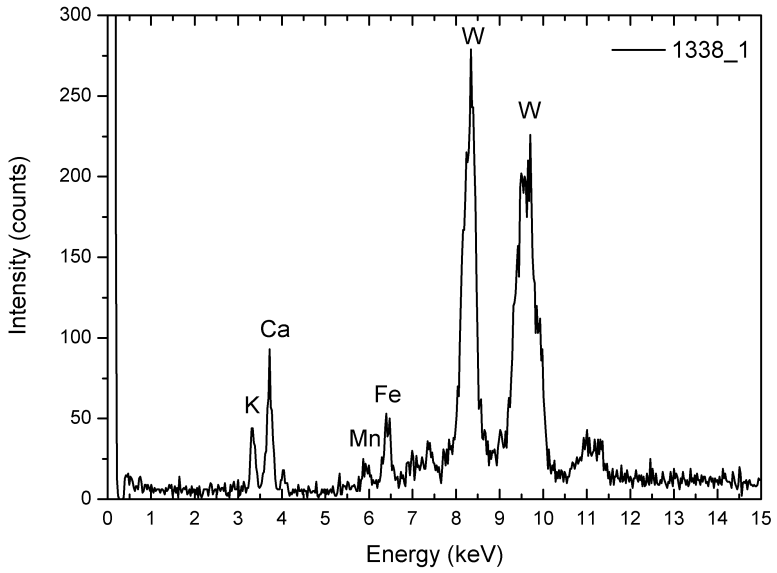

Figure A.3: XRF spectrum of the first sampled spot on the surface of the violin 1338. Tungsten peaks are attributable to the target of the instrument.

The XRF results for the violin 1338 are reported in table A.1. They were obtained by best fitting the emission peaks with Gaussian functions and computing their areas by subtracting both the background and the target signals.

The matrix of the Pearson correlation coefficients, calculated between the values of the areas for each element is reported in table A.2.

Table A.1: XRF results obtained from violin 1338 expressed as keV · counts.

Emission line	K K_{12}	Ca K_{12}	S K_{12}	Cl K_{12}	Fe K_{12}	Mn K_{12}	Ti K_{12}	Pb L_1	Zn K_{12}
1338_1	213	409	0	0	250	103	0	0	0
1338_2	163	312	0	0	248	66	0	0	0
1338_3	482	1604	0	0	2034	167	0	134	0
1338_4	189	474	0	0	392	104	0	0	0
1338_5	306	467	0	0	138	87	0	0	0
1338_6	150	343	0	0	305	44	0	0	0
1338_7	231	260	0	0	549	80	52	0	0
1338_8	218	376	0	0	194	0	0	0	0
1338_9	86	368	0	0	221	71	0	0	0
1338_10	155	640	48	0	636	52	0	0	0
1338_11	208	854	0	0	259	76	0	0	108
1338_12	179	458	0	0	363	81	0	0	0
1338_13	155	368	0	0	474	0	0	0	0
1338_14	140	417	0	0	332	0	0	0	0
1338_15	643	697	0	27	407	85	0	0	0
1338_16	229	529	26	0	398	93	0	0	0
1338_17	193	492	0	0	440	86	0	0	0
1338_18	198	761	0	0	543	84	0	0	100
1338_19	200	329	0	0	359	0	0	0	0
1338_20	309	356	0	0	297	127	0	0	75
1338_21	267	567	0	0	493	165	0	0	0
1338_22	218	346	0	0	230	97	0	0	0
1338_23	240	403	0	0	232	85	0	0	0
1338_24	440	692	0	0	713	147	0	124	119
1338_25	360	719	0	0	404	97	0	0	69
1338_26	166	334	0	0	181	64	0	88	0
1338_27	211	381	0	0	210	102	0	0	0
1338_28	116	313	0	0	91	62	0	0	0
1338_29	349	535	0	0	732	96	0	0	119
1338_30	117	222	0	0	118	62	0	0	0
1338_31	194	404	0	0	259	118	0	0	0
1338_32	262	463	0	0	744	84	0	0	0

Table A.2: Matrix of the correlation coefficients calculated between the values of the areas for each detected element on the violin 1338.

	K	Ca	S	Cl	Fe	Mn	Ti	Pb	Zn
K	1	0.59	-0.12	0.64	0.51	0.50	-0.01	0.42	0.31
Ca	0.59	1	0.10	0.14	0.83	0.48	-0.17	0.58	0.31
S	-0.12	0.10	1	-0.04	0.10	-0.09	-0.04	-0.08	-0.12
Cl	0.64	0.14	-0.04	1	0.00	0.02	-0.03	-0.06	-0.08
Fe	0.51	0.83	0.10	0.00	1	0.42	0.07	0.63	0.14
Mn	0.50	0.48	-0.09	0.02	0.42	1	0.00	0.41	0.27
Ti	-0.01	-0.17	-0.04	-0.03	0.07	0.00	1	-0.06	-0.08
Pb	0.42	0.58	-0.08	-0.06	0.63	0.41	-0.06	1	0.19
Zn	0.31	0.31	-0.12	-0.08	0.14	0.27	-0.08	0.19	1

Cello 1372

A picture under white and UV light of the instrument is shown in figure A.4.

Measures were carried out onto 23 spots. The sampling map is shown in figure A.5.

Among the others, three *special* spots were also analysed:

1. The sixth sampled spot, a carved part of the top;
2. The eleventh sampled spot, an area in which some *droplets* of varnish are visible;
3. The sixteenth sampled spot, a rough surface on the top of the scroll.

A typical spectrum recorded on the surface of the top of the cello 1372 is reported in figure A.6.

Spectra recorded on the surface of the cello 1372 are similar to the ones recorded onto the violin 1338. Signals relative to titanium, zinc and lead were found only in the spectra of the eleventh and the sixteenth analysed spots.

The XRF results for the cello 1372 are reported in table A.3. They were obtained with the same procedure of the ones calculated for violin 1338.

The matrix of the Pearson correlation coefficients calculated between the values of the areas for each element is reported in table A.4

Table A.3: XRF results obtained from cello 1372 expressed as keV · counts.

Emission line	K K_{12}	Ca K_{12}	S K_{12}	Cl K_{12}	Fe K_{12}	Mn K_{12}	Ti K_{12}	Pb L_1	Zn K_{12}
1372_1	297	424	33	27	235	115	0	0	0
1372_2	296	415	0	0	299	79	0	0	0
1372_3	227	360	0	0	88	46	0	0	0
1372_4	253	1712	113	0	1318	149	0	0	0
1372_5	287	485	35	0	726	84	0	0	0
1372_6	381	513	83	0	234	82	0	0	0
1372_7	134	397	18	0	103	56	0	0	0
1372_8	192	539	0	0	205	0	0	0	0
1372_9	360	493	25	0	541	0	0	0	0
1372_10	337	729	0	0	389	44	0	0	0
1372_11	540	2836	192	0	3621	166	47	181	78
1372_12	200	742	34	0	312	66	0	0	0
1372_13	473	403	0	0	233	51	0	0	0
1372_14	178	230	0	0	134	39	0	0	0
1372_15	109	356	0	0	199	57	0	0	0
1372_16	339	920	19	0	1217	107	41	94	122
1372_17	398	241	57	0	305	74	0	0	0
1372_18	308	328	0	0	144	89	0	0	0
1372_19	228	160	0	0	119	37	0	0	0
1372_20	348	174	0	0	181	77	0	0	0
1372_21	284	210	0	0	194	60	0	0	0
1372_22	412	365	22	0	185	53	0	0	0
1372_23	303	275	0	0	261	117	0	0	0

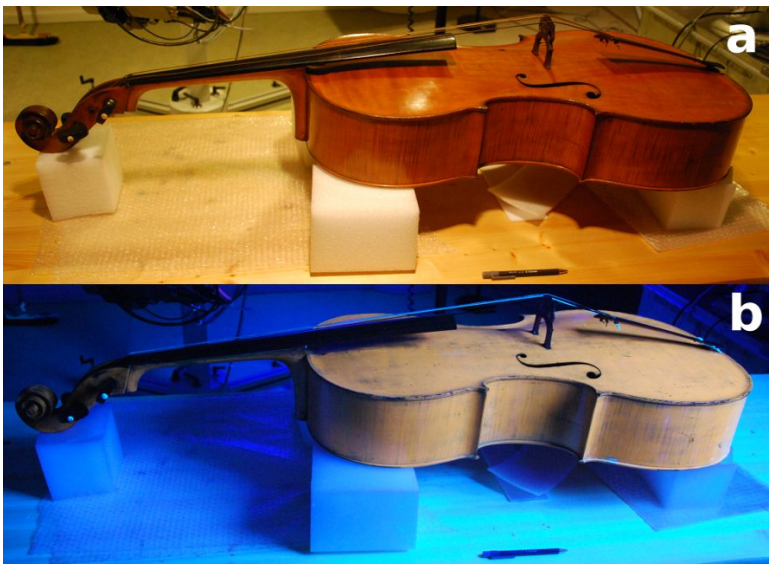

Figure A.4: The cello 1372 by B.-J. Boussu photographed under white (a) and UV (b) light. Picture used by permission of the "Musical Instruments Museum", Brussels.

Table A.4: Matrix of the correlation coefficients calculated between the values of the areas for each detected element on the cello 1372.

	K	Ca	S	Cl	Fe	Mn	Ti	Pb	Zn
K	1	0.40	0.48	0.00	0.51	0.35	0.44	0.49	0.35
Ca	0.40	1	0.88	-0.06	0.95	0.64	0.73	0.81	0.57
S	0.48	0.88	1	0.03	0.85	0.67	0.57	0.68	0.39
Cl	0.00	-0.06	0.03	1	-0.07	0.23	-0.07	-0.06	-0.06
Fe	0.51	0.95	0.85	-0.07	1	0.65	0.84	0.92	0.68
Mn	0.35	0.64	0.67	0.23	0.65	1	0.52	0.55	0.44
Ti	0.44	0.73	0.57	-0.07	0.84	0.52	1	0.97	0.96
Pb	0.49	0.81	0.68	-0.06	0.92	0.55	0.97	1	0.85
Zn	0.35	0.57	0.39	-0.06	0.68	0.44	0.96	0.85	1

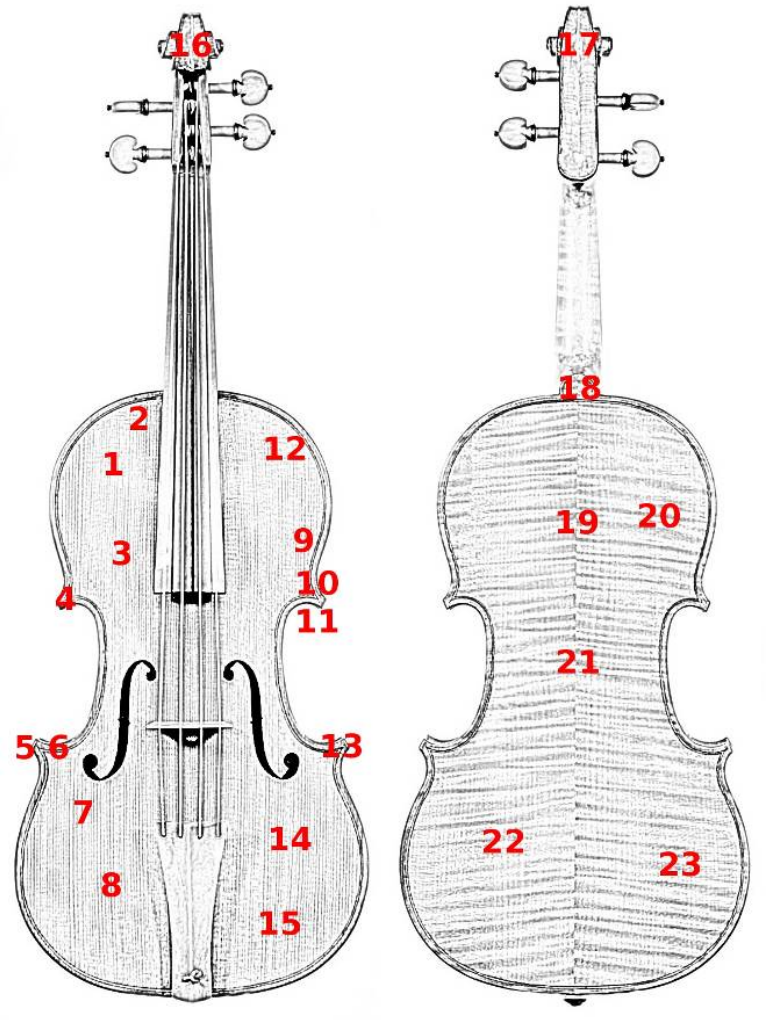

Figure A.5: The map of the spots of the cello 1372 by B.-J. Boussu analysed by μ-XRF.

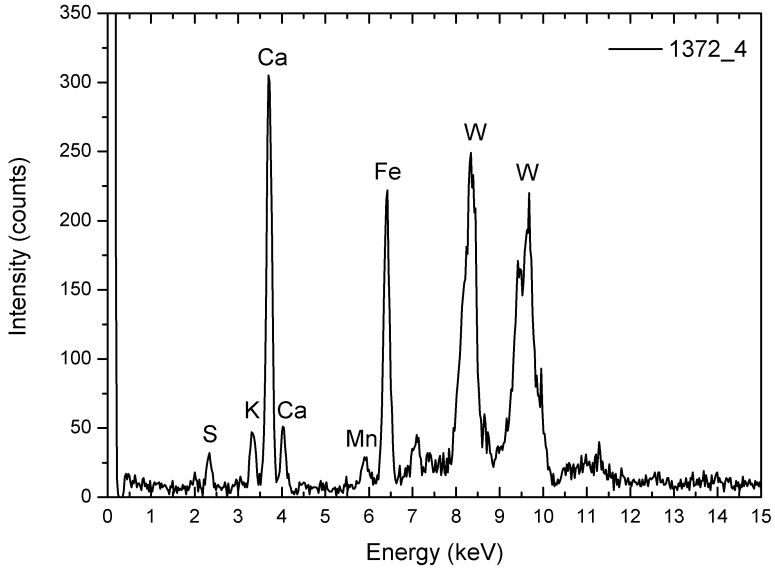

Figure A.6: XRF spectrum of the fourth sampled spot on the surface of the cello 1372. Tungsten peaks are attributable to the target of the instrument.

Cello 1374

A picture under white and UV light of the instrument is shown in figure A.7.

Measures were carried out onto 49 spots. The sampling map is shown in figure A.8.

A typical spectrum recorded on the surface of the top of the cello 1374 is reported in figure A.9.

Spectra recorded on the surface of the cello 1374 are significantly different from the ones recorded onto the previous instruments. In fact, chromium was ubiquitously found in the varnish of the cello 1374.

The XRF results for the cello 1374 are reported in table A.5. They were obtained with the same procedure of the ones calculated for the other instruments hitherto considered.

The matrix of the Pearson correlation coefficients calculated between the values of the areas for each element is reported in table A.6

Table A.5: XRF results obtained from cello 1374 expressed as keV · counts.

Emission line	K K_{12}	Ca K_{12}	S K_{12}	Cl K_{12}	Fe K_{12}	Mn K_{12}	Ti K_{12}	Pb L_1	Zn K_{12}	Cr K_{12}	Cu K_{12}	As K_{12}	Sr K_{12}
1374_1	492	1729	0	0	24609	117	369	657	172	1899	0	0	0
1374_2	566	3285	0	0	43746	146	0	1754	234	5027	0	0	0
1374_3	213	1118	0	0	2744	147	0	182	70	352	0	0	0
1374_4	226	1144	0	0	2090	78	44	162	0	578	0	0	0
1374_5	672	1632	0	0	5334	93	73	255	386	1148	0	0	0
1374_6	466	1248	0	0	829	0	0	257	119	4931	0	0	0
1374_7	310	852	0	0	1436	0	0	0	0	3792	0	0	0
1374_8	188	519	0	0	15196	94	0	235	342	156	0	0	0
1374_9	253	1094	0	0	1397	77	93	201	17	467	0	0	0
1374_10	267	1402	0	0	2282	111	41	68	65	503	0	0	0
1374_11	369	1244	0	0	1077	0	0	334	73	1763	0	0	0
1374_12	367	10312	0	61	4882	0	73	452	287	4819	410	0	276
1374_13	683	959	66	0	1846	0	46	0	0	1910	0	0	0
1374_14	264	977	0	0	795	0	0	85	0	505	0	0	0
1374_15	0	14161	0	0	3794	0	0	169	0	607	0	0	0
1374_16	538	1779	22	0	2284	0	40	100	79	2369	0	0	0
1374_17	387	1199	100	0	25817	0	81	481	678	2610	0	0	0
1374_18	198	782	0	0	43275	0	91	601	940	875	0	0	0
1374_19	134	1099	0	0	3502	84	19	138	67	302	0	0	0
1374_20	300	1051	0	0	1039	0	0	225	0	561	0	0	0
1374_21	232	1417	0	0	3750	0	29	251	106	1009	0	0	0
1374_22	377	1575	0	0	2144	0	33	204	79	218	0	0	0
1374_23	296	2522	0	0	78914	0	113	1279	1651	2428	0	0	0
1374_24	524	2015	0	0	9046	0	71	418	259	1931	0	0	0
1374_25	250	406	0	0	17150	42	53	486	543	121	0	0	0
1374_26	199	418	0	0	7826	0	0	316	258	625	0	0	0
1374_27	287	453	0	0	7913	58	0	566	301	154	0	0	0
1374_28	180	446	0	0	5831	0	57	210	158	0	0	0	0
1374_29	205	572	0	0	370	0	0	97	0	297	0	0	0
1374_30	311	1170	0	0	3540	0	43	317	0	3135	0	0	0
1374_31	243	599	0	0	283	0	40	0	0	290	0	0	0
1374_32	503	606	0	0	284	0	0	0	0	3880	0	0	0
1374_33	642	1081	0	0	2522	0	86	207	40	1215	0	0	0
1374_34	391	500	0	0	436	0	0	86	0	1162	0	0	0
1374_35	292	475	0	0	618	0	0	0	0	772	0	0	0
1374_36	383	948	0	0	1048	35	33	209	0	1071	0	0	0
1374_37	216	523	0	0	547	0	27	0	0	404	0	0	0
1374_38	202	519	0	0	443	0	37	133	0	388	0	0	0
1374_39	242	873	0	0	3245	0	62	91	59	85	0	0	0
1374_40	275	762	0	0	2252	0	0	74	0	469	0	0	0
1374_41	325	590	0	0	2153	0	26	100	0	510	0	0	0
1374_42	396	778	0	0	2699	19	0	222	0	223	0	0	0
1374_43	195	412	0	0	211	42	0	0	0	206	0	0	0
1374_44	273	414	0	0	1195	0	0	191	0	644	0	0	0
1374_45	551	915	0	0	16959	0	89	0	0	1534	0	420	0
1374_46	250	645	0	0	1143	1	0	116	122	674	0	0	0
1374_47	258	548	0	0	289	0	0	0	0	506	0	0	0
1374_48	298	2249	0	0	1689	0	52	278	0	3756	2287	0	0
1374_49	185	598	0	0	612	0	0	187	0	314	0	0	0

Figure A.7: The cello 1374 by G. Borbon photographed under white (a) and UV (b) light. Picture used by permission of the "Musical Instruments Museum", Brussels.

Table A.6: Matrix of the correlation coefficients calculated between the values of the areas for each detected element on the cello 1374.

	K	Ca	S	Cl	Fe	Mn	Ti	Pb	Zn	Cr	Cu	As	Sr
K	1	-0,13	0,29	0,04	0,10	0,05	0,30	0,18	0,01	0,50	-0,02	0,23	0,04
Ca	-0,13	1	-0,03	0,55	0,09	-0,02	0,06	0,19	0,07	0,29	0,14	-0,04	0,55
S	0,29	-0,03	1	-0,03	0,12	-0,13	0,10	0,01	0,18	0,17	-0,04	-0,03	-0,03
Cl	0,04	0,55	-0,03	1	-0,03	-0,08	0,09	0,09	0,07	0,37	0,16	-0,02	1,00
Fe	0,10	0,09	0,12	-0,03	1	0,18	0,40	0,82	0,89	0,25	-0,06	0,10	-0,03
Mn	0,05	-0,02	-0,13	-0,08	0,18	1	0,23	0,35	0,04	-0,04	-0,09	-0,08	-0,08
Ti	0,30	0,06	0,10	0,09	0,40	0,23	1	0,29	0,31	0,12	0,05	0,13	0,09
Pb	0,18	0,19	0,01	0,09	0,82	0,35	0,29	1	0,65	0,42	0,03	-0,12	0,09
Zn	0,01	0,07	0,18	0,07	0,89	0,04	0,31	0,65	1	0,15	-0,06	-0,07	0,07
Cr	0,50	0,29	0,17	0,37	0,25	-0,04	0,12	0,42	0,15	1	0,32	0,03	0,37
Cu	-0,02	0,14	-0,04	0,16	-0,06	-0,09	0,05	0,03	-0,06	0,32	1,00	-0,02	0,16
As	0,23	-0,04	-0,03	-0,02	0,10	-0,08	0,13	-0,12	-0,07	0,03	-0,02	1	-0,02
Sr	0,04	0,55	-0,03	1,00	-0,03	-0,08	0,09	0,09	0,07	0,37	0,16	-0,02	1

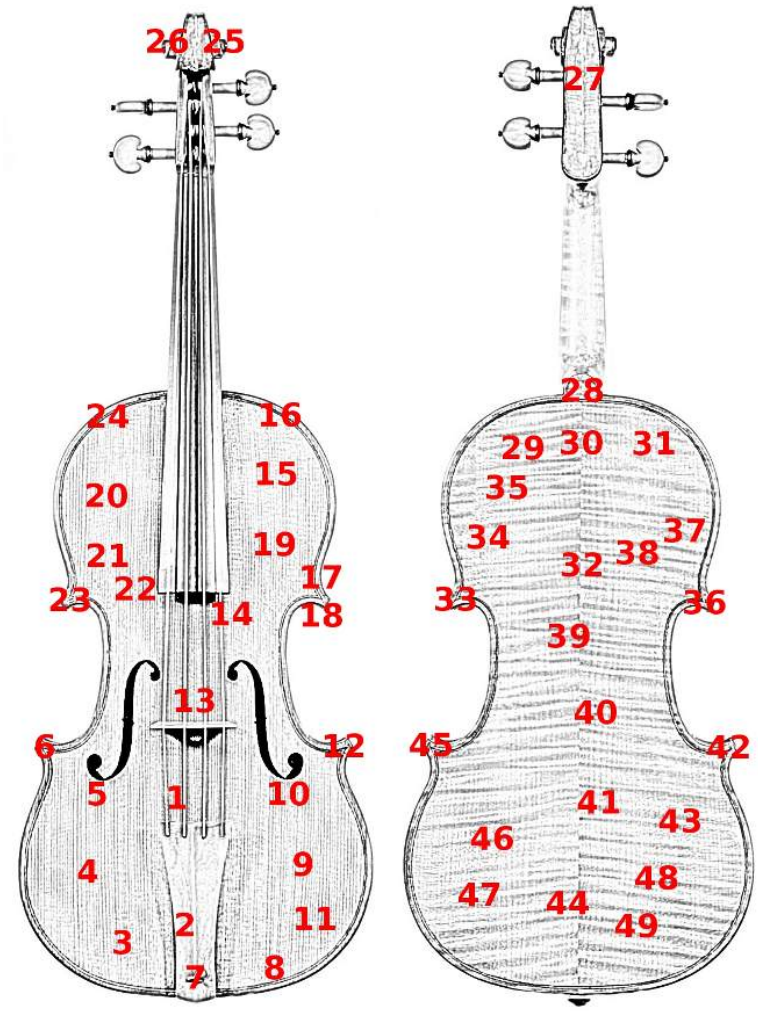

Figure A.8: The map of the spots of the cello 1374 by G. Borbon analysed by μ-XRF.

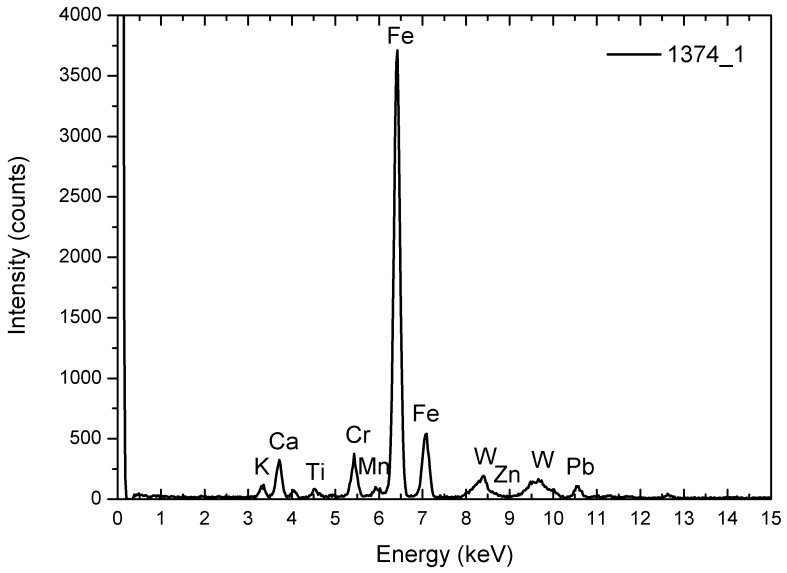

Figure A.9: XRF spectrum of the first sampled spot on the surface of the cello 1374. Tungsten peaks are attributable to the target of the instrument.

Pochette 2764

A picture under white and UV light of the instrument is shown in figure A.10.

Measures were carried out onto only seven spots because of the impossibility to reach other closer regions with the head of the μ-XRF instrument. The sampling map is shown in figure A.11.

A typical spectrum recorded on the surface of the back of the *pochette* 2764 is reported in figure A.12.

Spectra recorded on the surface of the *pochette* 2764 are similar to the ones recorded onto the violin 1338 and the cello 1372.

The XRF results for the *pochette* 2764 are reported in table A.7. They were obtained with the same procedure of the ones calculated for the other instruments hitherto considered.

The matrix of the Pearson correlation coefficients calculated between the values of the areas for each element is reported in table A.8

Figure A.10: The *pochette* 2764 by G. Borbon photographed under white (a) and UV (b) light. Picture used by permission of the "Musical Instruments Museum", Brussels.

Table A.7: XRF results obtained from *pochette* 2764 expressed as keV · counts.

Emission line	K K_{12}	Ca K_{12}	S K_{12}	Cl K_{12}	Fe K_{12}	Mn K_{12}	Ti K_{12}	Pb L_1	Zn K_{12}
2764_1	1119	1588	116	37	1387	142	0	226	140
2764_2	421	505	41	0	209	58	0	0	99
2764_3	390	448	40	0	119	68	0	0	60
2764_4	443	526	1	44	135	128	39	0	0
2764_5	553	595	0	30	297	58	0	118	109
2764_6	544	646	57	0	317	99	0	0	90
2764_7	454	492	20	0	119	128	0	0	130

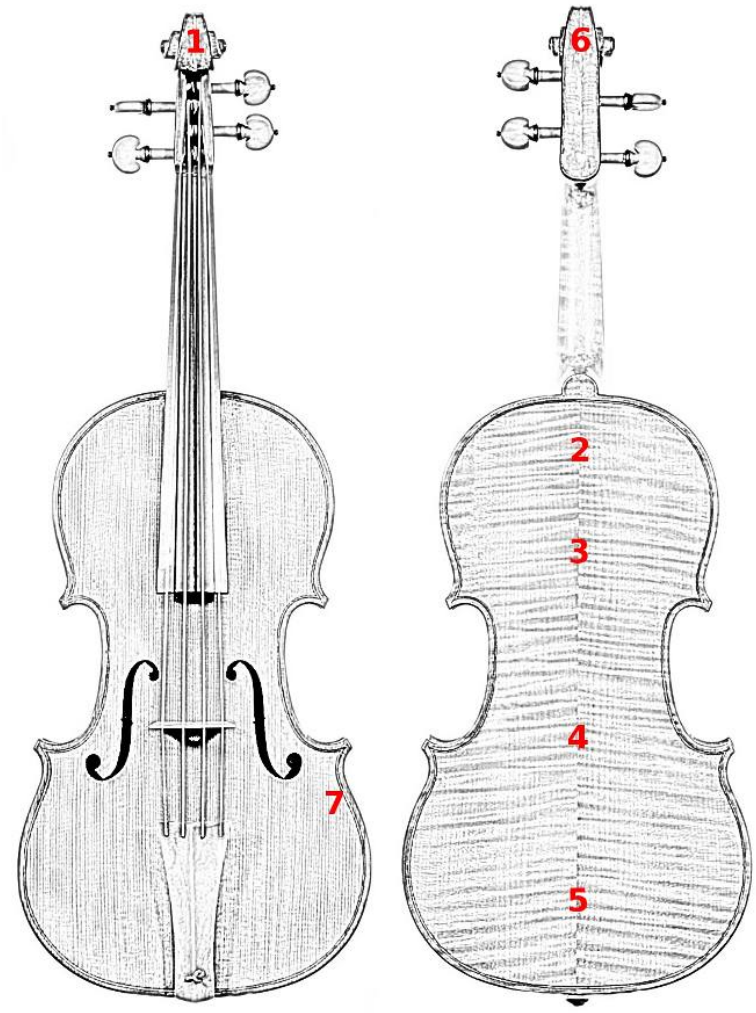

Figure A.11: The map of the spots of the *pochette* 2764 by G. Borbon analysed by μ-XRF.

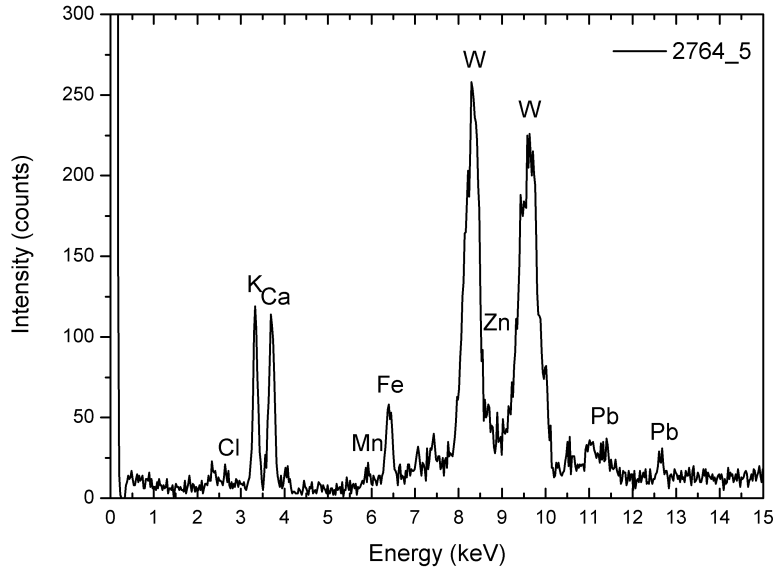

Figure A.12: XRF spectrum of the fifth sampled spot on the surface of the *pochette* 2764. Tungsten peaks are attributable to the target of the instrument.

Table A.8: Matrix of the correlation coefficients calculated between the values of the areas for each detected element on the *pochette* 2764.

	K	Ca	S	Cl	Fe	Mn	Ti	Pb	Zn
K	1	0.99	0.81	0.50	0.99	0.52	-0.20	0.92	0.53
Ca	0.99	1	0.84	0.48	1.00	0.54	-0.17	0.89	0.48
S	0.81	0.84	1	-0.01	0.85	0.36	-0.42	0.59	0.51
Cl	0.50	0.48	-0.01	1	0.46	0.42	0.61	0.59	-0.26
Fe	0.99	1.00	0.85	0.46	1	0.48	-0.23	0.90	0.51
Mn	0.52	0.54	0.36	0.42	0.48	1	0.37	0.28	0.05
Ti	-0.20	-0.17	-0.42	0.61	-0.23	0.37	1	-0.24	-0.83
Pb	0.92	0.89	0.59	0.59	0.90	0.28	-0.24	1	0.53
Zn	0.53	0.48	0.51	-0.26	0.51	0.05	-0.83	0.53	1

Violin 2774

A picture under white and UV light of the instrument is shown in figure A.13.

Figure A.13: The violin 2774 by G. Borbon photographed under white (a) and UV (b) light. Picture used by permission of the "Musical Instruments Museum", Brussels.

Measures were carried out onto 17 spots. The sampling map is shown in figure A.14.

A typical spectrum recorded on the surface of the top of the violin 2774 is reported in figure A.15.

Spectra recorded on the surface of the violin 2774 are similar to the ones recorded onto the instruments hitherto considered (excluding the cello 1374). Significant signals of copper and zinc (attributable to the secretion of human sweat [22, 79]) are noticeable in the spectra recorded on the first and second sampled spots. This is attributable to the thinner layer of residue varnish — due to a probable prolonged use of the instrument — and it is well visible when the instrument is observed under UV light (figure A.13 (b))

The XRF results for the violin 2774 are reported in table A.9. They were obtained with the same procedure of the ones calculated for the other instruments hitherto considered.

The matrix of the Pearson correlation coefficients calculated between the values of the areas for each element is reported in table A.10.

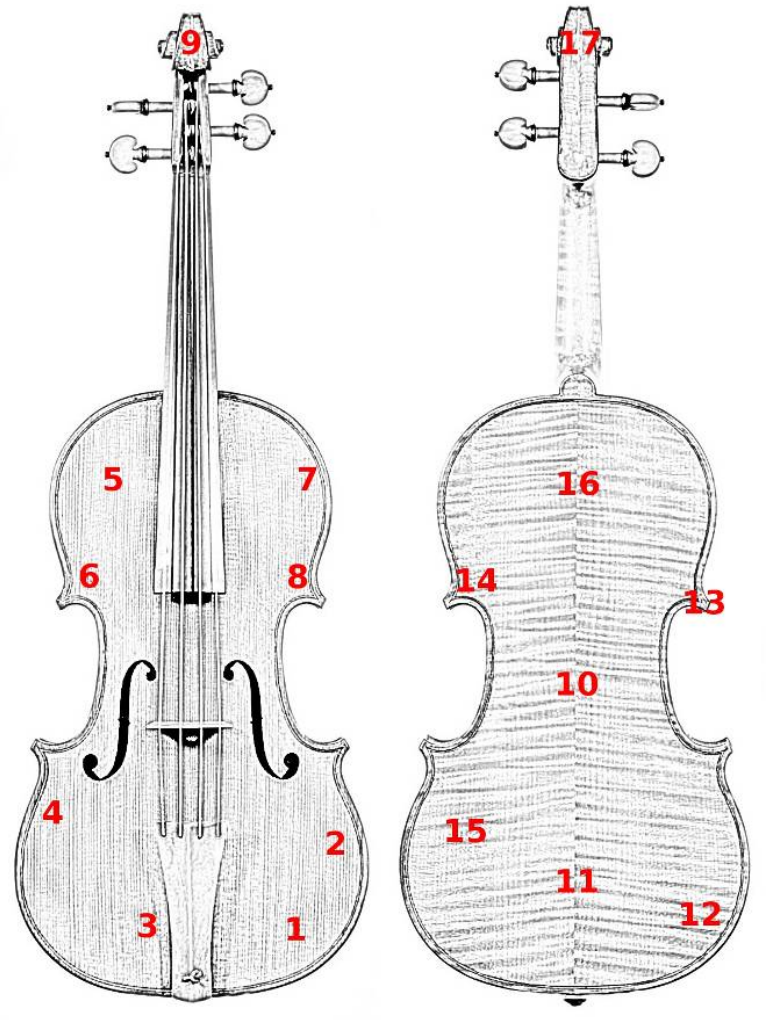

Figure A.14: The map of the spots of the violin 2774 by G. Borbon analysed by μ-XRF.

Table A.9: XRF results obtained from violin 2774 expressed as keV · counts.

Emission line	K K_{12}	Ca K_{12}	S K_{12}	Cl K_{12}	Fe K_{12}	Mn K_{12}	Ti K_{12}	Pb L_1	Zn K_{12}	Cu K_{12}
2774_1	448	1007	96	57	654	87	21	87	51	1184
2774_2	1052	1045	42	0	401	75	0	110	24	1020
2774_3	366	708	35	27	484	101	0	0	0	0
2774_4	383	469	16	0	276	63	0	0	0	0
2774_5	388	628	58	51	198	80	0	0	109	0
2774_6	637	725	75	60	278	96	0	0	72	0
2774_7	717	778	41	71	382	115	0	0	0	0
2774_8	1145	1248	94	74	1047	179	67	0	0	0
2774_9	357	1742	46	35	458	118	0	164	95	0
2774_10	313	545	52	0	267	49	0	0	0	0
2774_11	450	470	26	0	257	63	41	0	0	0
2774_12	571	905	35	31	1268	66	29	151	0	0
2774_13	613	947	0	0	1794	78	0	157	339	0
2774_14	547	1048	0	0	502	43	0	107	73	0
2774_15	279	561	9	46	145	74	0	0	0	0
2774_16	235	448	39	0	165	0	0	0	0	0
2774_17	254	455	8	44	206	52	0	141	0	0

Table A.10: Matrix of the correlation coefficients calculated between the values of the areas for each detected element on the violin 2774.

	K	Ca	S	Cl	Fe	Mn	Ti	Pb	Zn	Cu
K	1	0,46	0,37	0,24	0,42	0,61	0,49	0,06	0,07	0,31
Ca	0,46	1	0,30	0,22	0,43	0,58	0,21	0,55	0,31	0,24
S	0,37	0,30	1	0,58	-0,02	0,53	0,46	-0,29	-0,20	0,40
Cl	0,24	0,22	0,58	1	-0,02	0,69	0,28	-0,17	-0,16	0,02
Fe	0,42	0,43	-0,02	-0,02	1	0,31	0,36	0,52	0,62	0,02
Mn	0,61	0,58	0,53	0,69	0,31	1	0,49	-0,07	0,05	0,03
Ti	0,49	0,21	0,46	0,28	0,36	0,49	1	-0,11	-0,23	0,04
Pb	0,06	0,55	-0,29	-0,17	0,52	-0,07	-0,11	1	0,45	0,24
Zn	0,07	0,31	-0,20	-0,16	0,62	0,05	-0,23	0,45	1	-0,03
Cu	0,31	0,24	0,40	0,02	0,02	0,03	0,04	0,24	-0,03	1

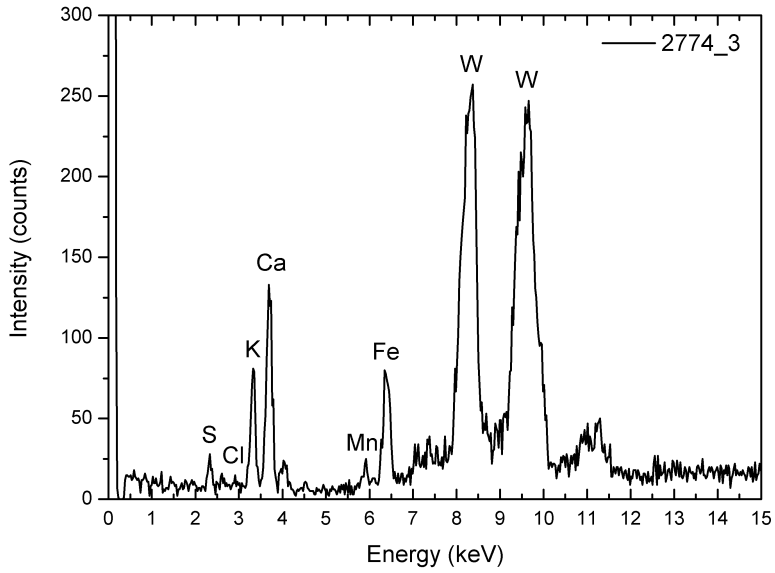

Figure A.15: XRF spectrum of the third sampled spot on the surface of the violin 2774. Tungsten peaks are attributable to the target of the instrument.

Violin 2781

A picture under white and UV light of the instrument is shown in figure A.16.

Measures were carried out onto 18 spots. The sampling map is shown in figure A.17.

A typical spectrum recorded on the surface of the top of the violin 2781 is reported in figure A.18.

Spectra recorded on the surface of the violin 2781 are similar to the ones recorded onto the instruments hitherto considered (excluding the cello 1374). Only the elemental composition of one analysed spot (already shown in the chapter of the results) is considerably different.

The XRF results for the violin 2781 are reported in table A.11. They were obtained with the same procedure of the ones calculated for the other instruments hitherto considered.

The matrix of the Pearson correlation coefficients calculated between the values of the areas for each element is reported in table A.12.

Figure A.16: The violin 2781 by B.-J. Boussu photographed under white (a) and UV (b) light. Picture used by permission of the "Musical Instruments Museum", Brussels.

Table A.11: XRF results obtained from violin 2781 expressed as keV · counts.

Emission line	K K_{12}	Ca K_{12}	S K_{12}	Cl K_{12}	Fe K_{12}	Mn K_{12}	Ti K_{12}	Pb L_1	Zn K_{12}	Sr K_{12}	Cd K_{12}	Ba L_1
2781_1	136	247	0	0	264	101	0	0	0	0	0	0
2781_2	359	564	12	35	541	112	34	0	24	0	0	0
2781_3	431	259	28	29	243	119	32	0	0	0	0	0
2781_4	97	180	50	22	808	50	0	0	500	140	212	1671
2781_5	132	257	0	0	273	147	0	0	0	0	0	0
2781_6	121	319	0	0	384	116	0	0	0	0	0	0
2781_7	244	242	0	0	173	84	0	0	19	0	0	0
2781_8	164	200	0	0	197	126	46	0	69	0	0	0
2781_9	153	221	0	0	357	106	0	0	0	0	0	0
2781_10	61	72	0	0	95	28	0	0	0	0	0	0
2781_11	115	267	0	0	222	54	0	0	0	0	0	0
2781_12	89	272	0	0	272	92	0	0	0	0	0	0
2781_13	143	249	0	0	307	70	0	0	0	0	0	0
2781_14	118	262	0	0	219	54	0	0	0	0	0	0
2781_15	327	549	0	0	519	120	42	39	136	0	0	0
2781_16	356	808	0	0	1773	133	0	72	569	98	0	0
2781_17	390	506	0	0	4291	0	0	142	896	0	0	0
2781_18	201	475	0	46	765	93	0	0	0	0	0	0

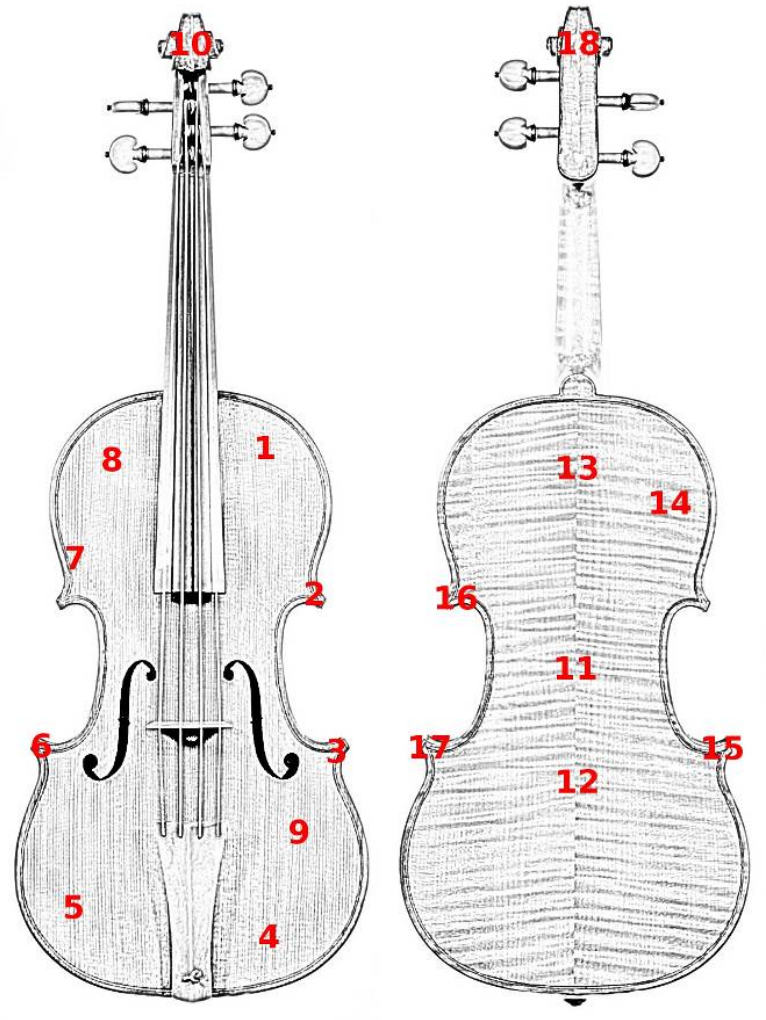

Figure A.17: The map of the spots of the violin 2781 by B.-J. Boussu analysed by μ-XRF.

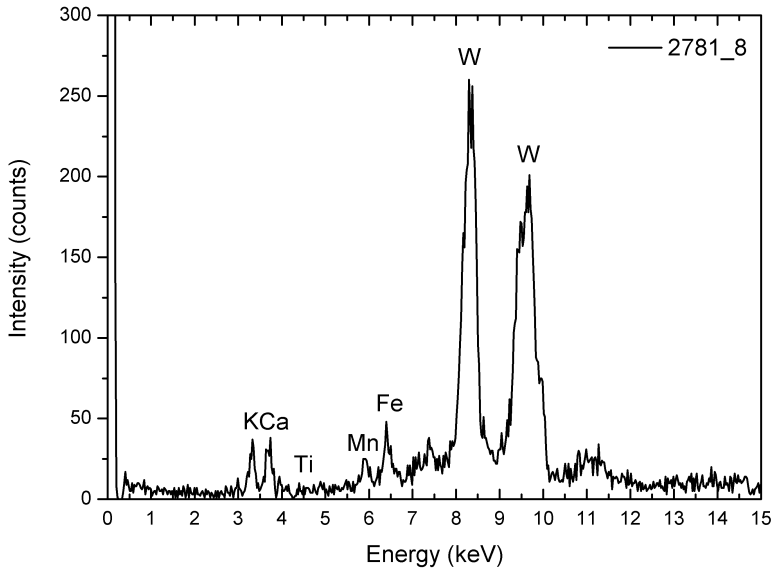

Figure A.18: XRF spectrum of the eighth sampled spot on the surface of the violin 2781. Tungsten peaks are attributable to the target of the instrument.

Table A.12: Matrix of the correlation coefficients calculated between the values of the areas for each detected element on the violin 2781.

	K	Ca	S	Cl	Fe	Mn	Ti	Pb	Zn	Sr	Cd	Ba
K	1	0,69	0,11	0,33	0,51	0,18	0,48	0,58	0,43	0,00	-0,22	-0,22
Ca	0,69	1	-0,17	0,21	0,53	0,27	0,17	0,60	0,48	0,22	-0,21	-0,21
S	0,11	-0,17	1	0,50	-0,02	-0,10	0,14	-0,15	0,25	0,66	0,85	0,85
Cl	0,33	0,21	0,50	1	-0,03	0,10	0,24	-0,20	-0,07	0,14	0,25	0,25
Fe	0,51	0,53	-0,02	-0,03	1	-0,43	-0,15	0,95	0,91	0,20	0,04	0,04
Mn	0,18	0,27	-0,10	0,10	-0,43	1	0,42	-0,34	-0,39	-0,05	-0,25	-0,25
Ti	0,48	0,17	0,14	0,24	-0,15	0,42	1	-0,05	-0,13	-0,18	-0,13	-0,13
Pb	0,58	0,60	-0,15	-0,20	0,95	-0,34	-0,05	1	0,88	0,15	-0,09	-0,09
Zn	0,43	0,48	0,25	-0,07	0,91	-0,39	-0,13	0,88	1	0,56	0,37	0,37
Sr	0,00	0,22	0,66	0,14	0,20	-0,05	-0,18	0,15	0,56	1	0,81	0,81
Cd	-0,22	-0,21	0,85	0,25	0,04	-0,25	-0,13	-0,09	0,37	0,81	1	1,00
Ba	-0,22	-0,21	0,85	0,25	0,04	-0,25	-0,13	-0,09	0,37	0,81	1,00	1

Violin 2782

A picture under white and UV light of the instrument is shown in figure A.19.

Figure A.19: The violin 2782 by B.-J. Boussu photographed under white (a) and UV (b) light. Picture used by permission of the "Musical Instruments Museum", Brussels.

Measures were carried out onto 22 spots. The sampling map is shown in figure A.20.

A typical spectrum recorded on the surface of the top of the violin 2782 is reported in figure A.21.

Spectra recorded on the surface of the violin 2782 are similar to the ones recorded onto the instruments hitherto considered (excluding the cello 1374).

The XRF results for the violin 2782 are reported in table A.13. They were obtained with the same procedure of the ones calculated for the other instruments hitherto considered.

The matrix of the Pearson correlation coefficients calculated between the values of the areas for each element is reported in table A.14.

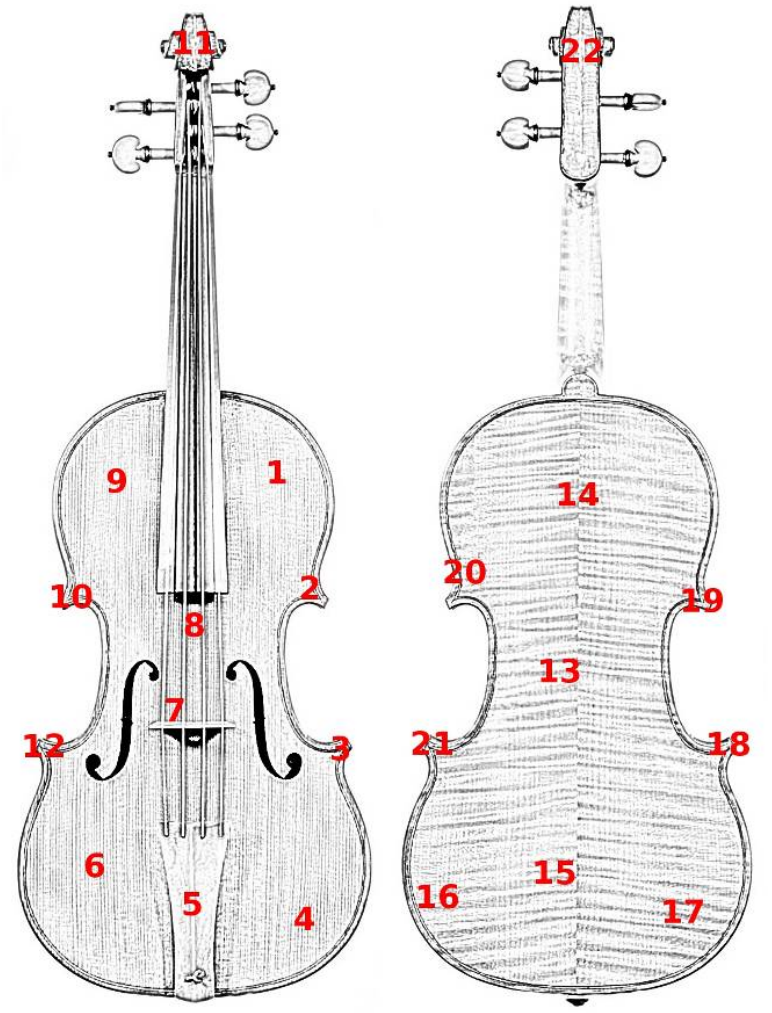

Figure A.20: The map of the spots of the violin 2782 by B.-J. Boussu analysed by μ-XRF.

Table A.13: XRF results obtained from violin 2782 expressed as keV · counts.

Emission line	K K_{12}	Ca K_{12}	S K_{12}	Cl K_{12}	Fe K_{12}	Mn K_{12}	Ti K_{12}	Pb L_1	Zn K_{12}	Sr K_{12}	Cu K_{12}
2782_1	738	769	0	6	441	129	0	0	163	0	0
2782_2	1021	1418	113	65	2222	82	93	94	377	0	0
2782_3	498	604	4	45	455	72	0	0	0	0	0
2782_4	271	417	12	33	197	118	0	0	33	0	0
2782_5	210	730	0	36	576	146	0	0	0	0	0
2782_6	505	693	26	63	411	105	0	117	103	0	0
2782_7	597	1185	66	48	792	117	50	0	146	0	0
2782_8	190	821	0	20	1490	104	82	57	98	77	0
2782_9	424	535	0	63	269	95	0	0	42	0	0
2782_10	293	1345	53	38	1285	84	55	76	128	0	0
2782_11	440	952	1	28	701	61	0	158	198	0	974
2782_12	360	624	0	0	461	145	0	0	61	0	0
2782_13	140	326	0	0	287	82	0	75	0	0	0
2782_14	253	346	0	38	139	40	0	0	0	0	0
2782_15	254	383	0	66	206	65	0	0	70	0	0
2782_16	305	423	0	39	293	57	0	0	26	0	0
2782_17	455	718	24	62	1128	53	0	0	132	0	0
2782_18	188	295	0	0	440	64	0	0	0	0	0
2782_19	276	560	30	25	438	79	45	0	0	0	0
2782_20	357	516	0	43	272	55	0	0	59	0	0
2782_21	355	400	0	0	342	55	44	77	0	0	0
2782_22	699	1873	71	63	1212	64	39	145	148	0	1028

Table A.14: Matrix of the correlation coefficients calculated between the values of the areas for each detected element on the violin 2782.

	K	Ca	S	Cl	Fe	Mn	Ti	Pb	Zn	Sr	Cu
K	1	0,66	0,71	0,42	0,55	0,07	0,36	0,32	0,81	-0,22	0,26
Ca	0,66	1	0,81	0,40	0,77	0,11	0,60	0,57	0,72	0,05	0,56
S	0,71	0,81	1	0,48	0,76	0,00	0,69	0,39	0,73	-0,13	0,20
Cl	0,42	0,40	0,48	1	0,29	-0,20	0,09	0,10	0,39	-0,15	0,15
Fe	0,55	0,77	0,76	0,29	1	0,03	0,79	0,45	0,79	0,36	0,20
Mn	0,07	0,11	0,00	-0,20	0,03	1	0,02	-0,18	0,06	0,14	-0,24
Ti	0,36	0,60	0,69	0,09	0,79	0,02	1	0,35	0,52	0,47	0,02
Pb	0,32	0,57	0,39	0,10	0,45	-0,18	0,35	1	0,49	0,09	0,70
Zn	0,81	0,72	0,73	0,39	0,79	0,06	0,52	0,49	1	0,04	0,32
Sr	-0,22	0,05	-0,13	-0,15	0,36	0,14	0,47	0,09	0,04	1	-0,07
Cu	0,26	0,56	0,20	0,15	0,20	-0,24	0,02	0,70	0,32	-0,07	1

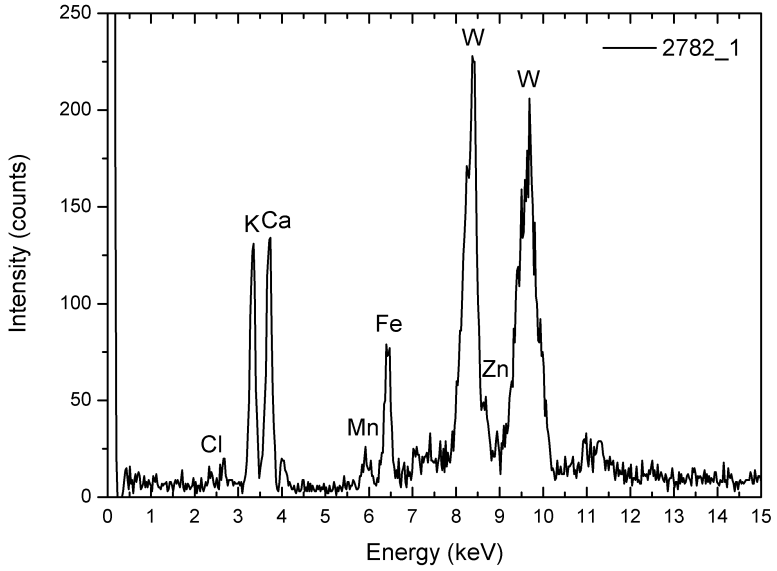

Figure A.21: XRF spectrum of the first sampled spot on the surface of the violin 2782. Tungsten peaks are attributable to the target of the instrument.

Violin 2784

A picture under white and UV light of the instrument is shown in figure A.22.

Measures were carried out onto 25 spots. The sampling map is shown in figure A.23.

A typical spectrum recorded on the surface of the top of the violin 2784 is reported in figure A.24.

Spectra recorded on the surface of the violin 2784 are similar to the ones recorded onto the instruments hitherto considered (excluding the cello 1374).

The XRF results for the violin 2784 are reported in table A.15. They were obtained with the same procedure of the ones calculated for the other instruments hitherto considered.

The matrix of the Pearson correlation coefficients calculated between the values of the areas for each element is reported in table A.16.

Figure A.22: The violin 2784 by B.-J. Boussu photographed under white (a) and UV (b) light. Picture used by permission of the "Musical Instruments Museum", Brussels.

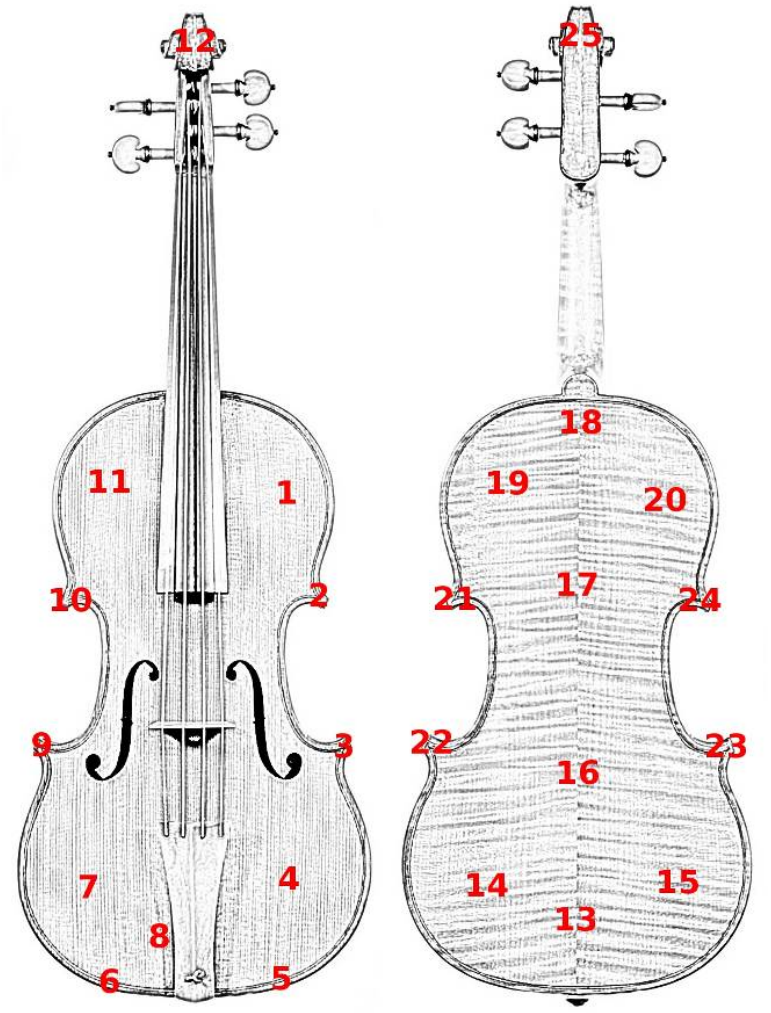

Figure A.23: The map of the spots of the violin 2784 by B.-J. Boussu analysed by μ-XRF.

Table A.15: XRF results obtained from violin 2784 expressed as keV · counts.

Emission line	K K_{12}	Ca K_{12}	S K_{12}	Cl K_{12}	Fe K_{12}	Mn K_{12}	Ti K_{12}	Pb L_1	Zn K_{12}	Cu K_{12}
2784_1	173	150	0	0	151	49	0	0	0	0
2784_2	504	299	0	0	219	85	0	0	33	0
2784_3	202	715	0	0	832	105	41	102	0	0
2784_4	109	227	1	18	353	96	0	0	0	0
2784_5	674	488	68	41	223	60	25	58	127	0
2784_6	1065	716	137	63	519	69	0	144	124	880
2784_7	190	152	0	0	115	62	0	0	0	0
2784_8	251	597	28	54	299	144	0	0	0	0
2784_9	193	410	0	0	336	76	0	71	1	0
2784_10	142	656	0	0	1776	79	66	168	0	796
2784_11	160	193	0	0	151	76	0	0	0	0
2784_12	206	304	23	0	175	42	0	0	0	0
2784_13	142	397	0	0	610	91	44	63	0	0
2784_14	110	199	0	0	133	0	0	0	0	0
2784_15	222	428	0	0	233	77	0	0	0	0
2784_16	178	437	0	0	246	48	0	114	0	0
2784_17	171	273	0	0	217	0	0	0	0	0
2784_18	198	242	0	0	184	72	42	0	72	0
2784_19	186	433	0	0	500	161	0	0	0	0
2784_20	194	326	0	0	195	77	0	103	0	0
2784_21	258	515	0	0	592	53	0	0	0	0
2784_22	133	396	13	25	321	70	0	0	0	0
2784_23	163	283	0	0	152	0	0	0	0	0
2784_24	187	298	0	0	247	0	0	0	0	0
2784_25	251	400	0	0	366	84	32	0	0	0

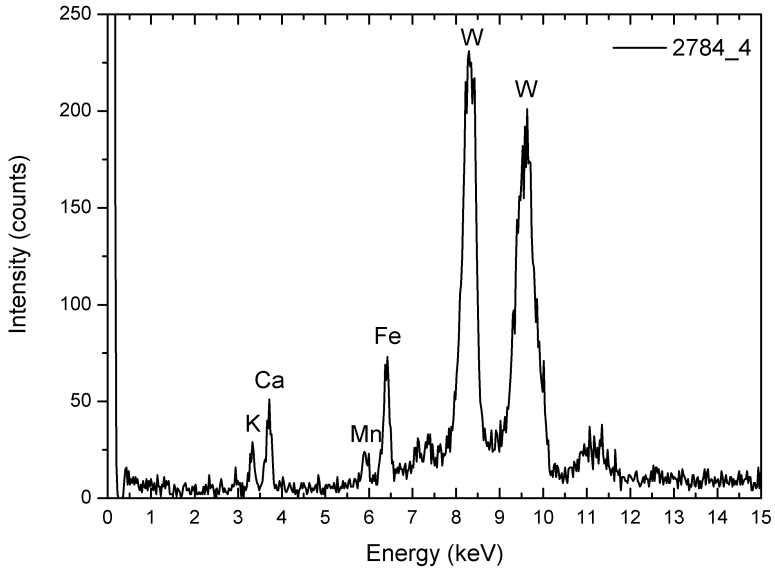

Figure A.24: XRF spectrum of the fourth sampled spot on the surface of the violin 2784. Tungsten peaks are attributable to the target of the instrument.

Table A.16: Matrix of the correlation coefficients calculated between the values of the areas for each detected element on the violin 2784.

	K	Ca	S	Cl	Fe	Mn	Ti	Pb	Zn	Cu
K	1	0,45	0,91	0,70	-0,01	0,07	-0,06	0,35	0,86	0,54
Ca	0,45	1	0,48	0,49	0,66	0,42	0,39	0,66	0,29	0,56
S	0,91	0,48	1	0,84	0,02	0,05	-0,07	0,38	0,81	0,61
Cl	0,70	0,49	0,84	1	-0,01	0,26	-0,12	0,21	0,63	0,41
Fe	-0,01	0,66	0,02	-0,01	1	0,29	0,70	0,64	-0,06	0,66
Mn	0,07	0,42	0,05	0,26	0,29	1	0,22	0,13	0,01	0,05
Ti	-0,06	0,39	-0,07	-0,12	0,70	0,22	1	0,46	0,15	0,33
Pb	0,35	0,66	0,38	0,21	0,64	0,13	0,46	1	0,29	0,69
Zn	0,86	0,29	0,81	0,63	-0,06	0,01	0,15	0,29	1	0,41
Cu	0,54	0,56	0,61	0,41	0,66	0,05	0,33	0,69	0,41	1

Violin 2836

A picture under white and UV light of the instrument is shown in figure A.25.

Figure A.25: The violin 2836 by G. Borbon photographed under white (a) and UV (b) light. Picture used by permission of the "Musical Instruments Museum", Brussels.

Measures were carried out onto 21 spots. The sampling map is shown in figure A.26.

A typical spectrum recorded on the surface of the top of the violin 2836 is reported in figure A.27.

The spectra recorded on the *stripe* on the upper right part of the top (in black under UV light, figure A.25 (b); spots 10, 11 and 12), show a very high content of lead with respect to the other ones. This could be due to a lump of the varnish. Spectra recorded on the surface of the violin 2836 features the presence of iron, relative low content of manganese and a considerable amount of zinc.

The XRF results for the violin 2836 are reported in table A.17. They were obtained with the same procedure of the ones calculated for the other instruments hitherto considered.

The matrix of the Pearson correlation coefficients calculated between the values of the areas for each element is reported in table A.18.

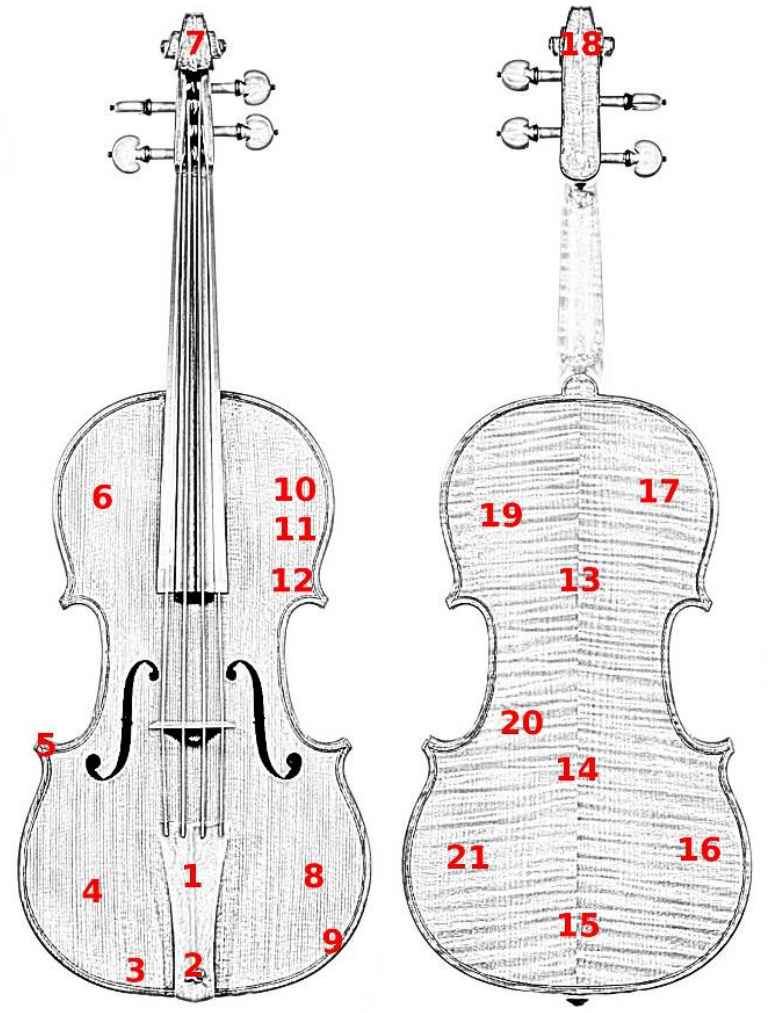

Figure A.26: The map of the spots of the violin 2836 by G. Borbon analysed by μ-XRF.

Table A.17: XRF results obtained from violin 2836 expressed as keV · counts.

Emission line	K K_{12}	Ca K_{12}	S K_{12}	Cl K_{12}	Fe K_{12}	Mn K_{12}	Ti K_{12}	Pb L_1	Zn K_{12}	Cu K_{12}	Sr K_{12}
2836_1	317	555	0	0	202	76	0	0	34	0	0
2836_2	479	1220	0	0	1187	83	39	424	170	936	0
2836_3	272	948	0	0	5963	61	187	8824	151	331	0
2836_4	126	585	0	0	324	219	0	0	0	0	0
2836_5	571	917	0	0	3845	638	25	151	115	0	0
2836_6	135	492	9	0	104	170	0	0	0	0	0
2836_7	214	1779	0	0	3048	71	32	316	0	0	0
2836_8	169	516	26	0	152	165	0	0	43	0	0
2836_9	330	867	45	46	1163	190	56	0	117	0	0
2836_10	15	210	0	0	358	0	0	24966	0	106	0
2836_11	124	2688	0	0	715	0	0	6571	175	0	170
2836_12	365	874	0	0	7614	179	84	24103	527	0	0
2836_13	230	313	27	0	191	0	0	0	0	0	0
2836_14	53	621	0	0	930	0	31	8984	0	0	0
2836_15	381	413	0	51	157	0	0	0	34	0	0
2836_16	186	442	0	0	131	0	0	0	0	0	0
2836_17	145	334	0	0	132	49	0	0	0	0	0
2836_18	388	916	47	37	789	67	31	0	103	0	0
2836_19	633	1049	58	40	1880	55	76	0	64	0	0
2836_20	145	1114	39	0	1769	44	37	0	92	808	0
2836_21	232	487	17	30	210	58	0	0	0	0	0

Table A.18: Matrix of the correlation coefficients calculated between the values of the areas for each detected element on the violin 2836.

	K	Ca	S	Cl	Fe	Mn	Ti	Pb	Zn	Cu	Sr
K	1	0,12	0,33	0,47	0,35	0,43	0,34	-0,25	0,36	0,10	-0,19
Ca	0,12	1	0,00	-0,08	0,27	-0,01	0,20	-0,03	0,34	0,19	0,75
S	0,33	0,00	1	0,57	-0,14	-0,07	0,13	-0,32	-0,05	0,04	-0,15
Cl	0,47	-0,08	0,57	1	-0,17	-0,11	0,06	-0,26	-0,05	-0,22	-0,12
Fe	0,35	0,27	-0,14	-0,17	1	0,34	0,78	0,49	0,77	0,12	-0,08
Mn	0,43	-0,01	-0,07	-0,11	0,34	1	0,05	-0,12	0,21	-0,12	-0,16
Ti	0,34	0,20	0,13	0,06	0,78	0,05	1	0,27	0,50	0,28	-0,15
Pb	-0,25	-0,03	-0,32	-0,26	0,49	-0,12	0,27	1	0,52	-0,04	0,09
Zn	0,36	0,34	-0,05	-0,05	0,77	0,21	0,50	0,52	1	0,18	0,19
Cu	0,10	0,19	0,04	-0,22	0,12	-0,12	0,28	-0,04	0,18	1	-0,09
Sr	-0,19	0,75	-0,15	-0,12	-0,08	-0,16	-0,15	0,09	0,19	-0,09	1

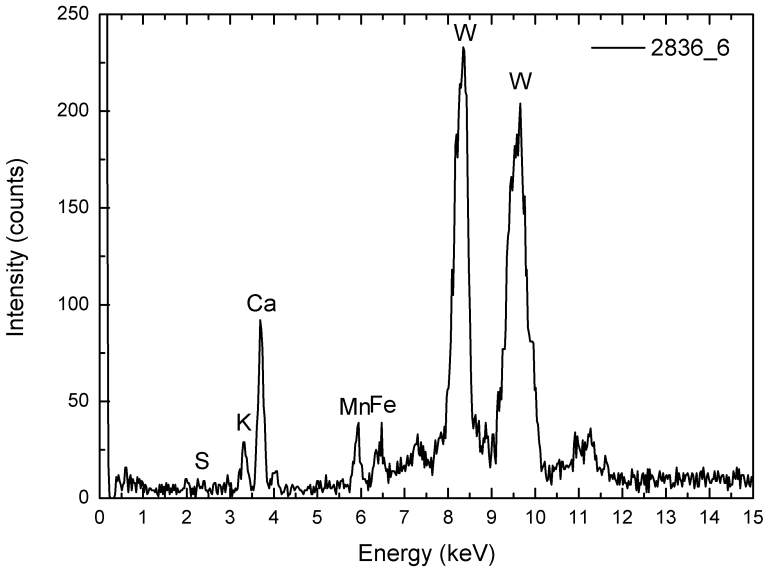

Figure A.27: XRF spectrum of the sixth sampled spot on the surface of the violin 2836. Tungsten peaks are attributable to the target of the instrument.

Appendix B

FTIR spectra and band assignments of reference materials

The FTIR spectra and the relative band assignments of the reference materials used in this work of thesis are reported in this appendix.

B.1 Diterpenic resins

Venetian Turpentine

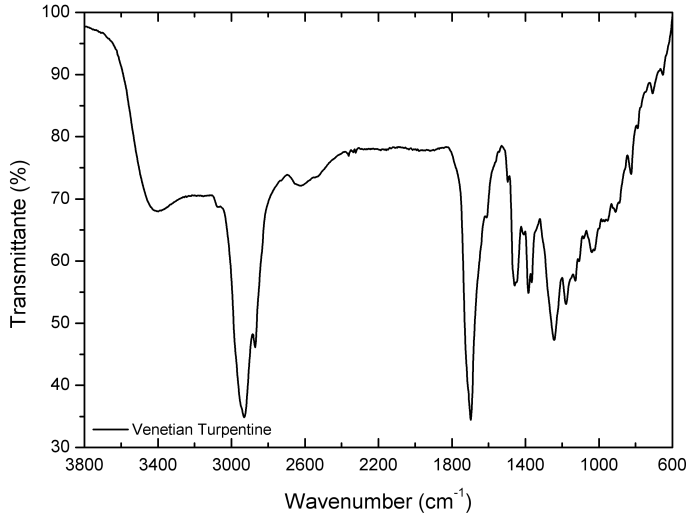

Figure B.1: Normalized FTIR spectrum of a microsample of Venetian turpentine.

Table B.1: Positions of the bands in the FTIR spectrum of the Venetian turpentine resin and their attribution.

Range (cm^{-1})	Bond and vibration
3710-3200	O-H stretching
3120-2700	C-H stretching
1810-1640	C=O stretching
1640-1580	C-C bending
1520-1320	C-H bending
1320-850	C-O stretching

Colophony

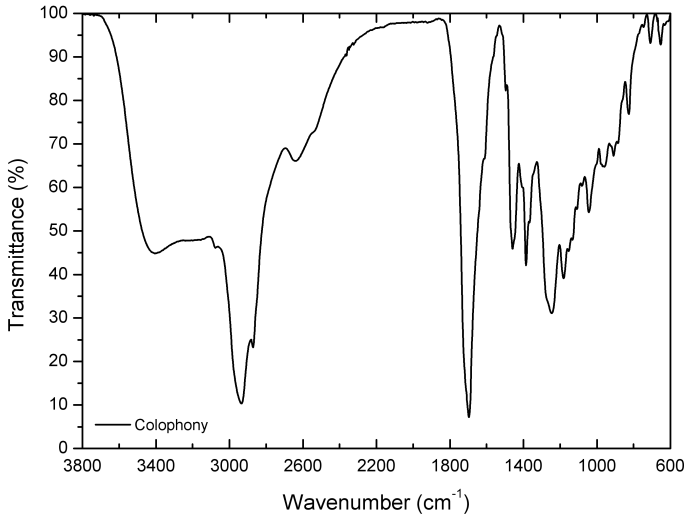

Figure B.2: Normalized FTIR spectrum of a microsample of colophony.

Table B.2: Positions of the bands in the FTIR spectrum of the colophony resin and their attribution.

Range (cm^{-1})	Bond and vibration
3700-3200	O-H stretching
3100-2700	C-H stretching
1840-1650	C=O stretching
1650-1580	C-C bending
1510-1320	C-H bending
1320-850	C-O stretching

Strasbourg Turpentine

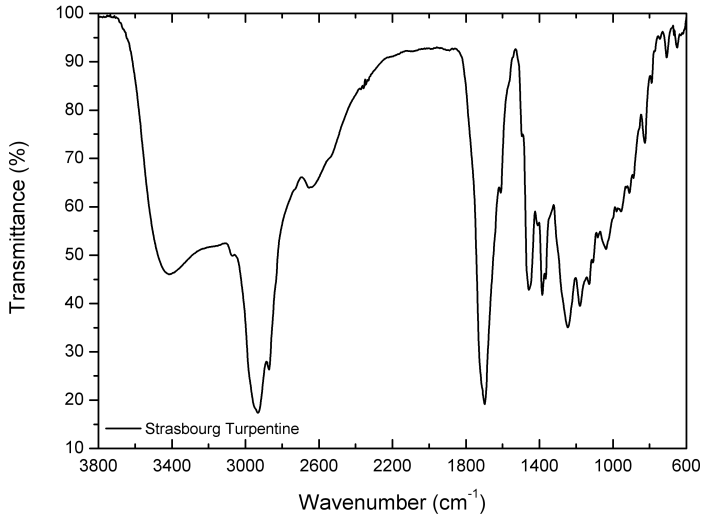

Figure B.3: Normalized FTIR spectrum of a microsample of Strasbourg turpentine.

Table B.3: Positions of the bands in the FTIR spectrum of the Strasbourg turpentine resin and their attribution.

Range (cm^{-1})	Bond and vibration
3700-3180	O-H stretching
3110-2690	C-H stretching
1850-1630	C=O stretching
1630-1580	C-C bending
1520-1320	C-H bending
1320-850	C-O stretching

Sandarac

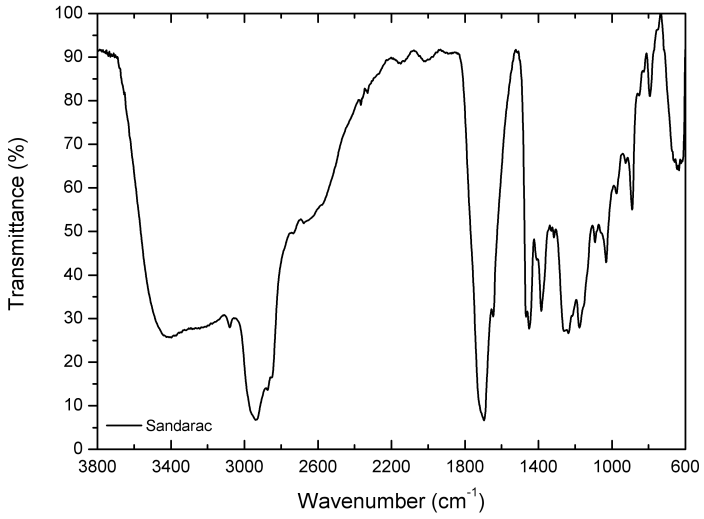

Figure B.4: Normalized FTIR spectrum of a microsample of sandarac.

Table B.4: Positions of the bands in the FTIR spectrum of the sandarac resin and their attribution.

Range (cm^{-1})	Bond and vibration
3730-3160	O-H stretching
3110-2690	C-H stretching
1840-1660	C=O stretching
1660-1620	C-C bending
1510-1330	C-H bending
1310-860	C-O stretching

Copal

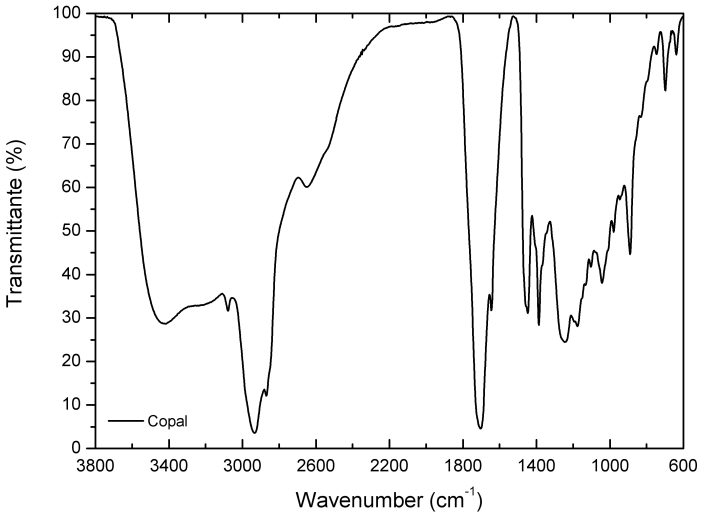

Figure B.5: Normalized FTIR spectrum of a microsample of copal.

Table B.5: Positions of the bands in the FTIR spectrum of the copal resin and their attribution.

Range (cm^{-1})	Bond and vibration
3730-3150	O-H stretching
3110-2700	C-H stretching
1850-1660	C=O stretching
1660-1620	C-C bending
1520-1330	C-H bending
1320-850	C-O stretching

B.2 Triterpenic resins

Mastic

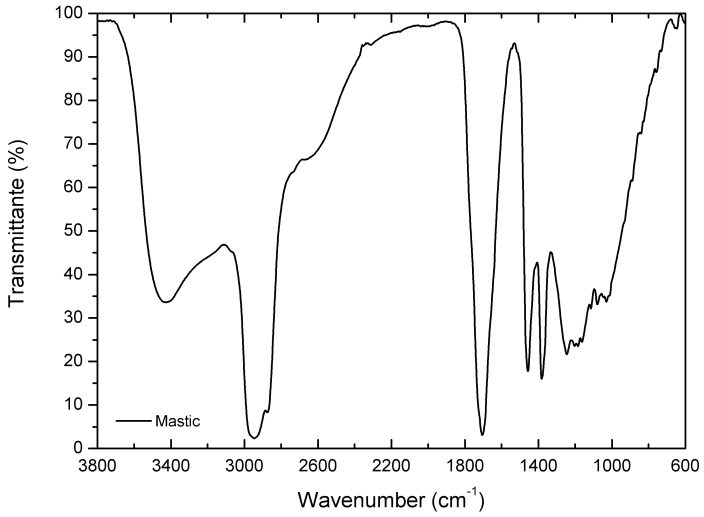

Figure B.6: Normalized FTIR spectrum of a microsample of mastic.

Table B.6: Positions of the bands in the FTIR spectrum of the mastic resin and their attribution.

Range (cm^{-1})	Bond and vibration
3700-3120	O-H stretching
3100-2730	C-H stretching
1850-1540	C=O stretching and C-C bending
1530-1330	C-H bending
1330-900	C-O stretching

Elemi

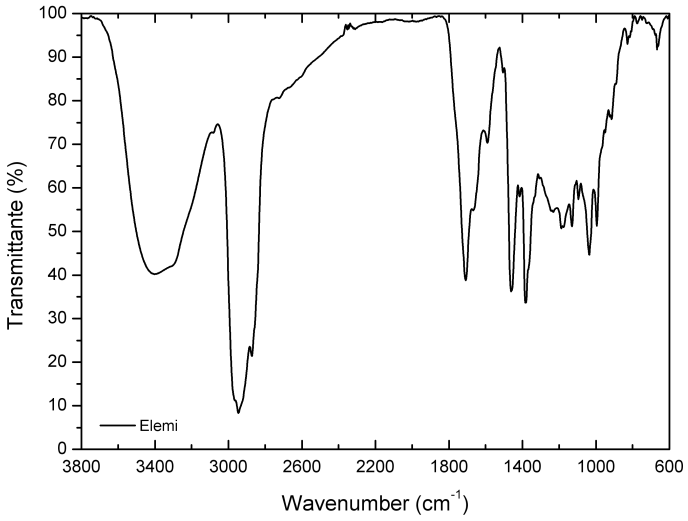

Figure B.7: Normalized FTIR spectrum of a microsample of elemi.

Table B.7: Positions of the bands in the FTIR spectrum of the elemi resin and their attribution.

Range (cm^{-1})	Bond and vibration
3730-3060	O-H stretching
3060-2750	C-H stretching
1820-1680	C=O stretching
1680-1630	C-C bending
1500-1320	C-H bending
1300-840	C-O stretching

Dammar

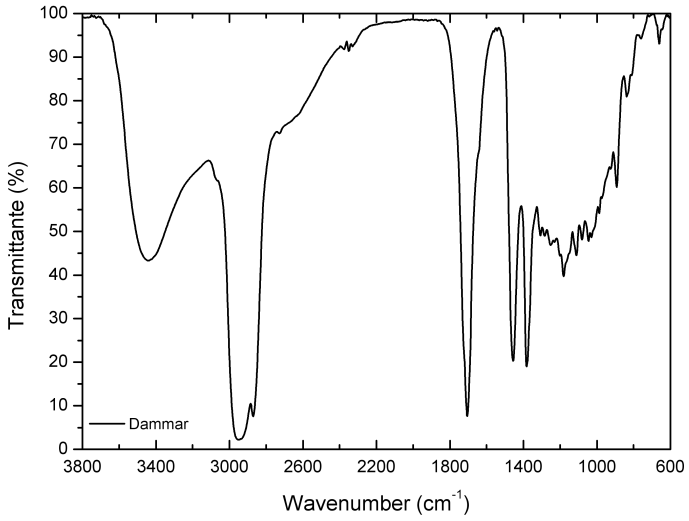

Figure B.8: Normalized FTIR spectrum of a microsample of dammar.

Table B.8: Positions of the bands in the FTIR spectrum of the dammar resin and their attribution.

Range (cm^{-1})	Bond and vibration
3710-3120	O-H stretching
3120-2730	C-H stretching
1860-1650	C=O stretching
1650-1620	C-C bending
1500-1330	C-H bending
1320-910	C-O stretching

B.3 Fossil and insect resins

Baltic Amber

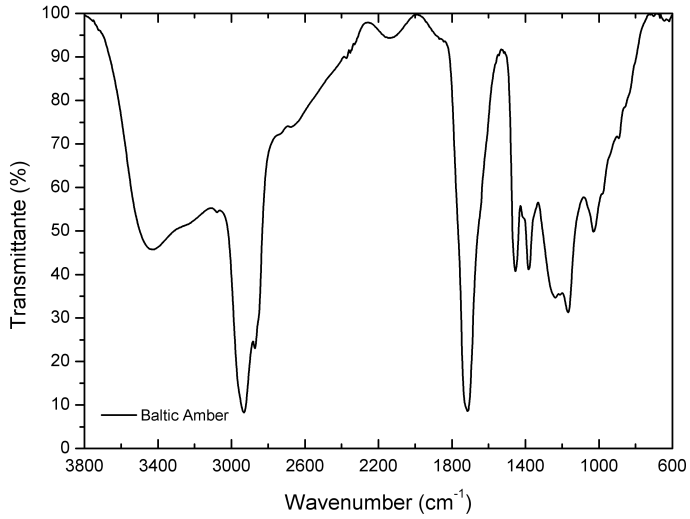

Figure B.9: Normalized FTIR spectrum of a microsample of Baltic amber.

Table B.9: Positions of the bands in the FTIR spectrum of the Baltic amber resin and their attribution.

Range (cm^{-1})	Bond and vibration
3800-3090	O-H stretching
3060-2760	C-H stretching
1830-1530	C=O stretching and C-C bending
1510-1330	C-H bending
1330-910	C-O stretching

Shellac

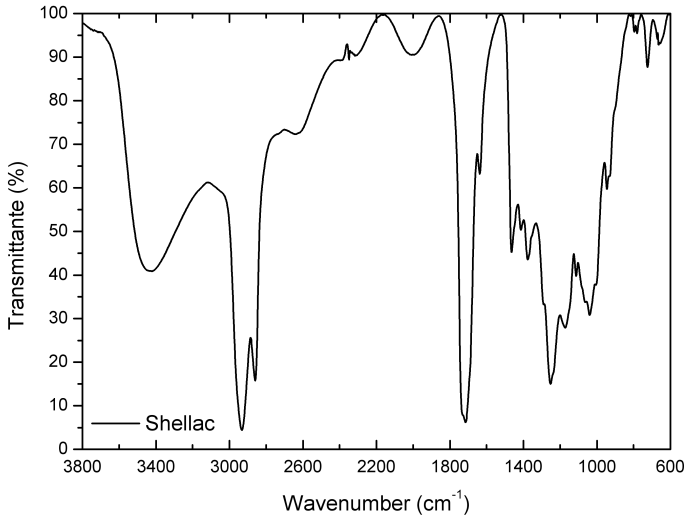

Figure B.10: Normalized FTIR spectrum of a microsample of shellac.

Table B.10: Positions of the bands in the FTIR spectrum of the shellac resin and their attribution.

Range (cm^{-1})	Bond and vibration
3680-3110	O-H stretching
3110-2760	C-H stretching
1850-1650	C=O stretching
1650-1610	C-C bending
1520-1330	C-H bending
1330-830	C-O stretching

B.4 Gum and Beeswax

Dragon's Blood

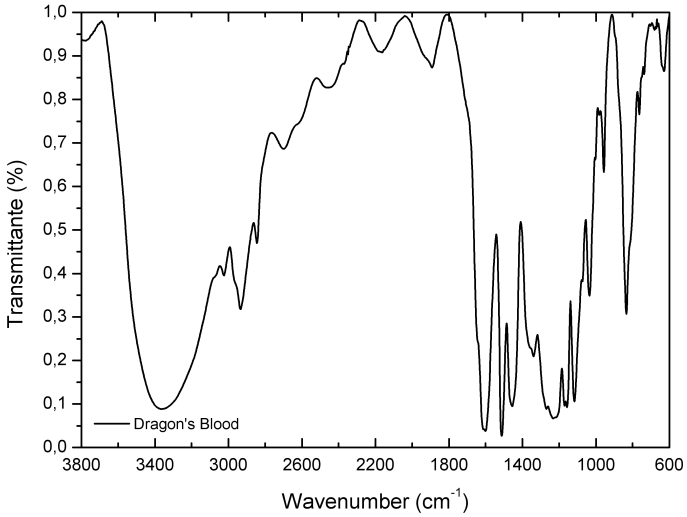

Figure B.11: Normalized FTIR spectrum of a microsample of Dragon's Blood.

Table B.11: Positions of the bands in the FTIR spectrum of the Dragon's Blood dye and their attribution.

Range (cm^{-1})	Bond and vibration
3690-3050	O-H stretching
3000-2770	C-H stretching
1810-1540	C=O stretching and C=C stretching
1540-1480	aromatic skeletal stretching
1480-1320	C-H bending
1320-910	C-O stretching

Beeswax

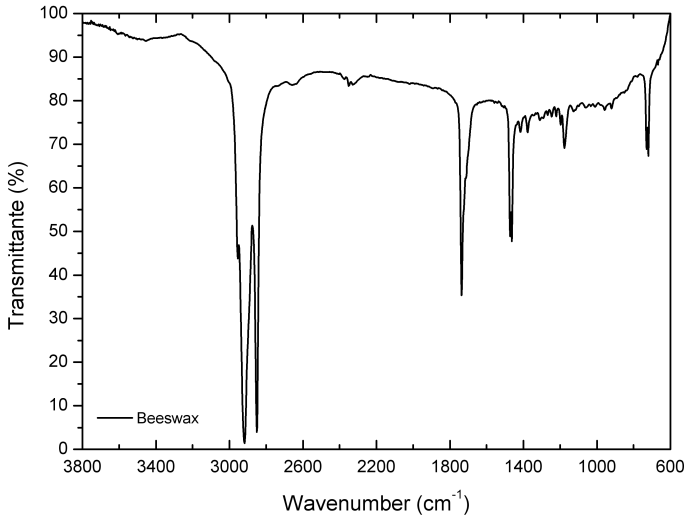

Figure B.12: Normalized FTIR spectrum of a microsample of beeswax.

Table B.12: Positions of the bands in the FTIR spectrum of the beeswax and their attribution.

Range (cm^{-1})	Bond and vibration
3800-3260	O-H stretching
3000-2750	C-H stretching
1770-1650	C=O stretching
1500-1430	C-H bending
1200-1140	C-O stretching
750-690	C-H torsion

Appendix C

Scientific activity

- Publications

  1. **F. Caruso**, C. Di Stefano, M.L. Saladino, and E. Caponetti. X-Ray Fluorescence spectroscopy applied to the study of three Sicilian works of art. In E.A. Varella and E. Caponetti, editors, *Proceedings of the 2nd Residential Summer School – Chemistry and Conservation Science 2008*, pages 77–85, 2009. ISBN 978-88-86208-60-4;
  2. **A. Spinella**, F. Caruso, and E. Caponetti. Solid state NMR application in the cultural heritage field. In E.A. Varella and E. Caponetti, editors, *Proceedings of the 2nd Residential Summer School – Chemistry and Conservation Science 2008*, pages 261–270, 2009. ISBN 978-88-86208-60-4;
  3. **F. Caruso**, S. Orecchio, M.G. Cicero, and C. Di Stefano. Determinazione di componenti della vernice e della colla del contrabbasso "Panormo" di Vincenzo Trusiano. In Regione Siciliana. Assessorato dei Beni Culturali, Ambientali e della Pubblica Istruzione. Dipartimento dei Beni Culturali, Ambientali e dell'Educazione Permanente. Centro Regionale per la Progettazione e il Restauro, editor, *Science and Cultural Heritage in the Mediterranean Area. Proceedings of the 3rd international congress "La materia e i segni della storia"*, pages 614–620, 2009. ISBN 978-88-6164-086-3;
  4. **M.G. Cicero**, C. Di Stefano, M.P. Casaletto, and F. Caruso. Un protocollo scientifico per la desalinizzazione di materiali lapidei: caso studio dei mosaici della Villa del Casale (Sicilia). In Regione Siciliana. Assessorato dei Beni Culturali, Ambientali e della Pubblica Istruzione. Dipartimento dei Beni Culturali, Ambientali e dell'Educazione Permanente. Centro Regionale per la Progettazione e il Restauro, editor, *Science and Cultural Heritage*

in the Mediterranean Area. Proceedings of the 3rd international congress "La materia e i segni della storia", pages 174–179, 2009. ISBN 978-88-6164-086-3;

5. **F. Caruso**, F. Giannici, M.A. Floriano and F. Caruso. A new procedure for the lightning experiment: Mn_2O_7 and ethanol. *The Chemical Educator*, 15:108–109, 2010. doi: 1007/s00897102220a;
6. **F. Caruso**, M.L. Saladino, A. Spinella, C. Di Stefano, P. Tisseyre, S. Tusa, and E. Caponetti. Physico-Chemical Characterization of the Acqualadrone *rostrum*. *Archaeometry*, XX:XXX-XXX, 2011. doi: 10.1111/j.1475-4754.2010.00567.x. In press;
7. **F. Caruso**, D.F. Chillura Martino, S. Saverwyns, M. Van Bos, L. Burgio, C. Di Stefano, and E. Caponetti. Multi-Analytical Approach to the Study of Varnishes from Historical Musical Instruments. In preparation;
8. **F. Caruso**, S. Saverwyns, M. Van Bos, D.F. Chillura Martino, and E. Caponetti. Micro-X-Ray Fluorescence Characterisation of the Varnish of Historical Low Countries Stringed Musical Instruments. In preparation;
9. **P. Frank**, F. Caruso, R. Sarangi, E. Caponetti, B. Hedman, and K.O. Hodgson. Sulfur and Volatiles in the Wood of the Acqualadrone Roman Ram After 2300 Years. In preparation.

- Participation and Communications to Scientific Congresses and Conferences

1. Scienza e Beni Culturali. V Congresso Nazionale di Archeometria. Siracusa (Italy), 26^{th}–29^{th} February 2008. Poster Presentation. E. Caponetti, D.F. Chillura Martino, **F. Caruso**, F. Di Maggio, "X-ray Fluorescence (XRF) analysis of a decorated 18^{th} century Sicilian floor tile";
2. 2^{nd} Residential Summer School: Chemistry and Conservation Science 2008. Università degli Studi di Palermo (Italy), 20^{th}–27^{th} July 2008. Invited Oral Contribution. C. Di Stefano, **F. Caruso**, "X-Ray Fluorescence (XRF) Spectroscopy Practical Information";
3. IV Convegno Congiunto delle Sezioni SCI Calabria e Sicilia 2008. Arcavacata di Rende (CS) (Italy), 1^{st}–2^{nd} December 2008. Oral Contribution. **M.L. Saladino**, D. Chillura Martino, F. Caruso, A. Zanotto, E. Caponetti, "Application of HR-TEM, Solid State NMR and SAXS techniques in the Cultural Heritage field";
4. Giornata Seminariale: Roma e il mare. A proposito del recente rinvenimento del rostro di Acqualadrone. Università degli Studi

di Messina (Italy), 23rd March 2009. Invited Oral Contribution. E. Caponetti, D.F. Chillura Martino, M.L. Saladino, **F. Caruso**, A. Spinella, G. Nasillo, R. Matassa, C. Vasi, F. Aliotta, R.C. Ponterio, S. Tusa, C. Di Stefano, P. Tisseyre, G. Manno, "Caratterizzazione chimico-fisica del rostro di Acqualadrone – Analisi preliminari";

5. Technart 2009. Non-destructive and Microanalytical Techniques in Art and Cultural Heritage. Athens (Greece), 27th–30th April 2009. Oral Contribution. E. Caponetti, **F. Caruso**, C. Di Stefano, M.L. Saladino, A. Spinella, P. Tisseyre, S. Tusa, "Preliminary study on the wood from an ancient Roman rostrum";

6. Technart 2009. Non-destructive and Microanalytical Techniques in Art and Cultural Heritage. Athens (Greece), 27th–30th April 2009. Poster Presentation. Best Poster Award. E. Caponetti, **F. Caruso**, D.F. Chillura Martino, C. Di Stefano, M.L. Saladino, "XRF characterisation of the varnishes of ancient stringed instruments";

7. XXXIX National Congress on Magnetic Resonance. Palermo (Italy), 21st–24th September 2009. Oral Contribution. **A. Spinella**, F. Caruso, E. Caponetti, "Preliminary solid state NMR characterization of wooden archaeological samples";

8. Cultural Heritage Cairo 2009. Science and Technology. Cairo (Egypt), 6th–8th December 2009. Oral Contribution. M. Romagnoli, S. Spina, U. Santamaria, **E. Caponetti**, F. Caruso, A. Spinella, M. Fedi, L. Caforio, S. Tusa, P. Tisseyre, C. Di Stefano, A. Valenti, "The wood in Acqualadrone (ME–Sicily) Roman Nostrum";

9. Second edition of YOCOCU. Youth in the Conservation of Cultural Heritage. Palermo (Italy), 24th–26th May 2010. Oral Contribution. **F. Caruso**, D.F. Chillura Martino, S. Saverwyns, M. Van Bos, L. Burgio, C. Di Stefano, E. Caponetti, "Multi-analytical approach to the study of varnishes from historical musical instruments";

10. Second edition of YOCOCU. Youth in the Conservation of Cultural Heritage. Palermo (Italy), 24th–26th May 2010. Poster Presentation. **M.L. Saladino**, F. Caruso, C. Di Stefano, V. Gennaro, E. Caponetti, "Artistic reproduction of the Guerriero da Petralia Sottana";

11. 10th Sigma Aldrich Young Chemists Symposium – SAYCS. Pesaro (Italy), 18th–20th October 2010. Flash communication. **F. Caruso**, S. Saverwyns, M. Van Bos, E. Caponetti, "Caratterizzazione di Antichi Strumenti Musicali Valloni mediante Micro-Fluorescenza a Raggi X";

12. 2010 LCLS/SSRL Annual Users' Meeting & Workshops. Menio Park (CA, USA), 17th–21th October 2010. Poster Presentation. **P. Frank**, R. Sarangi, F. Caruso, E. Caponetti, B. Hedman, K.O. Hodgson, "Shards of an Ancient Deathstar: Sulfur in a Recovered Roman Ram";
13. Convegno Congiunto delle Sezioni SCI Calabria e Sicilia 2010. Palermo (Italy), 2nd–3rd December 2010. Oral Contribution. **F. Caruso**, D. F. Chillura Martino, M.L. Saladino, S. Saverwyns, M. Van Bos, L. Burgio, C. Di Stefano, E. Caponetti, "Characterisation of the varnishes from historical musical instruments";
14. 5th Intensive School on Conservation Science. Marmara University, Istanbul (Turkey), July 2011. Invited Lecture. **F. Caruso**, "Chemistry between the notes. Characterisation of the varnishes from historical musical instruments".

- Research Periods Spent Abroad
  - October – November 2009: Internship at the Science Conservation section of the Conservation department of the Victoria and Albert in London (United Kingdom). Advisor: Dr Lucia Burgio (`l.burgio@vam.ac.uk`);
  - January – April 2010: Internship at the Laboratories Department of the Koninklijk Instituut voor het Kunstpatrimonium – Institut Royal du Patrimoine Artistique in Brussels (Belgium). Advisors: Dr Steven Saverwyns (`steven.saverwyns@kikirpa.be`) and Dr Marina Van Bos (`marina.vanbos@kikirpa.be`).

- Scholarships/Awards
  1. Technart 2009. Non-destructive and Microanalytical Techniques in Art and Cultural Heritage. Athens (Greece), 27th–30th April 2009. Poster Presentation. Best Poster Award. E. Caponetti, **F. Caruso**, D.F. Chillura Martino, C. Di Stefano, M.L. Saladino, "XRF characterisation of the varnishes of ancient stringed instruments";
  2. 3rd Residential Summer School on Conservation Science at Aristotle University of Thessaloniki (Greece). 19th–31st July 2009. Award for the best E-Chem Test in General Chemistry;
  3. Recipient of an Erasmus LLP Placement scholarship for an internship at the Koninklijkinstituut voor het Kunstpatrimonium – Institut Royal du Patrimoine Artistique in Brussels (Belgium) carried out from 11th January to 21st April 2010.

- Professional Qualifications
  - 2009: Member of the Società Chimica Italiana (Italian Chemical Society, SCI, member no. 16621);
  - 2010: Member of the Steering Committee (Division of Chemical Education) of the Younger Group of the Italian Chemical Society from 2010 to 2012;
  - 2010: Italian delegate of the European Young Chemists Network (EYCN);
  - 2010: Referee of Analytical and Bioanalytical Chemistry and Measurement.
- Organization of Scientific Conferences and Meetings
  - 2008: Organizing committee of the 2^{nd} Residential Summer School: Chemistry and Conservation Science 2008 organized by the Working Group on Chemistry and Cultural Heritage of the European Chemistry Thematic Network and by the Università degli Studi di Palermo. The Summer School was held at the Departments of Chemistry and the Centro Grandi Apparecchiature – UniNetLab of the Università degli Studi di Palermo. Palermo (Italy), 20^{th}–27^{th} July 2008;
  - 2010: Scientific committee of the 10^{th} Sigma Aldrich Young Chemists Symposium – SAYCS organized by the Younger Group of the Italian Chemical Society and Sigma-Aldrich. The symposium was held at Hotel Baia Flaminia. Pesaro (Italy), 18^{th}–20^{th} October 2010.